COMPOSITE MATERIALS EQUIVALENT PROPERTIES IN LAMINA, LAMINATE, AND STRUCTURE LEVELS

by

KAMRAN TAVAKOLDAVANI

Presented to the Faculty of the Graduate School of

The University of Texas at Arlington in Partial Fulfillment

of the Requirements

for the Degree of

MASTER OF SCIENCE IN MECHANICAL ENGINEERING

THE UNIVERSITY OF TEXAS AT ARLINGTON

December 2014

Acknowledgements

I would like to express my sincere appreciation to my research professor Dr. Chan. I admire his support and encouragement throughout my research period. I would like to thank my other committee members: Dr. Lawrence and Dr. Adnan for their support.

I would like to thank my wife and my boys for supporting me throughout my graduate program.

November 24, 2014

Abstract

COMPOSITE MATERIALS EQUIVALENT PROPERTIES

IN LAMINA, LAMINATE, AND

STRUCTURE LEVELS

Kamran Tavakoldavani, MS

The University of Texas at Arlington, 2014

Supervising Professor: Wen S Chan

Increasing use of thick composite structures requires a large model for structural analysis. In the analysis, equivalent properties of composites are often used. The equivalent properties of a composite are defined as the properties of a homogeneous orthotropic composite to representative an anisotropic heterogeneous composite material.

A set of equations for equivalent mechanical and thermal properties in lamina and laminate as well as structures was developed. The developed model for lamina and laminate of composite was based upon the equivalent structural characteristics of 0^0 lamina and homogenized 0^0 laminate for lamina and laminate level, respectively. The concept of narrow beam was enforced in an I-beam serving as an example for structural level. Laminates with symmetric/unsymmetrical, balanced/unbalanced or combined layup was used for study. Results indicate the equivalent properties exhibiting a significant difference in laminate with unsymmetrical and unbalanced layup comparing with FEM results.

Table of Contents

List of Illustrations

List of Tables

Chapter 1

Introduction

1.1 Background

Using composite materials in engineering industries requires complicated analysis and modeling which in most cases computer software runs the analysis. In the case of a thick laminate or a structure it would be a time consuming procedure to predict the mechanical and thermal properties of the desired laminate or structure by ply-by-ply approach.

In composite materials the properties are different depending on the fiber orientation in the matrix so knowing the properties or obtaining the correct and more accurate properties is a very important key when it comes to analyzing the structures. It's difficult and time consuming to calculate the properties of a very thick laminate with each layer having different stacking sequence. When analyzing a thick laminate, it would be simpler and less time consuming to use average properties that would represent the desired model, instead of going through the calculations and obtaining the stiffness matrices for each layer.

Three different levels are considered in this research for the analysis of composite materials such as Lamina, laminate and structure levels. When it comes to analyzing a thick laminate or a composite structure, it is difficult and it takes a large amount of computer memory. So in order to overcome these difficulties, equivalent properties of lamina or laminate are often used. Equivalent properties or effective stiffness properties are an average measure of the stiffness of the desired material. The actual averaging process in order to obtain equivalent properties must be done carefully and delicately. The process is to replace the heterogeneous medium by a macroscopic homogeneity material. This condition is so called effective or equivalent homogeneity. The basic problem is to utilize the averaging process to predict the equivalent properties of the idealized homogeneous medium. So the resulting equivalent properties are to be employed in the analysis of composite materials. Several methods have been proposed predicting equivalent properties. One would introduce a homogeneous volume element which is representing the heterogeneous material volume element. Average stress and average strain are defined for the representative volume element under the macroscopic homogeneous condition. Once the average stress and average strain are obtained, then the stiffness components can be calculated. Since predicting the properties of a laminate is time consuming so often in analysis of composite materials lumping group of plies into a single layer would reduce the size of the analysis and calculations. Equivalent properties are used in order to replace the lumped heterogeneous medium by an equivalent homogeneous material. For example consider a laminate with different layers and material orientation that has been lumped into one layer, so the equivalent properties would represent the lumped layers which behaves as if the fiber orientation in that layer is “0” degree.

Computer software such as ANSYS-APDL, and Mathematica can be used for numerical and analytical methods obtaining and predicting the mechanical and thermal properties of the lumped layers which represent the desired laminate or structure. A number of methods have been proposed for obtaining equivalent properties of composite materials such as conventional method and Modified method which are the focus of this research.

1.2 Objectives

The purpose of this thesis is to develop sets of procedures and calculations in order to obtain equivalent properties in all levels, lamina, laminate, and structure. The two methods that are considered in this thesis in order to obtain these properties are conventional properties method and modified method.

The conventional method uses smeared properties, but in the case of an angle ply, this method does not consider the shear strain produced by an applied axial force. Also In the case of a laminate under a simple tension, if the laminate is un-symmetric and/or un-balanced, it would produce curvature and shear strain which both of them are ignored by this method. The modified method considers the coupling effect of the combined axial and the bending loads that were induced in deriving the equivalent properties.

Analytical method which is done by using Mathematica software is considered in order to obtain equivalent properties and numerical method by ANSYS is considered in order to validate the results obtained from both methods. In Mathematica one program file is designed which contains all the three levels: lamina, laminate, and structure analysis and calculations. This file is divided into 3 different sections or subprograms. Program-1 contains lamina calculations, program-2 contains laminate calculations and program-3 contains structure calculations such as I-beam.

Numerical method is conducted by using ANSYS-APDL. For the case of a laminate which is subjected to an axial load, the stress results obtained by ANSYS are compared against ply-by-ply stress results from modified and conventional methods in order to confirm the accuracy of modified method. Also thermal load that are induced by temperature difference in the laminate is conducted in this thesis. Normal and shear stresses induced by thermal load are calculated by employing modified and conventional methods and the results are compared against ANSYS thermal analysis for accuracy confirmation.

At the structural level for the I-Beam cross section, the two methods that are considered are modified method and smeared properties approach. The equivalent axial stiffness and the bending stiffness of the I-beam are obtained by employing these two methods. Stress analysis is conducted using the modified and smeared properties approach, and the results are compared against the classical lamination theory and ANSYS software.

1.3 Outlines

Chapter 2 discusses the concepts of equivalent properties of materials in general view. It gives an over history and background about these properties and the important points about them.

Chapter 3 conducts the analysis and calculations for obtaining the equivalent properties for a lamina by employing the modified method and the conventional method.

Chapter 4 discusses the procedures in order to obtain the equivalent properties for a laminate by using the two methods.

Chapter 5, its focus is on I-beam structure, and calculating the sectional properties by employing the modified method and the smeared properties method. Also the stress analysis of the I-beam section is conducted, and the results obtained by both methods are illustrated.

Finally, chapter 6 is the conclusion of this thesis.

Chapter 2

Concepts of equivalent properties of materials

Materials have variety of properties, this includes mechanical and thermal properties. In the laboratories it has been found the combination of materials can improve the properties of materials. Engineers obtained a fundamental understanding of materials behavior in heterogeneous materials so that further improvements can be achieved. On scale of atoms and molecules all materials are heterogeneous. If materials were designed at this level of observation, the task would be very difficult to establish. To overcome this difficulty the continuum hypothesis is introduced. This hypothesis provides a statistical average process, and structure of the material is idealized as one in which the material is taken as a continuum. This continuum hypothesis involves the existence of certain measures associated with properties that govern the deformability of the media. These properties reflect averages of necessarily interactions on the molecular or atomic scale. Once the continuum model is constructed, the concept of homogeneity is of relevance. For a homogeneous medium the inherent properties that characterize it are the same at all points of the medium. Conditions of homogeneity and isotropy are assumed here to prevail within individual phases. The scale of the inhomogeneity is assumed to be orders of magnitude smaller than the characteristic dimension of the problem of interest. This condition just described is said to be that of effective or equivalent homogeneity. With the admissibility of equivalent homogeneity, the fundamental problem in heterogeneous material behavior can now be posed. The basic problem is to utilize the averaging process to predict the effective properties of the idealized homogeneous medium in terms of the properties of the individual phases and some information on the interfacial geometry. The resulting effective properties are those that would be employed in the analysis of a load bearing body composed of the composite material. The relationship between the effective properties and the individual phase properties plus the analysis of the structural problem of interest then provides the means of optimizing structural performance by varying individual phase properties or characteristics. One of the reasons that the effective properties are important is because it’s highly developed aspect of the subject of heterogeneous media behavior. An understanding of the role individual phase plays in the overall macroscopic behavior of composite materials provides the key by which materials can be judiciously selected for optimal combinations. Without such knowledge, the field of heterogeneous material behavior primarily would be just an offshoot of anisotropic elasticity. There many different geometric forms give drastically different reinforcing effects, so far as the effective moduli are concerned.

2.1 Literature review

They have been numbers of publications regarding predicting composite materials properties and equivalent or effective properties of composite materials. Micromechanics, Macromechanics in all levels of lamina, laminate, and structure analysis.

Fundamental principles of composite material stiffness predictions, Richardson [1] predicts stiffness used in this presentation are rule of mixtures (ROM), ROM with efficiency factor, Hart-Smith 10% rule, classical laminate analysis, and empirical formulae.

In, discussing effective properties of composites, Lydzba [2] used the homogenization method is to define for the heterogeneous medium that possesses the property of statistical homogeneity an equivalent homogeneous material that would have the same average properties. There are two methods in order to formulate the homogenization problem. One method incorporates the notion of representative volume element on volume averaging of the basic field variable. Fields that are discontinuous at the level of in-homogeneities undergo smoothing through the process of volume averaging. This method is called smoothing method or a micromechanics method. Other method is the mathematical theory of homogenization. The homogenization method is perceived as a smoothing method which is a representative volume element. Small volume is defined that has all the information to describe the structure and properties of the material on the macro scale. Representative volume element is large enough in order to include all elements of a microstructural arrangement. The transition from micro to macro scale is based on the averaging method.

Increasing the use of thick laminates and thick composite structures require a large model for structural analysis. Chan and his associates [3] represented the lumping procedures in which a group of plies lumped into a single layer to reduce the size of the problem and to increase the efficient computation which is often used in thick composite structure modeling. By doing so, the use of equivalent properties for replacing the lumped heterogeneous medium by an equivalent homogenous material is required. This study focuses on developing the equivalent coefficient of hygrothermal expansion of lumped layer by taking into account for induced curvature and shear deformation for an un-symmetrical and un-balanced laminates. The stress results for each ply by employing the modified method were almost identical as the results obtained by using a full model.

Closed form expansions of effective moduli that account for bending and shear induced deformation, used by Chan, and Chen [4] in layer lumping of finite element method analysis. The study demonstrates the accuracy of the present approach, quasi-3D and fully 3D FEM models of graphite/epoxy laminate which is subjected to a tension, bending, and torsion are investigated. The stress results for interlaminar stresses obtained by employing the present method were more appropriate than the results obtained by employing the conventional method.

In composite laminated structures, the idea of using rod reinforcement instead of conversional tape reinforcement, Chan, Wang [5] to ensure the structure fully exploits and fiber capability. The fiber waviness exists in the Prepreg tape when thin tape is unrolled for use. For a structure made of Prepreg tapes, fiber waviness also often occurs in the cured laminates. When such a structure is under a load, the stress distribution for a rod reinforced structure is more complex than for a tape reinforced structure. The main goal of this work is to conduct a buckling analysis of the Rodpack laminates with extreme damage. Damages considered in this study are broken rods. Rods split vertically and horizontally, and delamination between the rod layers and unidirectional plies.

This paper presents a theoretical and experimental study on the static structural response of composite I-Beams with elastic couplings. A Vlasov-type linear theory is developed to analyze composite open section beams made out of general composite laminates, where the transverse shear deformation of the beam cross section is included. Chandra, and Chopra [6] validate this analysis, graphite/epoxy and Kevlar/epoxy symmetric I-Beams were fabricated using an autoclave modeling technics. The beams were tested under tip bending and torsional load, and their structural response in terms of bending slope and twist were measured with a laser optical system. A good correlation between theoretical and experimental results was achieved. 630% increase in the torsional stiffness, and shear-bending coupling of flanges, increase the bending-torsion coupling stiffness of I-Beams.

This paper main objective is to study the laminate composite beam with C-Channel cross section under thermal environment. Kumton [7] developed the analytical method based on classical laminate theory in order to estimate stress on each lamina. The developed method includes the effect of coupling due to un-symmetrical of both laminate and structural configuration levels. The analytical method calculates the sectional properties such as centroid of the cross section, axial and bending stiffness for different laminate layups problems. ANSYS is used to model the 3D laminated composite with C-channel cross section beam. Results obtained by analytical method and FEM are compared against each other for accuracy.

Chapter 3

Lamina Equivalent Properties

3.1 Overview

A lamina consists of rows of parallel fibers surrounded by the matrix material. Figure 3—1 illustrates a lamina with fiber orientations: Θ_1, Θ_2, and Θ_3 which are in material principal coordinate system or it is also called local coordinate system. X, Y, and Z are the lamina coordinate system or global coordinate system. 'Θ' is positive if it is measured counter-clockwise from the X axis if the Z axis is upward to the lamina plane. 'Θ' is negative if it is measured clockwise from the X axis if the Z axis is downward to the lamina plane.

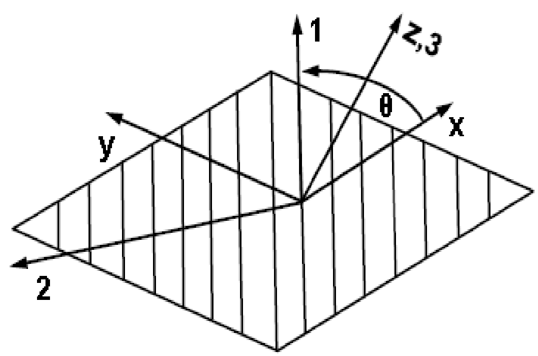

Figure 3—1 Fiber orientation

Laminar type considers material is homogenous, and uses average properties in the analysis, and it considers the unidirectional lamina as a quasi-homogeneous anisotropic material with average stiffness and strength properties. Lamina global elastic constants are: Modulus of elasticity: E_x, E_y, and E_z. Shear modulus: G_{xy}, G_{xz}, and G_{yz}. Poisson's ratio: υ_{xy}, υ_{yz}, and υ_{xz}. Local or principal material constants are: E_1, E_2, E_3, G_{12}, G_{13}, G_{23}, υ_{12}, υ_{13}, and υ_{23}. [S] is the compliance matrix in material orientation.

The general stress/strain relation (Hook's law) for zero degree lamina is:

$$\begin{pmatrix} \epsilon_1 \\ \epsilon_2 \\ \Upsilon_{12} \end{pmatrix} = \begin{pmatrix} S_{11} & S_{12} & S_{16} \\ S_{12} & S_{22} & S_{26} \\ S_{16} & S_{26} & S_{66} \end{pmatrix} \begin{pmatrix} \sigma_1 \\ \sigma_2 \\ \tau_{12} \end{pmatrix} \tag{3.1}$$

$$.S_{11} = \frac{1}{E_1},\ S_{22} = \frac{1}{E_2},\ S_{33} = \frac{1}{E_3},\ S_{12} = -\frac{\upsilon_{12}}{E_1} = -\frac{\upsilon_{21}}{E_2} \tag{3.2}$$

$$S_{13} = -\frac{\upsilon_{31}}{E_3} = -\frac{\upsilon_{13}}{E_1},\ S_{23} = -\frac{\upsilon_{23}}{E_2} = -\frac{\upsilon_{32}}{E_3},\ S_{66} = \frac{1}{G_{12}} \tag{3.3}$$

The relation between the engineering constants and compliance components are illustrated in the following matrix form.

$$\begin{pmatrix} \epsilon_x \\ \epsilon_y \\ \Upsilon_{xy} \end{pmatrix} = \begin{pmatrix} \frac{1}{E_x} & -\frac{\upsilon_{xy}}{E_x} & \frac{\eta_{xs}}{E_x} \\ -\frac{\upsilon_{yx}}{E_y} & \frac{1}{E_y} & \frac{\eta_{ys}}{E_y} \\ \frac{\eta_{xs}}{E_x} & \frac{\eta_{ys}}{E_y} & \frac{1}{G_{xy}} \end{pmatrix} \begin{pmatrix} \sigma_x \\ \sigma_y \\ \tau_{xy} \end{pmatrix} \tag{3.4}$$

$\frac{\eta_{xs}}{E_x} = \bar{S}_{16}$: shear coupling coefficient corresponding to normal stress in X-direction and shear strain in the X-Y plane and $\frac{\eta_{ys}}{E_y}$ = S_{26} in Y-direction.

Transformation relations for engineering constants in 2D:

$$\frac{1}{E_x} = \frac{m^2}{E_1}(m^2 - n^2\upsilon_{12}) + \frac{n^2}{E_2}(n^2 - m^2\upsilon_{21}) + \frac{m^2n^2}{G_{12}} \tag{3.5}$$

$$\frac{1}{E_y} = \frac{n^2}{E_1}(n^2 - m^2\upsilon_{12}) + \frac{m^2}{E_2}(m^2 - n^2\upsilon_{21}) + \frac{m^2n^2}{G_{12}} \tag{3.6}$$

$$\frac{1}{G_{xy}} = \frac{4m^2n^2}{E_1}(1 + \upsilon_{12}) + \frac{4m^2n^2}{E_2}(1 + \upsilon_{21}) + \frac{(m^2-n^2)^2}{G_{12}} \tag{3.7}$$

$$\frac{\upsilon_{xy}}{E_x} = \frac{\upsilon_{yx}}{E_y} = \frac{m^2}{E_1}(m^2\upsilon_{12} - n^2) + \frac{n^2}{E_2}(n^2\upsilon_{21} - m^2) + \frac{m^2n^2}{G_{12}} \tag{3.8}$$

$$\frac{\eta_{xs}}{E_x} = \frac{2m^3n}{E_1}(1 + \upsilon_{12}) - \frac{2mn^3}{E_2}(1 + \upsilon_{21}) - \frac{mn(m^2-n^2)}{G_{12}} \tag{3.9}$$

$$\frac{\eta_{ys}}{E_y} = \frac{2n^3m}{E_1}(1 + \upsilon_{12}) - \frac{2nm^3}{E_2}(1 + \upsilon_{21}) + \frac{mn(m^2-n^2)}{G_{12}} \tag{3.10}$$

In analysis of composite materials it is common and it would be more convenience to use equivalent elastic constants or average properties of the desired material. For instance, equivalent properties of an angle ply would represent the actual ply even though that’s a ply with fiber orientation. It means that a ply with equivalent properties would always be treated as if it was a zero degree ply. The important factor is that in the case of an angle ply when it is loaded under an axial load it will produce shear strain in addition to the normal strains. So the shear strain needs to be suppressed in order to represents a zero degree ply. Suppressing the shear strain induces the shear stress which it needs to be considered in the analysis for obtaining the equivalent properties for lamina with fiber orientation. The two methods that are considered in this thesis are traditional method and modified method.

3.2 Conventional method

The set of expressions for elastic constants in the loading or reference axis are: E_x, E_y, G_{xy}, and υ_{xy}. Elastic constants in lamina principal axis or local axis are: E_1, E_2, G_{12}, and υ_{12}. In order to obtain the equivalent properties under an applied axial load in X-direction the following equations are derived.

ϵ_x is the longitudinal strain or the normal strain and σ_x is the normal stress. For the case of a zero degree fiber orientation, Sin(0) =0, and Cos(0) =1, then the following equations are derived for the longitudinal modulus, $\overline{S_{11}}$:

$$\epsilon_x = \overline{S_{11}}\,\sigma_x \tag{3.11}$$

$$E_x = \frac{1}{\overline{S_{11}}} = \frac{1}{m^4 S_{11} + n^4 S_{22} + 2m^2 n^2 S_{12} + m^2 n^2 S_{66}} \tag{3.12}$$

$$\frac{1}{E_x} = \frac{m^4}{E_1} + \frac{n^4}{E_2} - 2m^2 n^2 \frac{\upsilon_{12}}{E_1} + \frac{n^2 m^2}{G_{12}}$$

(3.13)

m =Cos(Θ), n =Sin(Θ) (3.14)

For transverse modulus:

$$\frac{1}{E_y} = \frac{\epsilon_y}{\sigma_y} = \overline{S_{22}} = n^4 S_{11} + m^4 S_{22} + 2m^2 n^2 S_{12} + m^2 n^2 S_{66} \tag{3.15}$$

$$\frac{1}{E_y} = \frac{n^4}{E_1} + \frac{m^4}{E_2} - 2m^2 n^2 \frac{\upsilon_{12}}{E_1} + \frac{n^2 m^2}{G_{12}} \tag{3.16}$$

Poisson's ratio:

$$\epsilon_x = \overline{S_{11}}\sigma_x,\ \epsilon_y = \overline{S_{12}}\sigma_x \tag{3.17}$$

$$\upsilon_{xy} = -\frac{\epsilon_y}{\epsilon_x} = -\frac{\overline{S_{12}}}{\overline{S_{11}}} = E_x\left(\frac{\upsilon_{12}}{E_1}(m^4+n^4) - (\frac{1}{E_1}+\frac{1}{E_2}-\frac{1}{G_{12}})m^2n^2\right) \tag{3.18}$$

Shear modulus:

$$\Upsilon_{xy} = \overline{S_{66}}\tau_{xy} \tag{3.19}$$

$$\frac{1}{G_{xy}} = \frac{\Upsilon_{xy}}{\tau_{xy}} = \overline{S_{66}} = 2m^2n^2\left(\frac{2}{E_1}+\frac{2}{E_2}+\frac{4\upsilon_{12}}{E_1}-\frac{1}{G_{12}}\right)+\frac{m^4+n^4}{G_{12}} \tag{3.20}$$

Obtaining longitudinal and transverse modulus E_x and E_y, respectively:

$$E_x = \frac{1}{\overline{S_{11}}} \tag{3.21}$$

$$E_y = \frac{1}{\overline{S_{22}}} \tag{3.22}$$

Obtaining Poisson's ratio υ_{xy}:

$$\upsilon_{xy} = -\frac{\overline{S_{12}}}{\overline{S_{11}}} \tag{3.23}$$

Obtaining shear modulus G_{xy}:

$$G_{xy} = \frac{1}{\overline{S_{66}}} \tag{3.24}$$

Obtaining coefficient of thermal expansion:

$[\alpha_{x-y}] = [T_\epsilon(\Theta)]\ [\alpha_{1-2}]$

$$\alpha_x = m^2\,\alpha_1 + n^2\,\alpha_2,\ \alpha_y = n^2\,\alpha_1 + m^2\,\alpha_2,\ \alpha_{xy} = 2\,m\,n\,(\alpha_2 - \alpha_1) \tag{3.25}$$

The issue with this method is that in the case of an angle ply, the traditional method doesn't consider the induced shear stress when suppressing the shear strain. That's why the new modified method has been proposed which is discussed in the next section.

3.3 Modified method

In analysis of composite materials a ply with a fiber orientation 'Θ' (degree) when it's loaded under an axial load or a simple tensile load, it not only produces the normal strains, but also it produces the shear strain. In order to obtain equivalent properties for lamina by employing the modified method, enforcing the lamina to deform uniformly is required. For instance, lamina with fiber orientation 'Θ' is loaded under a simple tension in X-direction. In this case the shear deformation will be induced plus extension in X-direction (longitudinal strain ϵ_x) and contraction in Y-direction (transverse strain ϵ_y). Since lamina with equivalent properties represents a ply with fiber orientation as zero degree so the shear strain needs to be suppressed. By suppressing the shear strain, the shear stress will be induced in the ply. The induced shear stress affects the longitudinal strain and the transverse strain. In the following paragraph the equivalent properties of a lamina by employing the modified method will be derived.

It requires uniform deformation in order to obtain longitudinal modulus E_x also shear strain ΄Υ_{xy} should be suppressed, by doing so the shear stress will be induced. Equation (3.25) illustrates the condition for obtaining the longitudinal modulus.

$$\begin{pmatrix} \epsilon_x \\ \epsilon_y \\ 0 \end{pmatrix} = \begin{pmatrix} \overline{S_{11}} & \overline{S_{12}} & \overline{S_{16}} \\ \overline{S_{21}} & \overline{S_{22}} & \overline{S_{26}} \\ \overline{S_{16}} & \overline{S_{26}} & \overline{S_{66}} \end{pmatrix} \begin{pmatrix} \sigma_x \\ 0 \\ \tau_{xy} \end{pmatrix} \tag{3.25}$$

From the matrix above T_{xy} can be calculated by:

$$0 = \overline{S_{16}}\,\sigma_x + \overline{S_{66}}\tau_{xy} \tag{3.26}$$

The induced shear stress can be obtained by solving the equation above.

$$\tau_{xy} = -\frac{\overline{S_{16}}}{\overline{S_{66}}}\,\sigma_x \tag{3.27}$$

Longitudinal strain including the induced shear stress is:

$$\epsilon_x = \overline{S_{11}}\,\sigma_x + \overline{S_{16}}\tau_{xy} \tag{3.28}$$

Substituting the shear stress relation into the equation above as it follows:

$$\epsilon_x = \overline{S_{11}}\,\sigma_x + \overline{S_{16}}(-\frac{\overline{S_{16}}}{\overline{S_{66}}}\;\sigma_x) \tag{3.29}$$

Factor out normal stress:

$$\epsilon_x = \sigma_x \left(\overline{S_{11}} - \frac{\overline{S_{16}^2}}{\overline{S_{66}}}\right) \tag{3.30}$$

Finally the longitudinal modulus E_x is obtained as:

$$E_x = \frac{1}{\overline{S_{11}} - \frac{\overline{S_{16}^2}}{\overline{S_{66}}}} \tag{3.31}$$

Transverse strain will be calculated by:

$$\epsilon_y = \overline{S_{12}}\,\sigma_x + \overline{S_{26}}\tau_{xy} \tag{3.32}$$

By substituting in the equation above $\left(\overline{S_{12}} - \frac{\overline{S_{16}S_{26}}}{\overline{S_{66}}}\right)$ for the shear stress:

$$\epsilon_y = \sigma_x \left(\overline{S_{12}} - \frac{\overline{S_{16}S_{26}}}{\overline{S_{66}}}\right) \tag{3.33}$$

Obtain Poisson's ratio υ_{xy} by dividing the transverse strain by the longitudinal strain as it shows in equation (3.35).

$$\upsilon_{xy} = -\frac{\epsilon_y}{\epsilon_x} = -\frac{\overline{S_{12}} - \frac{\overline{S_{16}S_{26}}}{\overline{S_{66}}}}{\overline{S_{11}} - \frac{\overline{S_{16}^2}}{\overline{S_{66}}}} \tag{3.34}$$

Transverse modulus is obtained through applying σ_y:

$$E_y = \frac{1}{\overline{S_{22}} - \frac{\overline{S_{12}^2}}{\overline{S_{66}}}} \tag{3.35}$$

So far the equivalent properties are obtained under the applied load in the X-direction. Equation (3.37) illustrates the case for the applied load in the Y-direction. The same procedures are required in order to achieve the uniform deformation.

$$\begin{pmatrix} \epsilon_x \\ \epsilon_y \\ 0 \end{pmatrix} = \begin{pmatrix} \overline{S_{11}} & \overline{S_{12}} & \overline{S_{16}} \\ \overline{S_{21}} & \overline{S_{22}} & \overline{S_{26}} \\ \overline{S_{16}} & \overline{S_{26}} & \overline{S_{66}} \end{pmatrix} \begin{pmatrix} 0 \\ \sigma_y \\ \tau_{xy} \end{pmatrix} \tag{3.36}$$

Solve for transverse strain by deriving the above matrix.

$$\epsilon_y = \overline{S_{22}}\,\sigma_y + \overline{S_{26}}\left(-\frac{\overline{S_{26}}}{\overline{S_{66}}}\,\sigma_y\right) \tag{3.37}$$

Factor out the normal stress, then the transverse strain will be obtained by:

$$\epsilon_y = \sigma_y(\overline{S_{22}} - \frac{\overline{S_{26}^2}}{\overline{S_{66}}}) \tag{3.38}$$

Transverse moduli E_y can be obtained by:

$$E_y = \frac{1}{\overline{S_{22}} - \frac{\overline{S_{26}^2}}{\overline{S_{66}}}} \tag{3.39}$$

In order to obtain the shear modulus G_{xy}, pure shear deformation is required. To ensure the pure shear deformation for lamina under the applied shear load, the normal and the transverse strains need to be suppressed. By doing so the normal and the transverse stresses are induced.

$$\begin{pmatrix} 0 \\ 0 \\ \Upsilon_{xy} \end{pmatrix} = \begin{pmatrix} \overline{S_{11}} & \overline{S_{12}} & \overline{S_{16}} \\ \overline{S_{21}} & \overline{S_{22}} & \overline{S_{26}} \\ \overline{S_{16}} & \overline{S_{26}} & \overline{S_{66}} \end{pmatrix} \begin{pmatrix} \sigma_x \\ \sigma_y \\ \tau_{xy} \end{pmatrix} \tag{3.40}$$

The matrix above shows that after setting the strain in X and Y directions to zero, the normal and the transverse stresses can be calculated by the following equations.

$$0 = (\sigma_x \bar{S}_{11}) + (\sigma_y \bar{S}_{12}) + (\bar{S}_{16} \tau_{xy}) \tag{3.41}$$

$$0 = (\sigma_x \bar{S}_{11}) + (\sigma_y \bar{S}_{22}) + (\bar{S}_{26} \tau_{xy}) \tag{3.42}$$

$$\Upsilon_{xy} = (\sigma_x \bar{S}_{16}) + (\sigma_y \bar{S}_{26}) + (\bar{S}_{66} \tau_{xy}) \tag{3.43}$$

Solve for the normal stress and the transverse stress:

$$\sigma_x = \frac{\bar{S}_{12}\bar{S}_{26} - \bar{S}_{22}\bar{S}_{16}}{\bar{S}_{11}\bar{S}_{22} - \bar{S}_{12}^2} \tau_{xy} \tag{3.44}$$

$$\sigma_y = \frac{\bar{S}_{12}\bar{S}_{16} - \bar{S}_{11}\bar{S}_{26}}{\bar{S}_{11}\bar{S}_{22} - \bar{S}_{12}^2} \tau_{xy} \tag{3.45}$$

Shear strain can be calculated by substituting equation (3.44) and (3.45) into equation (3.43), and factor out the shear:

$$\Upsilon_{xy} = \left(\bar{S}_{66} + \bar{S}_{16} \frac{\bar{S}_{12}\bar{S}_{26} - \bar{S}_{22}\bar{S}_{16}}{\bar{S}_{11}\bar{S}_{22} - \bar{S}_{12}^2} + \bar{S}_{26} \frac{\bar{S}_{12}\bar{S}_{16} - \bar{S}_{11}\bar{S}_{26}}{\bar{S}_{11}\bar{S}_{22} - \bar{S}_{12}^2}\right) \tau_{xy} = \frac{\tau_{xy}}{G_{xy}} \tag{3.46}$$

Finally the shear modulus is obtained by:

$$G_{xy} = \left(\frac{1}{\bar{S}_{66} + \bar{S}_{16} \frac{\bar{S}_{12}\,\bar{S}_{26} - \bar{S}_{22}\bar{S}_{16}}{\bar{S}_{11}\,\bar{S}_{22} - \bar{S}_{12}^{2}} + \bar{S}_{26} \frac{\bar{S}_{12}\,\bar{S}_{16} - \bar{S}_{11}\bar{S}_{26}}{\bar{S}_{11}\,\bar{S}_{22} - \bar{S}_{12}^{2}}} \right) \tag{3.47}$$

3.4 Analytical method obtaining equivalent properties

Mathematica is used to obtain equivalent properties for lamina with different fiber orientations by employing conventional method and modified method. Three programs are developed in order to calculate the equivalent properties. Program 1 is used for calculating the equivalent properties for the case of lamina. This program would take the mechanical and thermal properties of a ply. It will calculate the reduced stiffness matrix [Q], and the compliance matrix [S] for the desire ply. It would implement both methods in order to obtain the equivalent properties for the desire lamina.

Material that is considered throughout this thesis is carbon/epoxy (IM6G/3501-6), with mechanical and thermal properties as:

Modulus elasticity, E_x =24.5(Msi), E_y =1.3(Msi)

Shear modulus, G_{xy} =0.94(Msi)

Poisson ration, υ_{xy} =0.31

Longitude thermal expansion, α_x =-0.5(10^{-6}/F), and α_y =13.9(10^{-6}/F)

3.4.1 Results and comparison of modified and conventional methods

Compliance matrix is constructed by Mathematica-10 by applying the equations below:

$$S_{11} = \frac{1}{E_1},\ S_{12} = S_{21} = -\frac{\upsilon_{12}}{E_1} = -\frac{\upsilon_{21}}{E_2} \tag{3.48}$$

$$S_{22} = \frac{1}{E_2},\ S_{66} = \frac{1}{G_{12}} \tag{3.49}$$

The matrix form constructed as:

$$\begin{pmatrix} \frac{1}{E_1} & -\frac{\upsilon_{12}}{E_1} & 0 \\ -\frac{\upsilon_{12}}{E_1} & \frac{1}{E_2} & 0 \\ 0 & 0 & \frac{1}{G_{12}} \end{pmatrix} \quad (3.50)$$

The fiber orientations that are considered for this program are: 0, 15, 30, 45, 60, 75 and 90 degrees. Once the equivalent properties are obtained for both methods then Excel program is used to plot the results. The plots that are constructed for all the cases are illustrated in the following pages.

Figure 3—2 illustrates longitudinal and transverse modulus obtained from both methods. Each data is related to its ply orientation for both methods. The left vertical axis is the longitudinal modulus and the right vertical axis is the transverse modulus. The horizontal axis is the fiber orientation which starts with 0 degree to 90 degree with increment rate of 15 degree. As it is showing in the figure the longitudinal modulus is decreasing as the angle ply is increasing for both methods. The transverse modulus is increasing as the angle ply also is increasing. As expected for the 0 and 90 degree ply the value is the same for both methods.

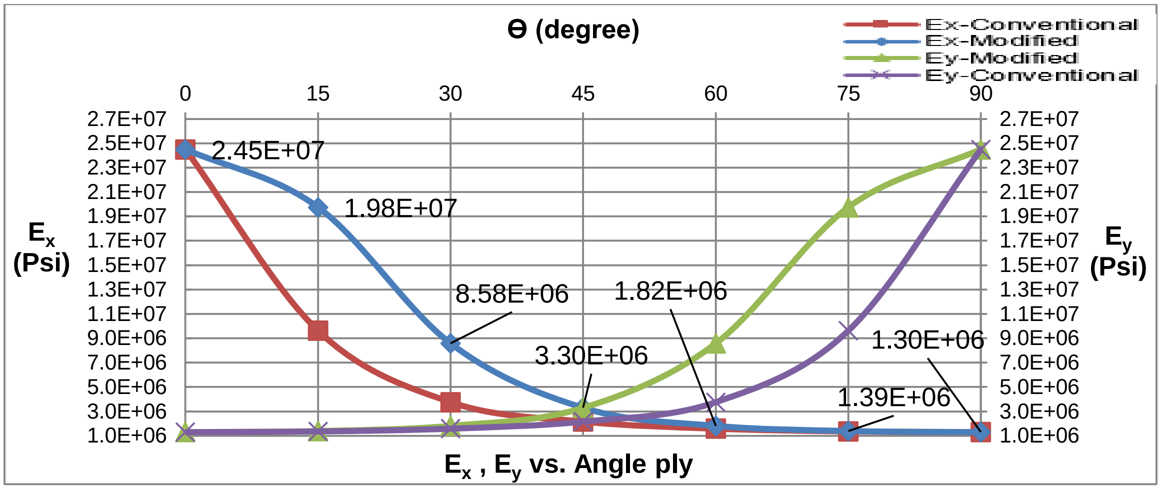

Figure 3—2 Longitudinal & Transverse Modulus

Table 3—1 displays the results from Figure 3—2 for longitudinal modulus. The highest percentage difference is for 30 degree ply.

Table 3—1 Longitudinal Modulus

E_x(Psi)			
Ɵ ply	Modified method	Conventional method	% Difference
0	2.45E+07	2.45E+07	0.0
15	1.98E+07	9.63E+06	51.3
30	8.58E+06	3.76E+06	56.1
45	3.30E+06	2.16E+06	34.4
60	1.82E+06	1.59E+06	12.6
75	1.39E+06	1.36E+06	2.4
90	1.30E+06	1.30E+06	0.0

Table 3—2 display the results for the transverse modulus. The highest percent difference is for 60 degree ply.

Table 3—2 Transverse Modulus

E_y(Psi)			
Ɵ ply	Modified method	Conventional method	% Difference
0	1.30E+06	1.30E+06	0.0
15	1.39E+06	1.36E+06	2.4
30	1.82E+06	1.59E+06	12.6
45	3.30E+06	2.16E+06	34.4
60	8.58E+06	3.76E+06	56.1
75	1.98E+07	9.63E+06	51.3
90	2.45E+07	2.45E+07	0.0

Figure 3—3 illustrates Poisson's ratio for both methods. For the 0 and 90 degree ply the results are identical. For the 75 degree ply the results are in very close range. There is a big difference for the 15, 30, 45 and 60 degree ply.

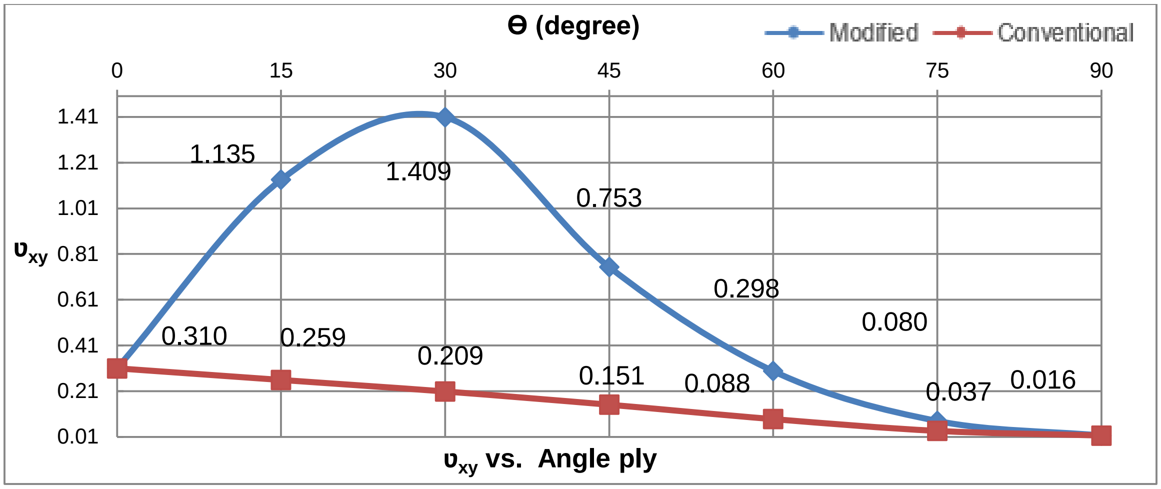

Figure 3—3 Poisson's ratio vs. Angle ply

Table 3—3 displays the results from Figure 3—3. The percent difference is zero for the cases of 0 and 90 degree plies. The highest value for the percent difference is for the case of 30 degree ply which is 85.2%.

Table 3—3 Poisson's Ratio

υ_{xy}			
ϴ ply	Modified method	Conventional Method	% Difference
0	0.310	0.310	0.0
15	1.135	0.259	77.2
30	1.409	0.209	85.2
45	0.753	0.151	80.0
60	0.298	0.088	70.5
75	0.080	0.037	54.2
90	0.016	0.016	0.0

Figure 3—4 illustrates the shear modulus for both methods. For the cases of 0 and 90 degree plies the results for both methods are identical. For the case of 45 degree ply it has the most disagreement between the results.

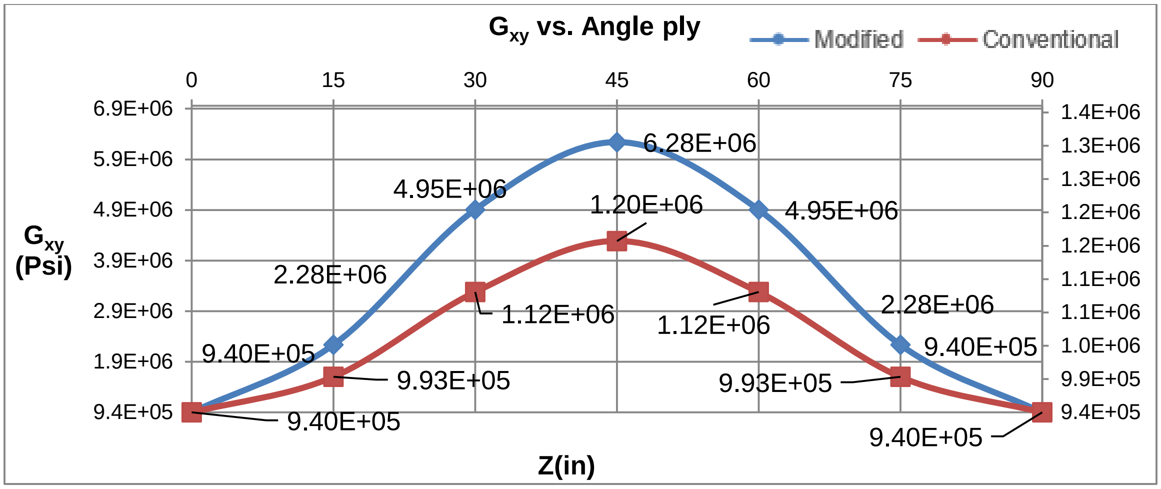

Figure 3—4 Shear Modulus

Table 3—4 displays the results from. For 0 and 90 degree plies the percent difference is zero. But the rest of plies the percent difference is high value especially the highest value for α_x is for 30 degree ply.

Table 3—4 Shear Modulus

G_{xy}(Psi)			
ϴ ply	Modified method	Conventional method	% Difference
0	9.40E+05	9.40E+05	0.0
15	2.28E+06	9.93E+05	56.3
30	4.95E+06	1.12E+06	77.3
45	6.28E+06	1.20E+06	80.9
60	4.95E+06	1.12E+06	77.3
75	2.28E+06	9.93E+05	56.3
90	9.40E+05	9.40E+05	0.0

Chapter 4

Laminate Equivalent Properties

4.1 Overview

It's known that the use of the composite materials have been growing in industries, such as, aerospace, manufacturing, civil, oil and gas, biomedical, and many other industries around the globe especially in the aerospace industries in the U.S. When it comes to analysis of composites it takes a large amount of memory in order to run computer software. It could become a great challenge and time consuming matter when dealing with a structure that is constructed of layers of same or different materials with each ply with different fiber orientation. In order to resolve these issues is to obtain equivalent properties that would represent the laminate or the structure that is considered for analysis. The procedure starts with lumping group of layers with different fiber orientation into a single layer (zero degree) that would represent the actual structure or the actual laminate. The purpose is to replace the lumped heterogeneous material by an equivalent homogenous material. Briefly constructing the laminate stiffness matrices are discussed first.

[A]=Extensional Stiffness matrix, (lb/in)

[B]=Extensional-Bending Coupling Stiffness matrix, (lb)

[D] Bending Stiffness matrix, (lb-in)

Laminate stiffness matrices:

$$[A] = \sum_{k=1}^{n} [Q]\,(h_k - h_{k-1}) \tag{4.1}$$

$$[B] = \frac{1}{2} \sum_{k=1}^{n} [Q]\,(h_k^2 - h_{k-1}^2) \tag{4.2}$$

$$[D] = \frac{1}{3} \sum_{k=1}^{n} [Q]\,(h_k^3 - h_{k-1}^3) \tag{4.3}$$

Force and moment resultants in laminate: Sum of the force and moment in each layer:

$$\begin{pmatrix} N_x \\ N_y \\ N_{xy} \end{pmatrix} = \sum_{k=1}^{n} \int_{h_{k-1}}^{h_k} \begin{pmatrix} \sigma_x \\ \sigma_y \\ \tau_{xy} \end{pmatrix} dz \ \frac{lb}{in} \quad , \quad \begin{pmatrix} M_x \\ M_y \\ M_{xy} \end{pmatrix} = \sum_{k=1}^{n} \int_{h_{k-1}}^{h_k} \begin{pmatrix} \sigma_x \\ \sigma_y \\ \tau_{xy} \end{pmatrix} z \, dz \ \frac{lb-in}{in} \tag{4.4}$$

After obtaining the force and moment in each layer, then the total force and moment in laminate with respect to mid plane strain and curvature are as follow:

$$\begin{pmatrix} N \\ M \end{pmatrix} = \begin{pmatrix} A & B \\ B & D \end{pmatrix} \begin{pmatrix} \epsilon^0 \\ K \end{pmatrix} \tag{4.5}$$

Expand and derive the matrix above in order to solve for the resultant forces:

$$\begin{pmatrix} N_x \\ N_y \\ N_{xy} \end{pmatrix} = \begin{pmatrix} A_{11} & A_{12} & A_{16} \\ A_{21} & A_{22} & A_{26} \\ A_{16} & A_{26} & A_{66} \end{pmatrix} \begin{pmatrix} \epsilon_x^0 \\ \epsilon_y^0 \\ \Upsilon_{xy}^0 \end{pmatrix} + \begin{pmatrix} B_{11} & B_{12} & B_{16} \\ B_{21} & B_{22} & B_{26} \\ B_{16} & B_{26} & B_{66} \end{pmatrix} \begin{pmatrix} K_x \\ K_y \\ K_{xy} \end{pmatrix} \tag{4.6}$$

A_{11} and A_{22} are the axial extension stiffness

A_{12} is stiffness due to the Poisson's ratio effect

A_{16} and A_{26} are stiffness due to the shear coupling

B_{11} and B_{22} are coupling stiffness due to the direct curvature

B_{12} is the coupling stiffness due to the Poisson's ratio effect

B_{16} and B_{26} are the extension-twisting coupling stiffness (shear-bending coupling)

B_{66} is the shear-twisting coupling stiffness

D_{11} and D_{22} are the bending stiffness

D_{12} is the bending stiffness due to the Poisson's ratio effect

D_{16} and D_{26} are the bending and twisting coupling

D_{66} is the twisting stiffness

Expand and solve equation (4.5) for the moments:

$$\begin{pmatrix} M_x \\ M_y \\ M_{xy} \end{pmatrix} = \begin{pmatrix} B_{11} & B_{12} & B_{16} \\ B_{21} & B_{22} & B_{26} \\ B_{16} & B_{26} & B_{66} \end{pmatrix} \begin{pmatrix} \epsilon_x^0 \\ \epsilon_y^0 \\ \Upsilon_{xy}^0 \end{pmatrix} + \begin{pmatrix} D_{11} & D_{12} & D_{16} \\ D_{21} & D_{22} & D_{26} \\ D_{16} & D_{26} & D_{66} \end{pmatrix} \begin{pmatrix} K_x \\ K_y \\ K_{xy} \end{pmatrix} \tag{4.7}$$

Concept of equivalent homogenous solid Consider a microscopic heterogeneous material so the procedure is to construct the equivalent homogeneous medium to represents the original material structure.

The average stress/strain tensor over the volume of the representing volume element:

$$[\bar{\sigma}] = \frac{1}{V}\int [\sigma(x, y, z)]dV \quad (4.8)$$

$$[\bar{\epsilon}] = \frac{1}{V}\int [\epsilon(x, y, z)]dV \quad (4.9)$$

Equivalent homogeneous solids are defined as:

$$[\bar{\sigma}] = [\bar{C}].[\bar{\epsilon}], [\bar{\epsilon}] = [\bar{S}].[\bar{\sigma}] \quad (4.10)$$

[C] and [S] are the equivalent stiffness matrix and compliance matrix, respectively in a homogeneous medium.

Equivalent Elastic constant Similar to the lamina, a laminate with equivalent properties should be deformed uniformly under an axial load. The two methods that were discussed in chapter 3 are also discussed in this chapter except this time it's regarding the laminate equivalent properties.

4.2 Conventional method

To obtain equivalent properties, we apply the corresponding load on the laminate. Let, $N_x \neq 0$, and $N_{xy}=N_y=M=0$, and 't' is the laminate thickness.

$$\begin{pmatrix} \epsilon^0 \\ \kappa \end{pmatrix} = \begin{pmatrix} a & b \\ b^T & d \end{pmatrix} \begin{pmatrix} N \\ M \end{pmatrix}, \epsilon_x = N_x\, a_{11} = a_{11}\, t\, \sigma_x = \sigma_x \frac{1}{E_x} \quad (4.11)$$

Longitudinal and transverse modulus:

$$E_x = \frac{1}{a_{11}\, t},\ E_y = \frac{1}{a_{22}\, t} \quad (4.12)$$

Poisson's ratio and shear modulus:

$$\upsilon_{xy} = -\frac{a_{12}}{a_{11}},\ G_{xy} = \frac{1}{a_{66}\, t} \quad (4.13)$$

Let replace the mechanical load by the thermal induced load, then the coefficient of thermal expansion CTE would be:

$$[\alpha] = \{[a]\,[N^{TH}] + [b]\,[M]^{TH}\}\frac{1}{\Delta T} \tag{4.14}$$

$$[N^{TH}] = \sum_{k=1}^{n}[\bar{Q}]\,[\alpha_{x-y}](z_k - z_{k-1})\,\Delta T$$

$$[M^{TH}] = \frac{1}{2}\sum_{k=1}^{n}[\bar{Q}]\,[\alpha_{x-y}](z_k^2 - z_{k-1}^2)\,\Delta T$$

4.3 Modified method

The main objective is to lump several plies into a single ply with 0 degree fiber orientation. Stress at any given ply remains the same as compare with the un-lumped model. In this analysis a coupling effect of combined axial and bending loads were included in deriving the equivalent properties. Conventional method the effect of curvature and shear deformation on the equivalent properties was ignored for un-symmetrical and un-balanced laminates. Shear deformation and out of plane curvatures, this is due to the non-zero value of the extension-bending coupling stiffness which is the B matrix. In plane extension-shear coupling stiffness which are A_{16} and A_{26}. Bending twisting coupling stiffness are D_{16} and D_{26}. The representing 0 degree layer will not induce in plane shear and out of plane couplings. So in order to accomplish the results with no shear deformation and neither curvature is to suppress the shear deformation and curvature for analysis of obtaining the equivalent properties.

Unlike the conventional method, this method ensures zero curvature and shear deformation when it's evaluating the equivalent properties.

Let $N_x \neq 0$, and $N_{xy}=N_y=M=0$, so only N_x is the applied load, then curvature needs to be suppressed in order to obtain the equivalent properties. After suppressing the curvature, moment equation will be induced.

$$\begin{pmatrix} \epsilon^0 \\ 0 \end{pmatrix} = \begin{pmatrix} a & b \\ b^T & d \end{pmatrix} \begin{pmatrix} N \\ M \end{pmatrix}, 0 = b^T\,N + d\,M \tag{4.15}$$

$$M = -b^T N d^{-1}, \ \epsilon^0 = N(a - b^T b\, d^{-1}) \tag{4.16}$$

The value inside the parenthesis is a 3 by 3 matrix that it's called [P] matrix. So the new mid plane strain would be:

$$[P] = [a] - [b^T][b]\,[d]^{-1} \tag{4.17}$$

$$\epsilon^0 = [P][N] \tag{4.18}$$

Now let the mid plane shear strain be suppressed and N_{xy} is induced, with applying load in the X direction:

$$\begin{pmatrix} \epsilon_x^0 \\ \epsilon_y^0 \\ 0 \end{pmatrix} = \begin{pmatrix} P_{11} & P_{12} & P_{16} \\ P_{12} & P_{22} & P_{26} \\ P_{16} & P_{26} & P_{66} \end{pmatrix} \begin{pmatrix} N_x \\ 0 \\ N_{xy} \end{pmatrix} \tag{4.19}$$

From the matrix above, the mid strains can be solved:

$$\epsilon_x^0 = \left(P_{11} - \frac{P_{16}^2}{P_{66}}\right) N_x, \ \epsilon_y^0 = \left(P_{12} - \frac{P_{16}\,P_{26}}{P_{66}}\right) N_x \tag{4.20}$$

Once the mid strains equations are formed then the equivalent properties: longitudinal, transverse, and Poisson's ratio can be obtained:

$$E_x = \frac{1}{\left(P_{11} - \frac{P_{16}^2}{P_{66}}\right) t} \ E_y = \frac{1}{\left(P_{12} - \frac{P_{16}\,P_{26}}{P_{66}}\right) t} \ \upsilon_{xy} = -\frac{\epsilon_y^0}{\epsilon_x^0} = \frac{P_{12} - \frac{P_{16}\,P_{26}}{P_{66}}}{P_{11} - \frac{P_{16}^2}{P_{66}}} \tag{4.21}$$

To obtain shear modulus G_{xy} with applied N_{xy} it requires to $\epsilon^0{}_x = \epsilon^0{}_y = 0$, to ensure the pure shear deformation.

$$\begin{pmatrix} 0 \\ 0 \\ \Upsilon_{xy} \end{pmatrix} = \begin{pmatrix} P_{11} & P_{12} & P_{16} \\ P_{12} & P_{22} & P_{26} \\ P_{16} & P_{26} & P_{66} \end{pmatrix} \begin{pmatrix} N_x \\ N_y \\ N_{xy} \end{pmatrix} \tag{4.22}$$

By suppressing normal strains, normal axial forces will be induced.

$$\begin{pmatrix} N_x \\ N_y \end{pmatrix} = -\begin{pmatrix} P_{11} & P_{12} \\ P_{12} & P_{22} \end{pmatrix}^{-1} \begin{pmatrix} P_{16} \\ P_{26} \end{pmatrix} N_{xy} = -\frac{1}{\Delta} \begin{pmatrix} P_{22} & -P_{12} \\ -P_{12} & P_{11} \end{pmatrix} \begin{pmatrix} P_{16} \\ P_{26} \end{pmatrix} N_{xy} \tag{4.23}$$

$$\Delta = P_{22}\,P_{11} - P_{12}^2 \tag{4.24}$$

Normal axial forces can be solved:

$$N_x = -\frac{P_{22}\,P_{16} - P_{12}\,P_{26}}{\Delta} N_{xy},\;\; N_y = -\frac{P_{11}\,P_{26} - P_{12}\,P_{26}}{\Delta} N_{xy} \tag{4.25}$$

From the matrix above and by having the normal axial forces induced, then shear strain would be:

$$\Upsilon_{xy} = P_{16}\,N_x + P_{26}\,N_y + P_{66}\,N_{xy} \tag{4.26}$$

$$\Upsilon_{xy} = \left(P_{66} - \frac{P_{16}(P_{22}\,P_{16} - P_{12}\,P_{26})}{\Delta} - \frac{P_{26}(P_{11}\,P_{26} - P_{12}\,P_{26})}{\Delta}\right) N_{xy} \tag{4.27}$$

Assuming shear strain to be 1, shear modulus can be obtained with t being the laminate thickness:

$$G_{xy} = \frac{1}{\left(P_{66} - \frac{P_{16}(P_{22}\,P_{16} - P_{12}\,P_{26})}{\Delta} - \frac{P_{26}(P_{11}\,P_{26} - P_{12}\,P_{26})}{\Delta}\right) t} \tag{4.28}$$

Coefficient of Thermal Expansion CTE, in the previous calculations the [P] matrix was constructed:

$$\begin{pmatrix} \epsilon_x^0 \\ \epsilon_y^0 \end{pmatrix} = \begin{pmatrix} P_{11} - \frac{P_{16}^2}{P_{66}} & P_{12} - \frac{P_{16}\,P_{26}}{P_{66}} \\ P_{12} - \frac{P_{16}\,P_{26}}{P_{66}} & P_{22} - \frac{P_{26}^2}{P_{66}} \end{pmatrix} \begin{pmatrix} N_x \\ N_y \end{pmatrix} \tag{4.29}$$

Mid strain in X and Y directions can be solved:

$$\epsilon_x^0 = \left(P_{11} - \frac{P_{16}^2}{P_{66}}\right) N_x + \left(P_{12} - \frac{P_{16}\,P_{26}}{P_{66}}\right) N_y \tag{4.30}$$

$$\epsilon_y^0 = \left(P_{12} - \frac{P_{16}\,P_{26}}{P_{66}}\right) N_x + \left(P_{22} - \frac{P_{26}^2}{P_{66}}\right) N_y \tag{4.31}$$

Force and moment resultants for thermal loads are:

$$[N^{TH}]_{3X1} = \sum_{k=1}^{n} [Q].[\underset{\sim}{\alpha}]\,(h_k - h_{k-1})\,\Delta T,\;\; \frac{lb}{in} \tag{4.32}$$

$$[M^{TH}]_{3X1} = \frac{1}{2} \sum_{k=1}^{n} [Q].[\underset{\sim}{\alpha}]\,(h_k^2 - h_{k-1}^2)\Delta T,\;\; lb \tag{4.33}$$

Considering the equation for the thermal load and the mid plane strain equation, coefficient of thermal expansion can be obtained by:

$$\alpha_x = \left\{\left(P_{11} - \frac{P_{16}^2}{P_{66}}\right) N_x^{TH} + \left(P_{12} - \frac{P_{16}\,P_{26}}{P_{66}}\right) N_y^{TH}\right\} \frac{1}{\Delta T} \tag{4.34}$$

$$\alpha_y = \left\{\left(P_{12} - \frac{P_{16}\,P_{26}}{P_{66}}\right) N_x^{TH} + \left(P_{22} - \frac{P_{26}^2}{P_{66}}\right) N_y^{TH}\right\} \frac{1}{\Delta T} \tag{4.35}$$

4.4 Analytical method obtaining equivalent properties

As it was discussed in the previous chapter in order to calculate equivalent properties software Mathematica-10 is used. Mechanical and thermal properties are the same as it was for chapter 1. In the software file Program-2A and Program-2B are for analysis and calculations for laminate using both conventional and modified properties methods.

4.4.1 Result obtained by employing modified and conventional methods

Consider a laminate with stacking sequence: $[+\Theta/-\Theta/0/90]_S$, $[+\Theta/-\Theta/0/90]_{2T}$, $[\theta_2/0/90]_S$, and $[\theta_2/0/90]_{2T}$. 'S' is for a symmetrical laminate and "Θ" is the ply orientation which varies as 0, 15, 30, 45, 60, 75, and 90 degree. For the case of a symmetrical laminate coupling stiffness [B] =0. For the case of a balanced laminate stiffness due to shear coupling $A_{16} = A_{26} = 0$.

Figure 4—1 illustrates the longitudinal modulus for symmetrical and balanced laminate for both conventional method and modified method. The laminates that are considered for this figure are: $[0_2/0/90]_S$, $[15/-15/0/90]_S$, $[30/-30/0/90]_S$, $[45/-45/0/90]_S$, $[60/-60/0/90]_S$, $[75/-75/0/90]_S$, and $[90_2/0/90]_S$. As expected since it's a balanced symmetrical laminate the results obtained from both methods are identical.

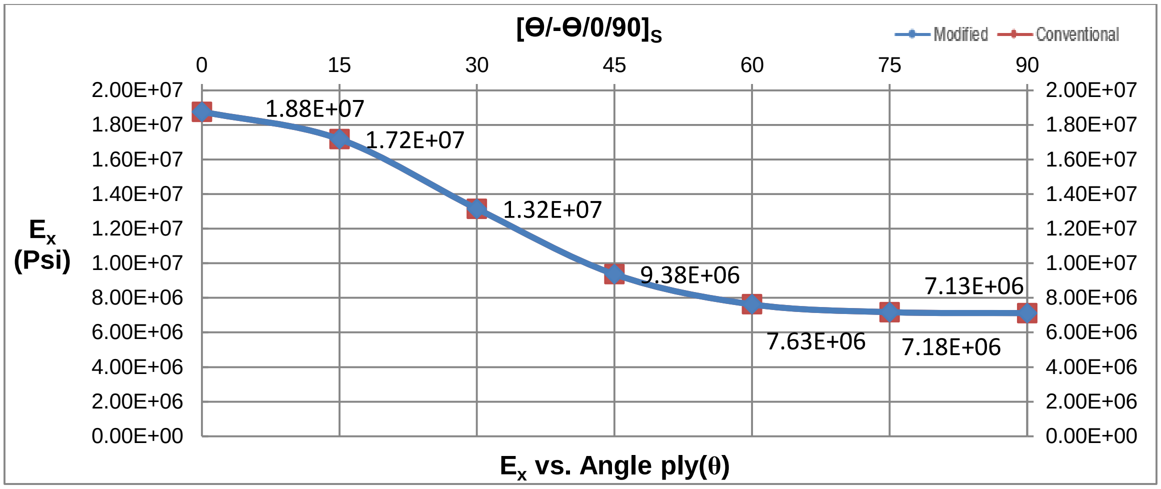

Figure 4—1 Longitudinal Modulus for $[\Theta/\text{-}\Theta/0/90]_S$

Table 4—1 displays the results from Figure 4—1 As it's displayed in the table all the values are the same for both methods.

Table 4—1 Longitudinal Modulus for $[\Theta/\text{-}\Theta/0/90]_S$

E_x(Psi)			
Θ/-Θ	Modified method	Conventional method	% Difference
0/0	1.88E+07	1.88E+07	0.0
15/-15	1.72E+07	1.72E+07	0.0
30/-30	1.32E+07	1.32E+07	0.0
45/-45	9.38E+06	9.38E+06	0.0
60/-60	7.63E+06	7.63E+06	0.0
75/-75	7.18E+06	7.18E+06	0.0
90/90	7.13E+06	7.13E+06	0.0

Figure 4—2 illustrates the longitudinal modulus for un-symmetrical, and balanced laminates with stacking sequence as $[+\Theta/\text{-}\Theta/0/90]_{2T}$. Since it's an un-symmetrical laminate the results are not identical.

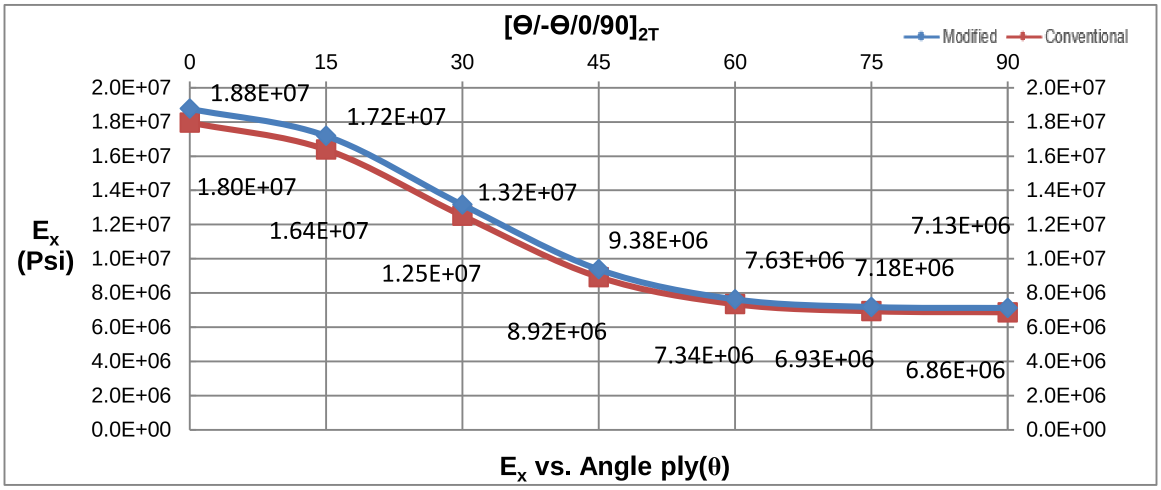

Figure 4—2 Longitudinal Modulus for $[+\Theta/-\Theta/0/90]_{2T}$

Table 4—2 displays the results from Figure 4—2. As it's displayed in the table under the difference column none of the values are identical even though it's a balanced laminate.

Table 4—2 Longitudinal Modulus for $[+\Theta/-\Theta/0/90]_{2T}$

E_x(Psi)			
Θ/-Θ	Modified method	Conventional method	% Difference
0/0	1.88E+07	1.80E+07	4.3
15/-15	1.72E+07	1.64E+07	4.7
30/-30	1.32E+07	1.25E+07	4.9
45/-45	9.38E+06	8.92E+06	4.8
60/-60	7.63E+06	7.34E+06	3.8
75/-75	7.18E+06	6.93E+06	3.6
90/90	7.13E+06	6.86E+06	3.7

Figure 4—3 illustrates the longitudinal modulus for symmetrical laminate with stacking sequence as $[\theta_2/0/90]_S$. For the cases of $[0_2/0/90]$ and $[90_2/0/90]$ the laminate is balanced so the results are identical. But for rest of the cases the laminates are not balanced anymore and the results are not identical.

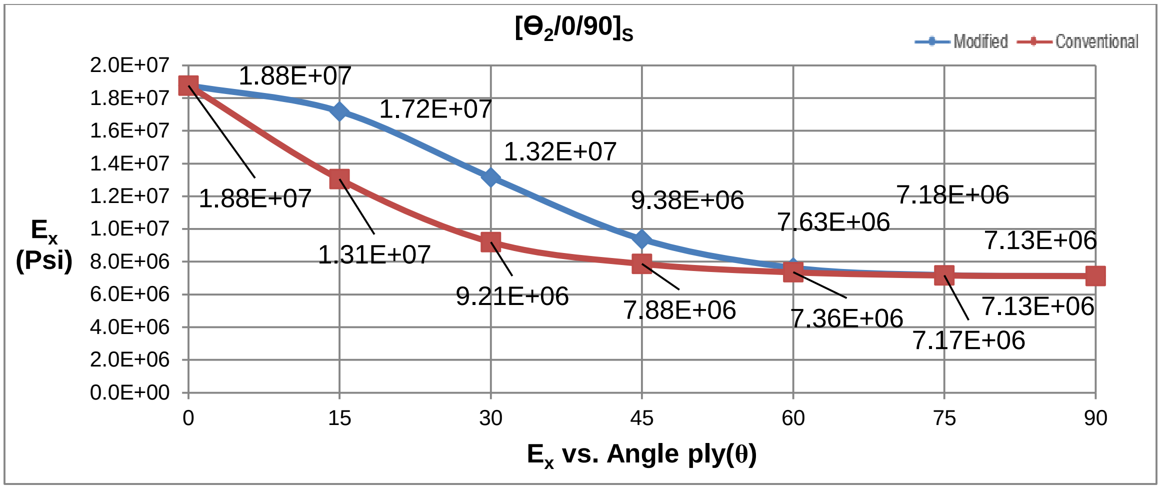

Figure 4—3 Longitudinal Modulus for $[\theta_2/0/90]_S$

Table 4—3 displays the results from Figure 4—3. As it's displayed in the table for the cases of $[0_2/0/90]$ and $[90_2/0/90]$ the percent difference is zero. The percent differences are non-zero values for the rest of the stacking sequences.

Table 4—3 Longitudinal Modulus for $[\theta_2/0/90]_S$

E_x(Psi)			
Θ/Θ	Modified method	Conventional method	% Difference
0/0	1.88E+07	1.88E+07	0.0
15/15	1.72E+07	1.31E+07	24.1
30/30	1.32E+07	9.21E+06	30.0
45/45	9.38E+06	7.88E+06	16.0
60/60	7.63E+06	7.36E+06	3.5
75/75	7.18E+06	7.17E+06	0.2
90/90	7.13E+06	7.13E+06	0.0

Figure 4—4 illustrates the longitudinal modulus for un-symmetrical laminate with stacking sequence as $[\Theta_2/0/90]_{2T}$. The laminates are un-symmetrical so the results are not identical even though $[0_2/0/90]_{2T}$ and $[90_2/0/90]_{2T}$ are balanced laminates.

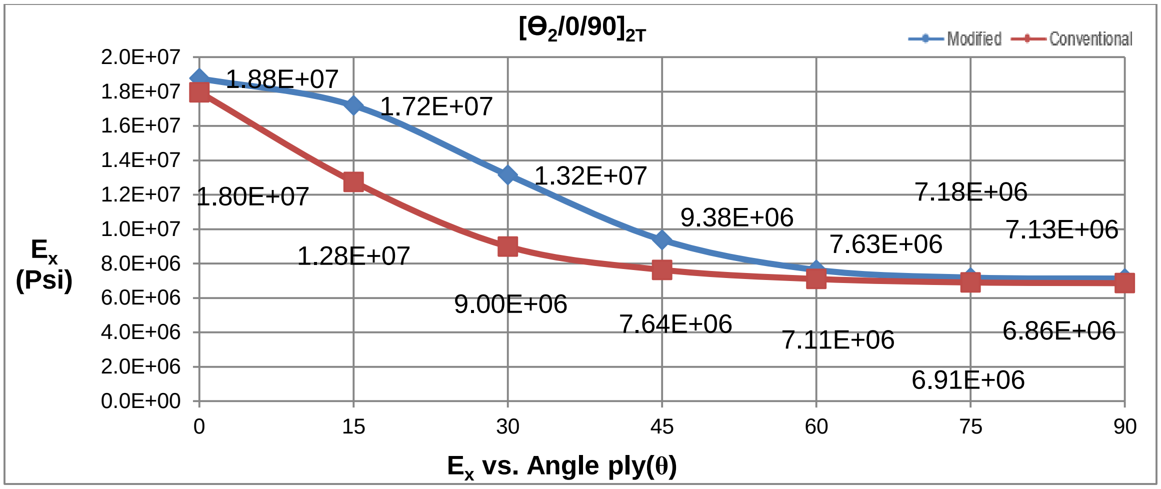

Figure 4—4 Longitudinal Modulus for $[\theta_2/0/90]_{2T}$

Table 4—4 displays the results from Figure 4—4. As it's displayed in the table the percent difference is non-zero values for all the cases.

Table 4—4 Longitudinal Modulus for $[\theta_2/0/90]_{2T}$

E_x(Psi)			
Ɵ/Ɵ	Modified method	Conventional method	% Difference
0/0	1.88E+07	1.80E+07	4.3
15/15	1.72E+07	1.28E+07	25.8
30/30	1.32E+07	9.00E+06	31.6
45/45	9.38E+06	7.64E+06	18.5
60/60	7.63E+06	7.11E+06	6.9
75/75	7.18E+06	6.91E+06	3.8
90/90	7.13E+06	6.86E+06	3.7

Figure 4—5 illustrates the transverse modulus for symmetrical balanced laminates with stacking sequence as $[+\Theta/-\Theta/0/90]_S$. All the obtained results for both methods are identical.

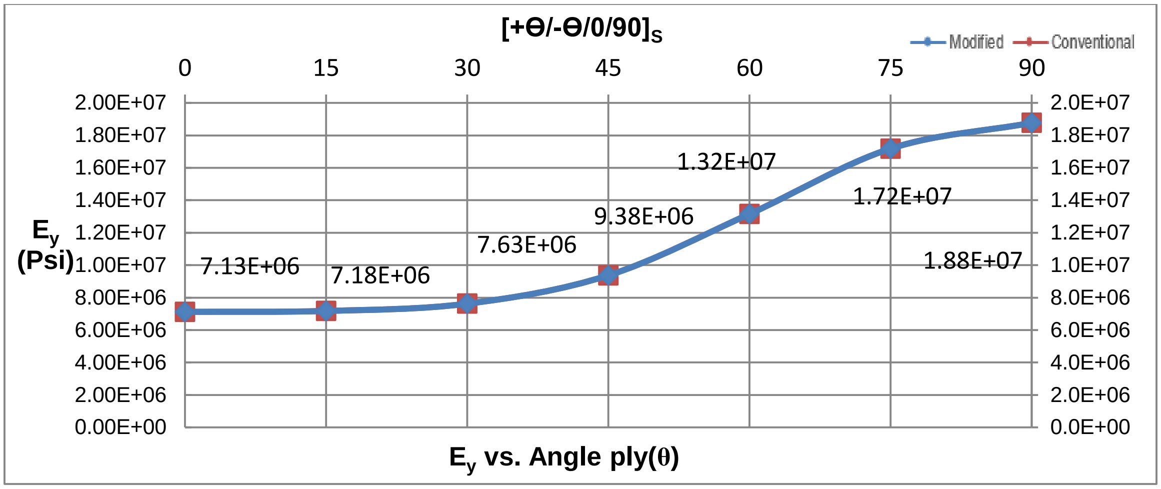

Figure 4—5 Transverse Modulus for [Θ/-Θ/0/90]S

Table 4—5 displays the results from Figure 4—5. As it's displayed in the table the percent difference is zero for all cases.

Table 4—5 Transverse Modulus for [Θ/-Θ/0/90]S

E_y(Psi)			
Θ/-Θ	Modified method	Conventional method	% Difference
0/0	7.13E+06	7.13E+06	0.0
15/-15	7.18E+06	7.18E+06	0.0
30/-30	7.63E+06	7.63E+06	0.0
45/-45	9.38E+06	9.38E+06	0.0
60/-60	1.32E+07	1.32E+07	0.0
75/-75	1.72E+07	1.72E+07	0.0
90/90	1.88E+07	1.88E+07	0.0

Figure 4—6 illustrates the transverse modulus for un-symmetrical balanced laminates with stacking sequence as $[+\Theta/-\Theta/0/90]_{2T}$. Even though the laminate is balanced for all the cases the results are not identical and for the case of $[90_2/0/90]_{2T}$ the results are in very close range for both methods.

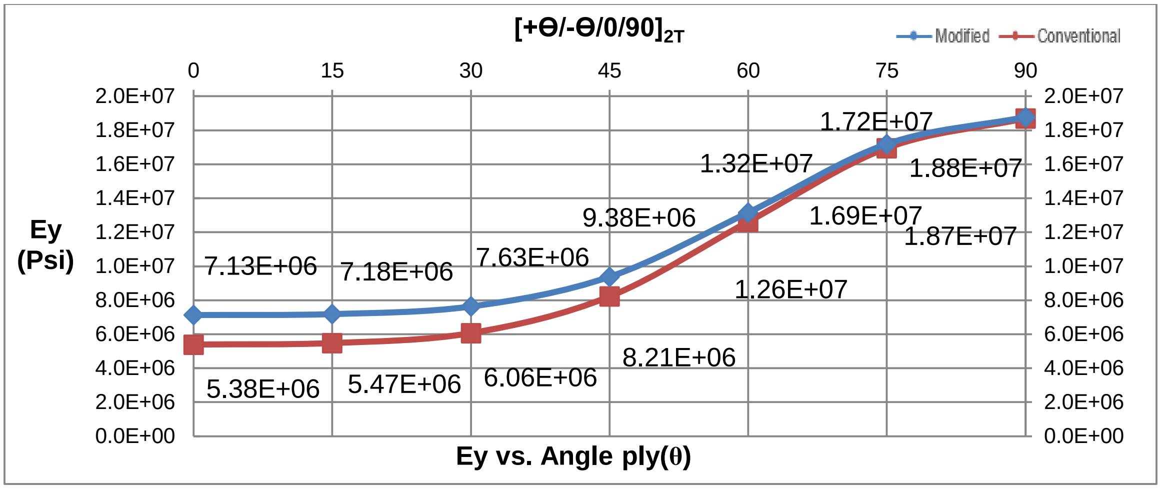

Figure 4—6 Transverse Modulus for $[\Theta/\text{-}\Theta/0/90]_{2T}$

Table 4—6 displays the results from Figure 4—6. As it's displayed in the table for the case of [90/90] the results are very close but rest of cases the percent difference is greater than one.

Table 4—6 Transverse Modulus for $[\Theta/\text{-}\Theta/0/90]_{2T}$

E_y(Psi)			
Θ/-Θ	Modified method	Conventional method	% Difference
0/0	7.13E+06	5.38E+06	24.5
15/-15	7.18E+06	5.47E+06	23.8
30/-30	7.63E+06	6.06E+06	20.6
45/-45	9.38E+06	8.21E+06	12.4
60/-60	1.32E+07	1.26E+07	4.1
75/-75	1.72E+07	1.69E+07	1.4
90/90	1.88E+07	1.87E+07	0.4

Figure 4—7 illustrates the transverse modulus for symmetrical laminates with stacking sequence as $[\theta_2/0/90]_S$. The cases of $[90_2/0/90]_S$ and $[0_2/0/90]_S$ the laminates are balanced and the results are identical but for the rest of cases the laminates are un-balanced and the results are not identical.

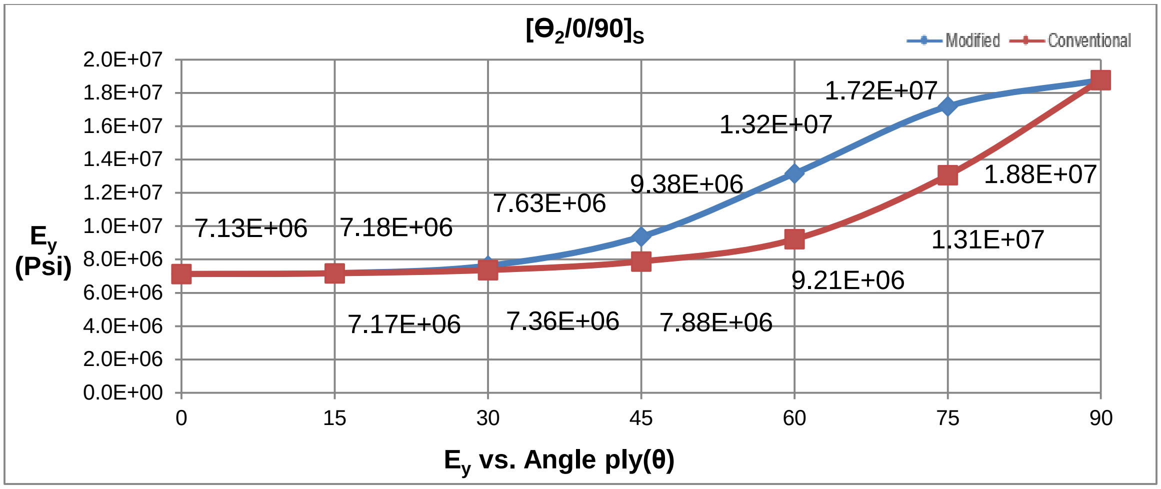

Figure 4—7 Transverse Modulus for $[\theta_2/0/90]_S$

Table 4—7 displays the results from Figure 4—7 As it's shown in the table the only laminates that are balanced are [0/0] and [90/90] with identical results unlike the rest of the laminates that are un-balanced with no identical results. Also the case of [15/15] laminate even though it's an un-balanced laminate but the result is very close only 0.2%.

Table 4—7 Transverse Modulus for $[\theta_2/0/90]_S$

E_y			
Θ/Θ	Modified method	Conventional method	% Difference
0/0	7.13E+06	7.13E+06	0.0
15/15	7.18E+06	7.17E+06	0.2
30/30	7.63E+06	7.36E+06	3.5
45/45	9.38E+06	7.88E+06	16.0
60/60	1.32E+07	9.21E+06	30.0
75/75	1.72E+07	1.31E+07	24.1
90/90	1.88E+07	1.88E+07	0.0

Figure 4—8 illustrates the transverse modulus for un-symmetrical laminates with stacking sequence as $[\theta_2/0/90]_{2T}$. Laminates $[90_2/0/90]_{2T}$ and $[0_2/0/90]_{2T}$ are balanced but only $[90_2/0/90]_{2T}$ has very close results for both methods. The rest of the laminates including the balanced laminate $[0_2/0/90]_{2T}$ have no identical results.

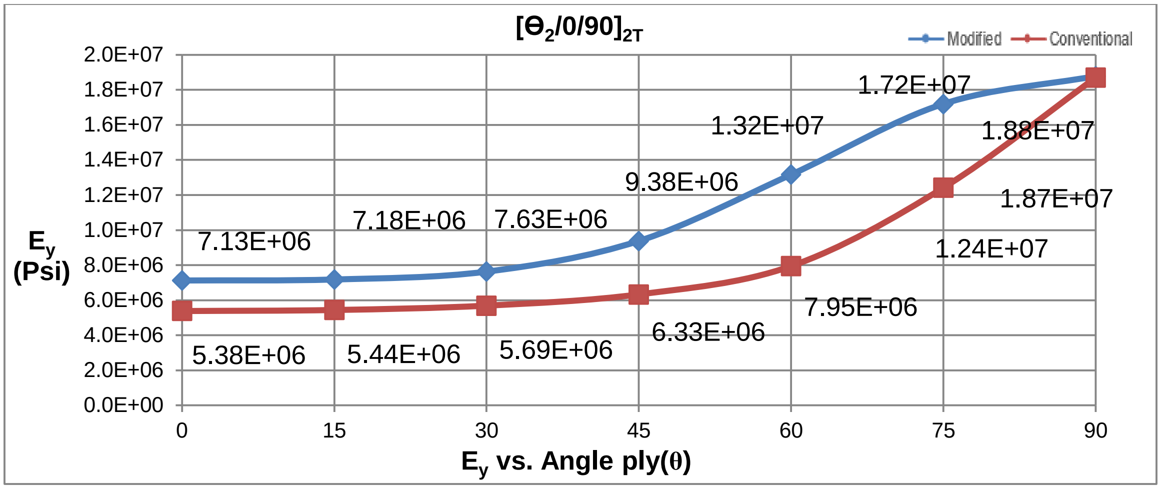

Figure 4—8 Transverse Modulus for $[\theta_2/0/90]_{2T}$

Table 4—8 displays the results from Figure 4—8. As it's shown in the table laminate with [90/90] has very close results 0.4%. Rest of laminates the percent difference is much greater than one percent.

Table 4—8 Transverse Modulus for $[\theta_2/0/90]_{2T}$

E_y(Psi)			
Θ/Θ	Modified method	Conventional method	% Difference
0/0	7.13E+06	5.38E+06	24.5
15/15	7.18E+06	5.44E+06	24.2
30/30	7.63E+06	5.69E+06	25.4
45/45	9.38E+06	6.33E+06	32.5
60/60	1.32E+07	7.95E+06	39.6
75/75	1.72E+07	1.24E+07	27.8
90/90	1.88E+07	1.87E+07	0.4

Figure 4—9 illustrates the shear modulus for un-symmetrical balanced laminates with stacking sequence as $[+\Theta/-\Theta/0/90]_{2T}$. Even though the laminate is balanced for all cases but only laminates $[0_2/0/90]_{2T}$ and $[90_2/0/90]_{2T}$ have identical results for both methods.

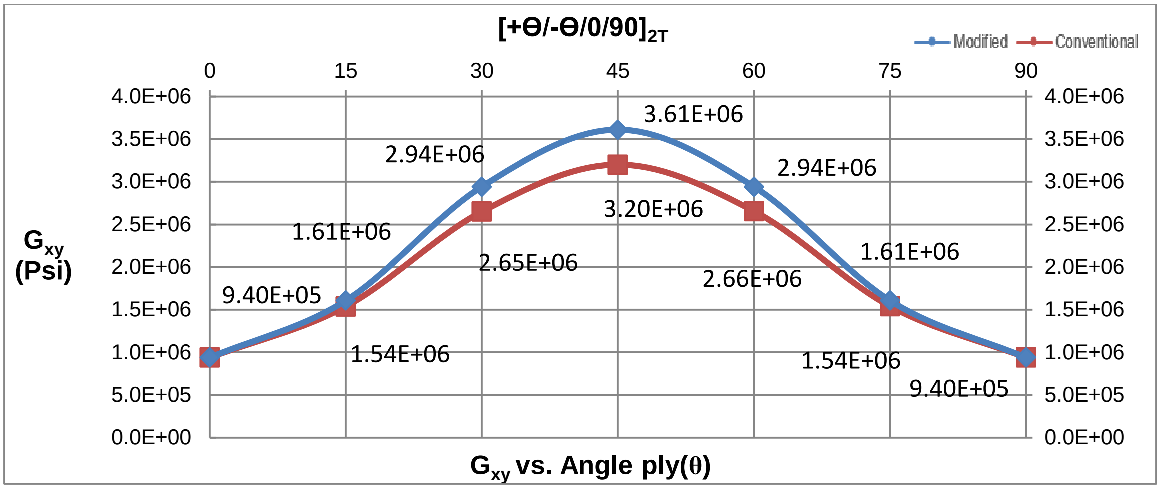

Figure 4—9 Shear Modulus for $[\Theta/-\Theta/0/90]_{2T}$

Table 4—9 shows the results from Figure 4—9. Cases of [0/0] and [90/90] the percent difference is zero but for the rest of the laminates the percent difference is greater than one.

Table 4—9 Shear Modulus for $[\Theta/-\Theta/0/90]_{2T}$

G_{xy}(Psi)			
Ө/-Ө	Modified method	Conventional method	% Difference
0/0	9.40E+05	9.40E+05	0.0
15/-15	1.61E+06	1.54E+06	4.3
30/-30	2.94E+06	2.65E+06	9.9
45/-45	3.61E+06	3.20E+06	11.3
60/-60	2.94E+06	2.66E+06	9.7
75/-75	1.61E+06	1.54E+06	4.1
90/90	9.40E+05	9.40E+05	0.0

Figure 4—10 illustrates the shear modulus for symmetrical balanced laminates with stacking sequence as $[\Theta/-\Theta/0/90]_S$. The results obtained from both methods are identical for all cases.

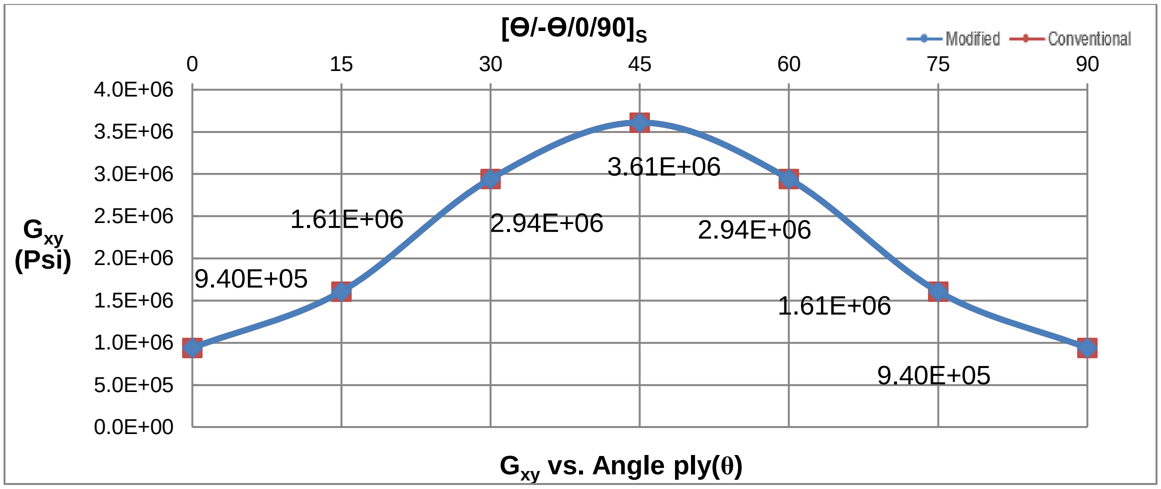

Figure 4—10 Shear Modulus for $[\Theta/\text{-}\Theta/0/90]_S$

Table 4—10 displays the results from Figure 4—10. The percent difference is zero for all of the cases.

Table 4—10 Shear modulus for $[\Theta/\text{-}\Theta/0/90]_S$

G_{xy}(Psi)			
Θ/-Θ	Modified method	Conventional method	% Difference
0/0	9.40E+05	9.40E+05	0.0
15/-15	1.61E+06	1.61E+06	0.0
30/-30	2.94E+06	2.94E+06	0.0
45/-45	3.61E+06	3.61E+06	0.0
60/-60	2.94E+06	2.94E+06	0.0
75/-75	1.61E+06	1.61E+06	0.0
90/90	9.40E+05	9.40E+05	0.0

Figure 4—11 illustrates the shear modulus for un-symmetrical laminates with stacking sequence as $[\theta_2/0/90]_{2T}$. Laminates $[90_2/0/90]_{2T}$ and $[0_2/0/90]_{2T}$ are the only balanced laminates with the identical results obtained from both methods. The rest of the laminates are un-balanced and their results are not identical.

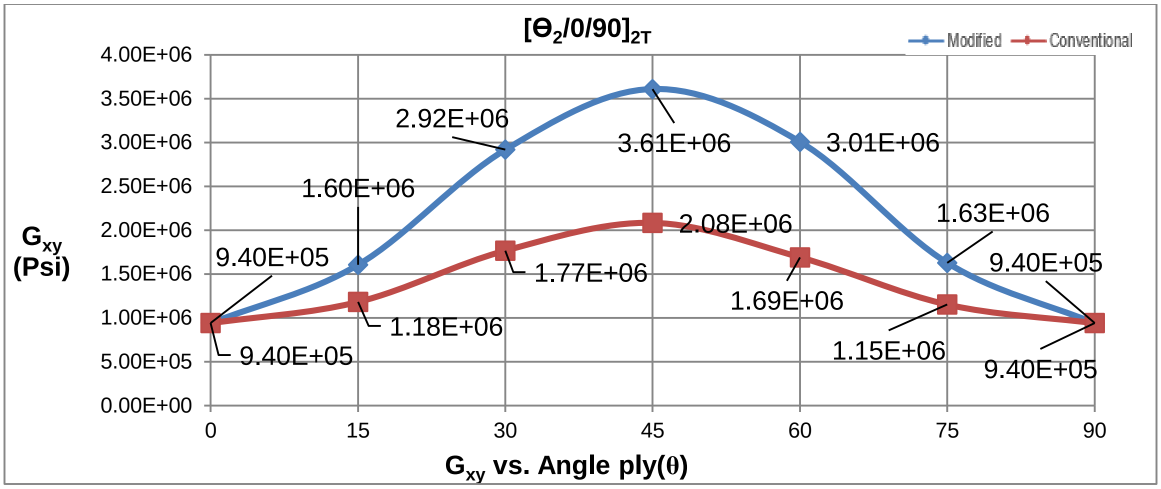

Figure 4—11 Shear Modulus for $[\Theta_2/0/90]_{2T}$

Table 4—11 displays the results for both methods from Figure 4—11. Cases of [0/0] and [90/90] have zero values for the percent difference unlike the rest of the laminates with non-zero values for the percent difference.

Table 4—11 Shear modulus for $[\theta_2/0/90]_{2T}$

G_{xy}(Psi)			
Θ/Θ	Modified method	Conventional method	% Difference
0/0	9.40E+05	9.40E+05	0.0
15/15	1.60E+06	1.18E+06	26.4
30/30	2.92E+06	1.77E+06	39.5
45/45	3.61E+06	2.08E+06	42.3
60/60	3.01E+06	1.69E+06	43.8
75/75	1.63E+06	1.15E+06	29.2
90/90	9.40E+05	9.40E+05	0.0

Figure 4—12 illustrates the shear modulus for symmetrical laminates with stacking sequence as $[\theta_2/0/90]_S$. Laminates $[90_2/0/90]_S$ and $[0_2/0/90]_S$ are the only balanced laminates and their results obtained from both methods are identical. For the rest of the un-balanced laminates the results are not identical.

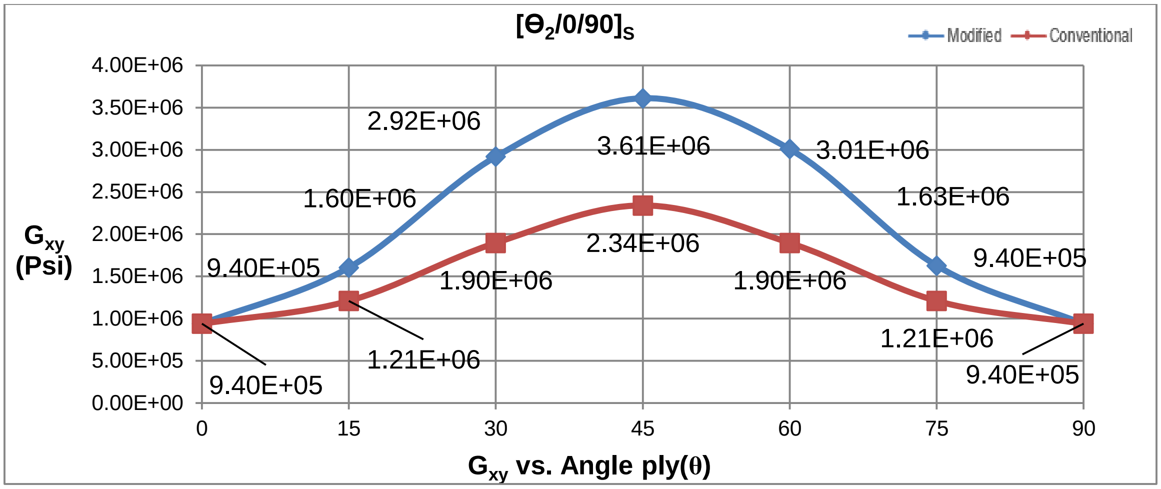

Figure 4—12 Shear Modulus for $[\theta_2/0/90]_S$

Table 4—12 displays the results from Figure 4—12. Laminates $[90_2/0/90]_S$ and $[0_2/0/90]_S$ have zero values for the percent difference unlike the rest of the laminates with non-zero values for the percent difference.

Table 4—12 Shear modulus for $[\theta_2/0/90]_S$

G_{xy}(Psi)			
Θ/Θ	Modified method	Conventional method	% Difference
0/0	9.40E+05	9.40E+05	0.0
15/15	1.60E+06	1.21E+06	24.5
30/30	2.92E+06	1.90E+06	35.0
45/45	3.61E+06	2.34E+06	35.2
60/60	3.01E+06	1.90E+06	36.9
75/75	1.63E+06	1.21E+06	25.6
90/90	9.40E+05	9.40E+05	0.0

Figure 4—13 illustrates the Poisson's ratio for un-symmetrical balanced laminates with stacking sequence as $[\Theta/-\Theta/0/90]_{2T}$. The results obtained from both methods for laminate $[90_2/0/90]$ are in very close range.

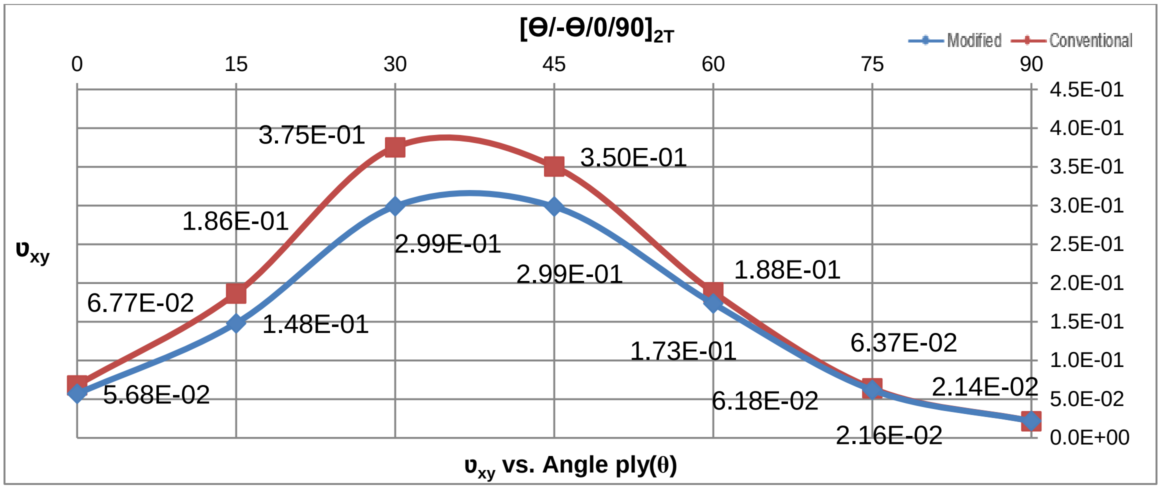

Figure 4—13 Poisson's Ratio for $[\Theta/\text{-}\Theta/0/90]_{2T}$

Table 4—13 displays the results from Figure 4—13. For the case of [90/90] the percent difference is very small as 0.9. For the rest of the laminates the percent differences are much larger.

Table 4—13 Poisson's Ratio for $[\Theta/\text{-}\Theta/0/90]_{2T}$

υ_{xy}			
Θ/-Θ	Modified method	Conventional method	% Difference
0/0	5.68E-02	6.77E-02	16.2
15/-15	1.48E-01	1.86E-01	20.6
30/-30	2.99E-01	3.75E-01	20.3
45/-45	2.99E-01	3.50E-01	14.8
60/-60	1.73E-01	1.88E-01	7.8
75/-75	6.18E-02	6.37E-02	3.0
90/90	2.16E-02	2.14E-02	0.9

Figure 4—14 illustrates the Poisson's ratio for symmetrical balanced laminates with stacking sequence as $[\Theta/\text{-}\Theta/0/90]_S$. The results obtained from both methods are identical for all the laminates.

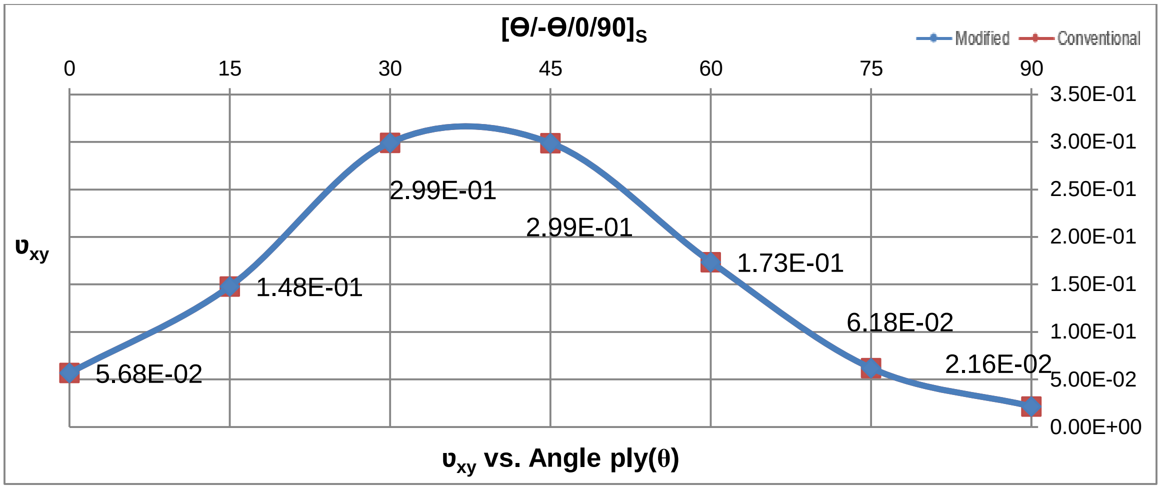

Figure 4—14 Poisson's Ratio for $[\Theta/\text{-}\Theta/0/90]_S$

Table 4—14 displays the results from Figure 4—14. The percent differences for all the laminates are zero.

Table 4—14 Poisson's Ratio for $[\Theta/\text{-}\Theta/0/90]_S$

υ_{xy}			
Ɵ/-Ɵ	Modified method	Conventional method	% Difference
0/0	5.68E-02	5.68E-02	0.0
15/-15	1.48E-01	1.48E-01	0.0
30/-30	2.99E-01	2.99E-01	0.0
45/-45	2.99E-01	2.99E-01	0.0
60/-60	1.73E-01	1.73E-01	0.0
75/-75	6.18E-02	6.18E-02	0.0
90/90	2.16E-02	2.16E-02	0.0

Figure 4—15 illustrates the Poisson's ratio for un-symmetrical laminates with stacking sequence as $[\theta_2/0/90]_{2T}$. Laminates $[90_2/0/90]_{2T}$ and $[0_2/0/90]_{2T}$ are the only balanced laminates for the case of $[\theta_2/0/90]_{2T}$ but $[90_2/0/90]_{2T}$ is the only laminate with the results obtained from both methods are in very close range. The results of the other laminates are not identical.

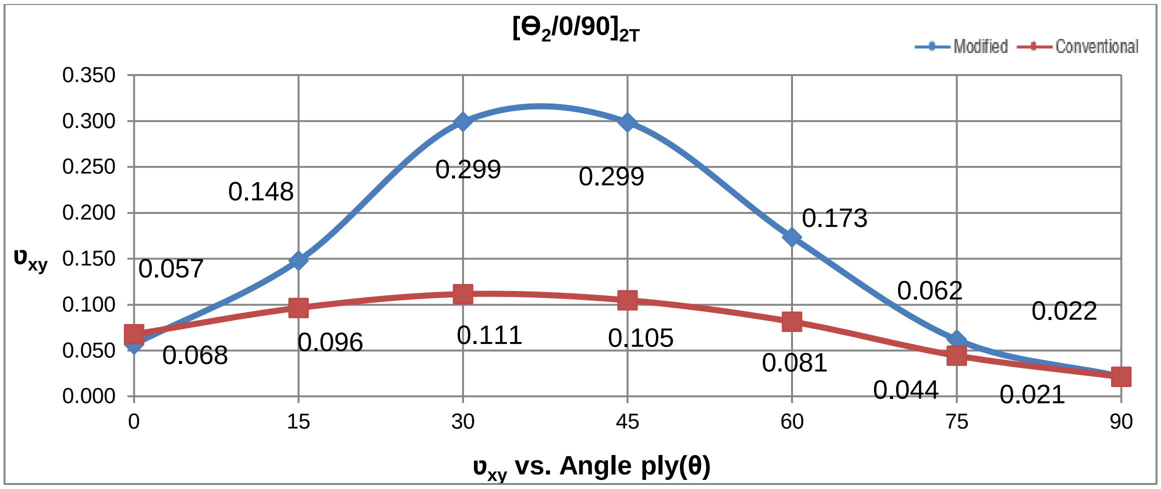

Figure 4—15 Poisson's ratio for $[\theta_2/0/90]_{2T}$

Table 4—15 displays the results from Figure 4—15. For the case of [90/90] the percent difference is very small as 0.9 unlike the rest of the laminates the percent differences are much larger.

Table 4—15 Poisson's Ratio for $[\theta_2/0/90]_{2T}$

υ_{xy}			
Ɵ/Ɵ	Modified method	Conventional method	% Difference
0/0	0.057	0.068	16.2
15/15	0.148	0.096	34.9
30/30	0.299	0.111	62.8
45/45	0.299	0.105	65.0
60/60	0.173	0.081	53.1
75/75	0.062	0.044	28.1
90/90	0.022	0.021	0.9

Figure 4—16 illustrates the Poisson's ratio for symmetrical laminates with stacking sequence as $[\Theta_2/0/90]_S$. Laminates $[90_2/0/90]_S$ and $[0_2/0/90]_S$ are the only balanced laminates with the identical results obtained from both methods. The rest of the laminates are un-balanced with no identical results.

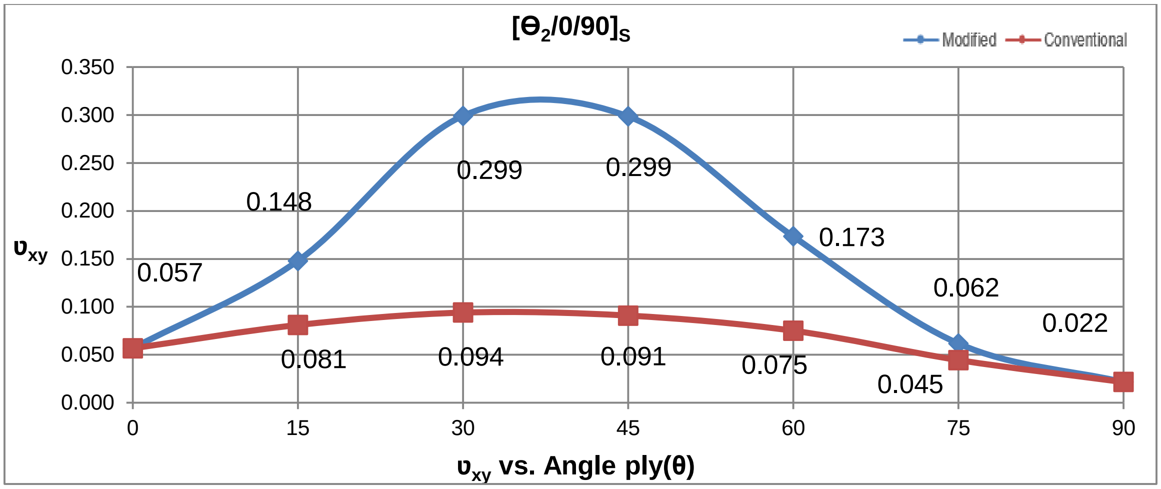

Figure 4—16 Poisson's Ratio for $[\theta_2/0/90]_S$

Table 4—16 displays the results from Figure 4—16. The percent difference for the cases of [0/0] and [90/90] is zero. The rest of the laminates have non-zero values for the percent difference.

Table 4—16 Poisson's ratio for $[\theta_2/0/90]_S$

υ_{xy}			
Θ/Θ	Modified method	Conventional method	% Difference
0/0	5.68E-02	5.68E-02	0.0
15/15	1.48E-01	8.10E-02	45.2
30/30	2.99E-01	9.40E-02	68.6
45/45	2.99E-01	9.09E-02	69.6
60/60	1.73E-01	7.51E-02	56.7
75/75	6.18E-02	4.45E-02	28.0
90/90	2.16E-02	2.16E-02	0.0

Figure 4—17 illustrates the Coefficient of Thermal Expansion for un-symmetrical laminate with stacking sequence as $[\Theta/\text{-}\Theta/0/90]_{2T}$. There is no identical result from both methods for this case.

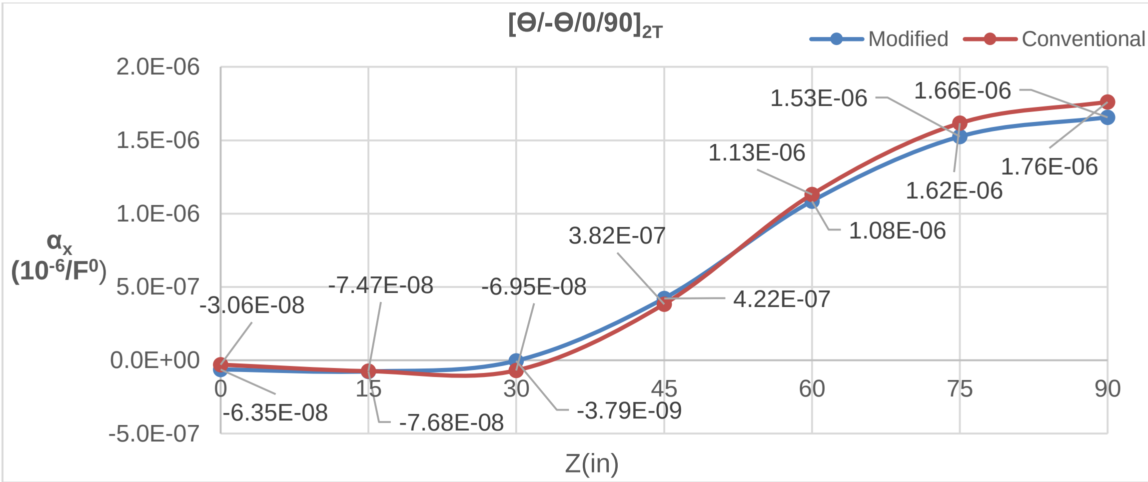

Figure 4—17 Longitudinal Coefficient of Thermal Expansion $[\Theta/\text{-}\Theta/0/90]_{2T}$

Table 4—17 displays the plotted values from Figure 4—17. The percent difference is a none zero value for all the cases.

Table 4—17 Longitudinal Coefficient of Thermal Expansion $[\Theta/\text{-}\Theta/0/90]_{2T}$

$\alpha_x(10^{-6}/F^0)$			
Θ/-Θ	Modified method	Conventional method	% Difference
0/0	-6.35E-08	-3.06E-08	51.8
15/-15	-7.68E-08	-7.47E-08	2.7
30/-30	-3.79E-09	-6.95E-08	94.6
45/-45	4.22E-07	3.82E-07	9.3
60/-60	1.08E-06	1.13E-06	4.1
75/75	1.53E-06	1.62E-06	5.6
90/90	1.66E-06	1.76E-06	6.0

Figure 4—18 illustrates the Coefficient of Thermal Expansion for symmetrical laminate with stacking sequence as $[\Theta/\text{-}\Theta/0/90]_S$. It's a balanced laminate for all the cases. So the results from both methods are identical.

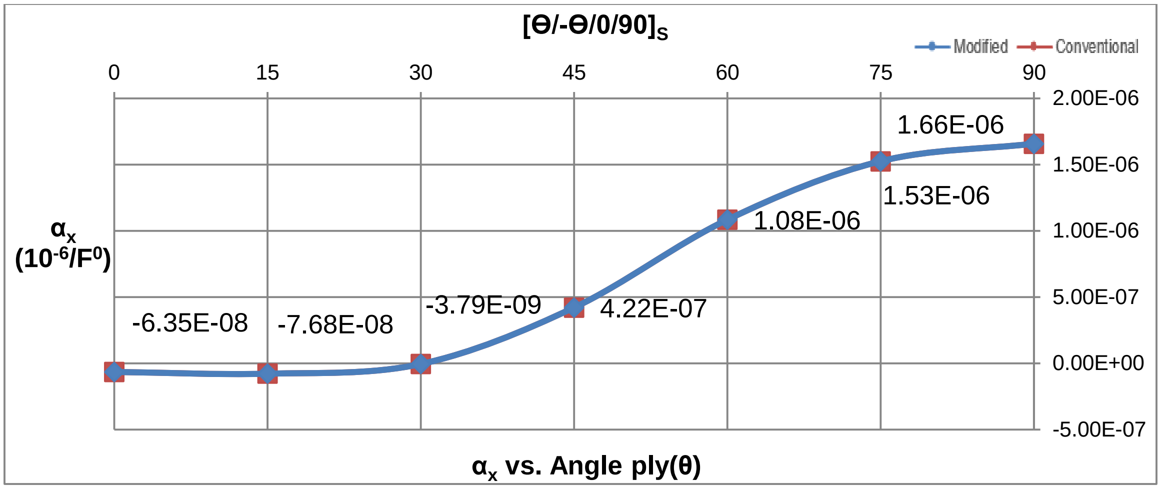

Figure 4—18 Longitudinal Coefficient of Thermal Expansion $[\Theta/-\Theta/0/90]_S$

Table 4—18 displays the results from Figure 4—18. The percent difference is zero for all the cases.

Table 4—18 Longitudinal Coefficient of Thermal Expansion $[\Theta/-\Theta/0/90]_S$

$\alpha_x(10^{-6}/F^0)$			
Ɵ/-Ɵ	Modified method	Conventional method	% Difference
0/0	-6.35E-08	-6.35E-08	0.0
15/-15	-7.68E-08	-7.68E-08	0.0
30/-30	-3.79E-09	-3.79E-09	0.0
45/-45	4.22E-07	4.22E-07	0.0
60/-60	1.08E-06	1.08E-06	0.0
75/-75	1.53E-06	1.53E-06	0.0
90/90	1.66E-06	1.66E-06	0.0

Figure 4—19 illustrates the longitudinal Coefficient of Thermal Expansion for un-symmetrical laminate with stacking sequence as $[\theta_2/0/90]_{2T}$. None of the results are identical obtained from both methods.

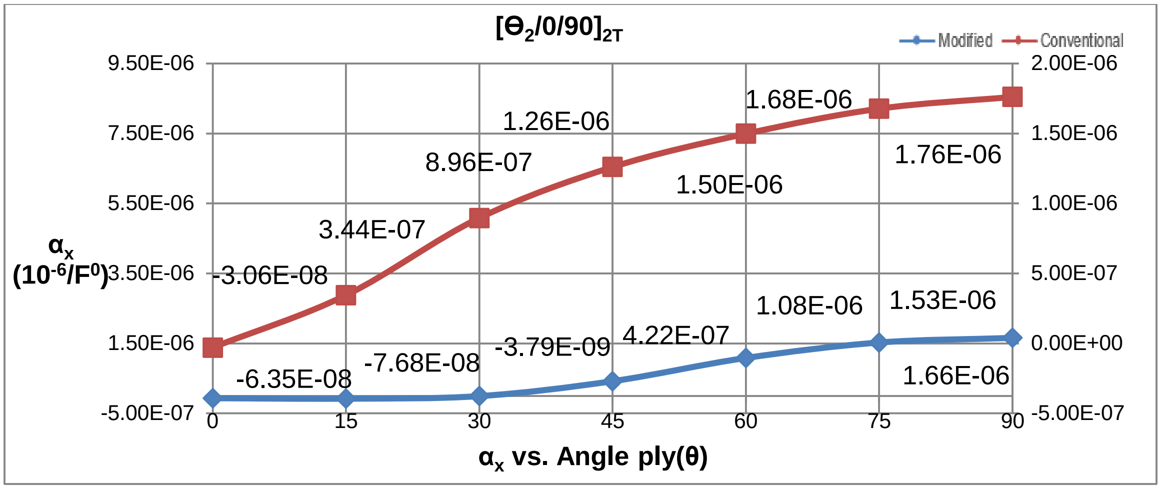

Figure 4—19 Longitudinal Coefficient of Thermal Expansion $[\theta_2/0/90]_{2T}$

Table 4—19 displays the results from Figure 4—19. The percent difference is large for all the cases from both methods.

Table 4—19 Longitudinal Coefficient of Thermal Expansion $[\theta_2/0/90]_{2T}$

$\alpha_x(10^{-6}/F^0)$			
Ө/Ө	Modified method	Conventional method	% Difference
0/0	-6.35E-08	-3.06E-08	51.8
15/15	-7.68E-08	3.44E-07	122.4
30/30	-3.79E-09	8.96E-07	100.4
45/45	4.22E-07	1.26E-06	66.5
60/60	1.08E-06	1.50E-06	27.6
75/75	1.53E-06	1.68E-06	9.1
90/90	1.66E-06	1.76E-06	6.0

Figure 4—20 illustrates the longitudinal Coefficient of Thermal Expansion for symmetrical laminate with stacking sequence as $[\theta_2/0/90]_S$. Only for the cases of 0 and 90 degree the results are identical from both methods and the rest of the cases the results are not identical. Also for the case of 75 degree the results are in very close range.

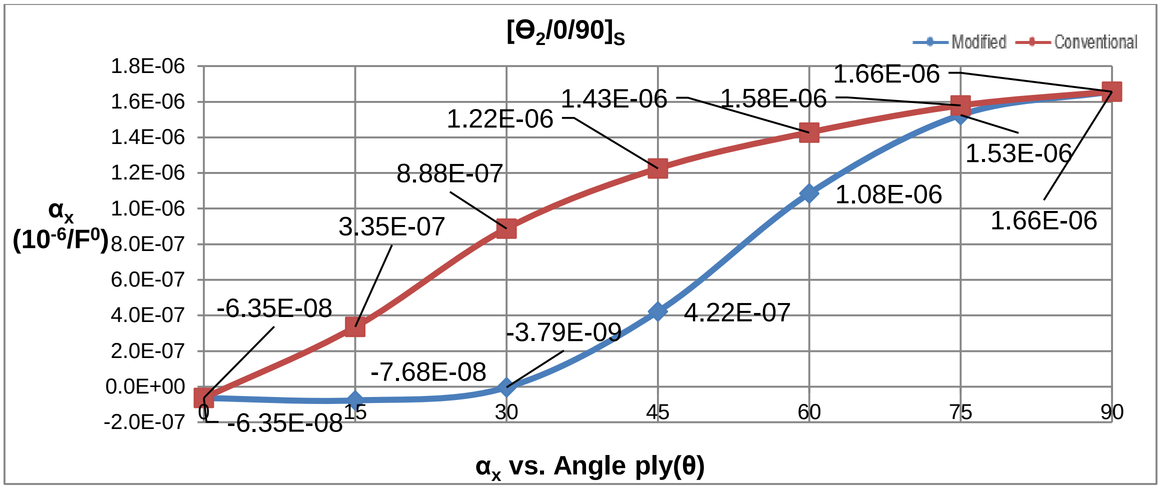

Figure 4—20 Longitudinal Coefficient of Thermal Expansion $[\theta_2/0/90]_S$

Table 4—20 displays the results from Figure 4—20. The percent difference for the cases of 0 and 90 degree is 0 and for the case of 75 degree is very small value.

Table 4—20 Longitudinal Coefficient of Thermal Expansion $[\theta_2/0/90]_S$

$\alpha_x(10^{-6}/F^0)$			
Θ/Θ	Modified method	Conventional method	% Difference
0/0	-6.35E-08	-6.35E-08	0.0
15/15	-7.68E-08	3.35E-07	122.9
30/30	-3.79E-09	8.88E-07	100.4
45/45	4.22E-07	1.22E-06	65.6
60/60	1.08E-06	1.43E-06	24.0
75/75	1.53E-06	1.58E-06	3.4
90/90	1.66E-06	1.66E-06	0.0

Figure 4—21 illustrates the transverse coefficient of thermal expansion for the stacking sequence of $[\Theta/-\Theta/0/90]_{2T}$. The data from both methods is not the same for all the cases.

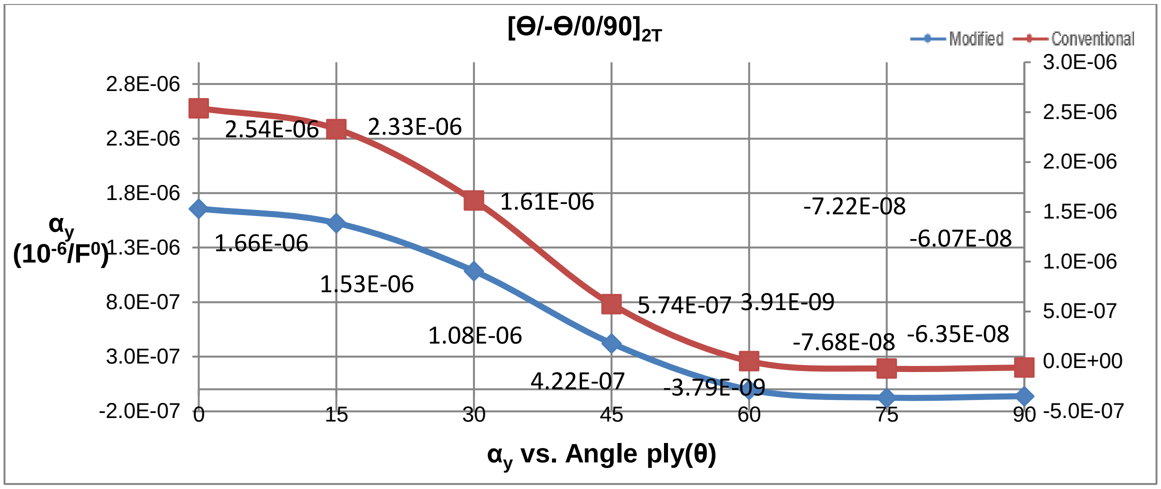

Figure 4—21 Transverse Coefficient of Thermal Expansion [Θ/-Θ/0/90]$_{2T}$

Table 4—21 displays the results from Figure 4—21. The percent difference is none zero value for all the cases. The highest percent difference value is for the case of 60/-60.

Table 4—21 Transverse Coefficient of Thermal Expansion [Θ/-Θ/0/90]$_{2T}$

$\alpha_y(10^{-6}/F^0)$			
Θ/-Θ	Modified method	Conventional method	% Difference
0/0	1.66E-06	2.54E-06	34.8
15/-15	1.53E-06	2.33E-06	34.6
30/-30	1.08E-06	1.61E-06	32.8
45/-45	4.22E-07	5.74E-07	26.5
60/-60	-3.79E-09	3.91E-09	196.8
75/-75	-7.68E-08	-7.22E-08	5.9
90/90	-6.35E-08	-6.07E-08	4.4

Figure 4—22 illustrates the transverse coefficient of thermal expansion for the symmetrical laminates with stacking sequence of [Θ/-Θ/0/90]$_S$. The results obtained from both methods are the same.

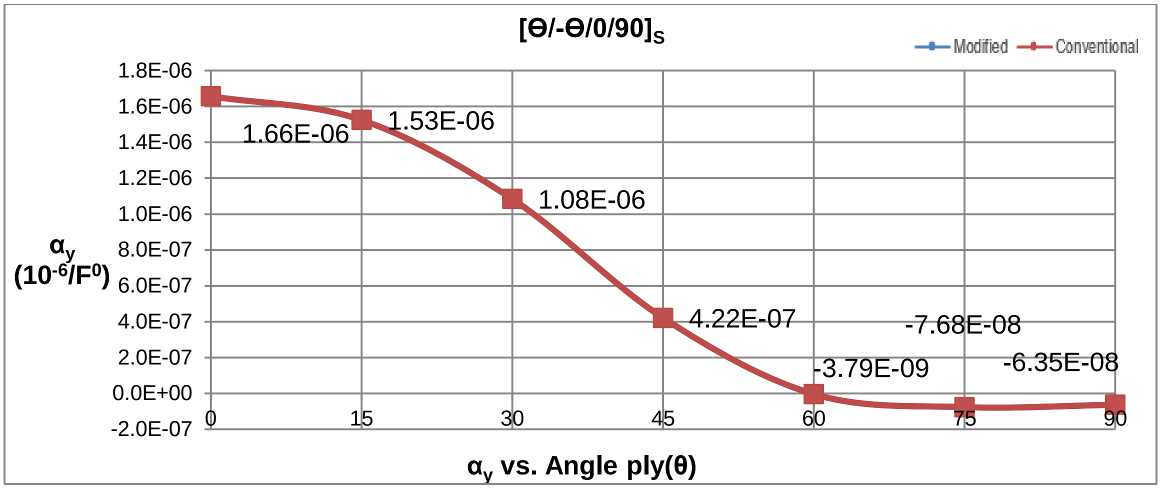

Figure 4—22 Transverse Coefficient of Thermal Expansion [Ө/-Ө/0/90]$_S$

Table 4—22 displays the results from Figure 4—22. For the symmetrical laminate the percent difference for all the cases are zero value.

Table 4—22 Transverse Coefficient of Thermal Expansion [Ө/-Ө/0/90]$_S$

$\alpha_y(10^{-6}/F^0)$			
Ө/-Ө	Modified method	Conventional method	% Difference
0/0	1.66E-06	1.66E-06	0
15/-15	1.53E-06	1.53E-06	0
30/-30	1.08E-06	1.08E-06	0
45/-45	4.22E-07	4.22E-07	0
60/-60	-3.79E-09	-3.79E-09	0
75/-75	-7.68E-08	-7.68E-08	0
90/90	-6.35E-08	-6.35E-08	0

Figure 4—23 illustrates the transverse coefficient of thermal expansion for the un-symmetrical laminates with stacking sequence as [θ_2/0/90]$_{2T}$. None of the results are the same from both methods. The biggest difference is for the case of 75/75.

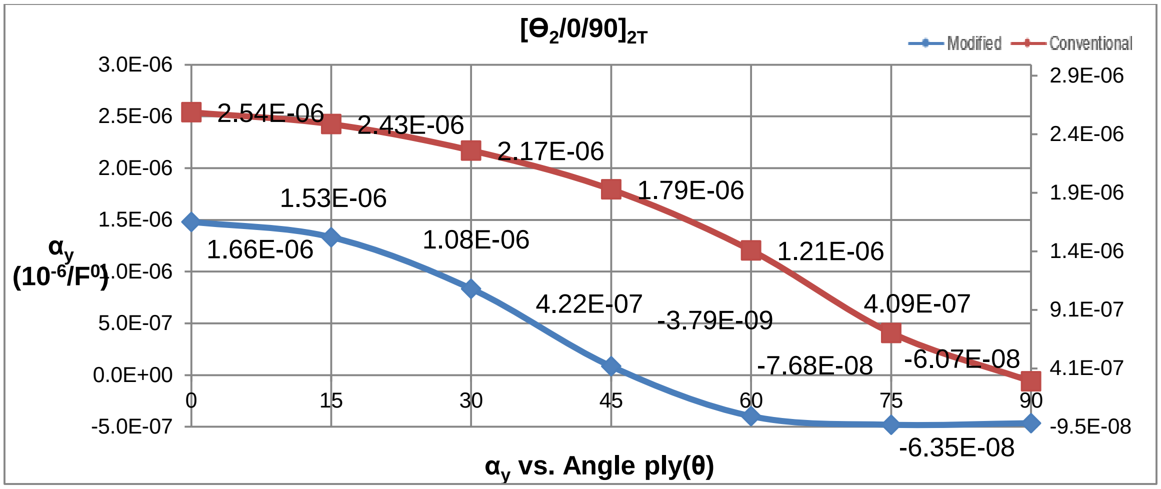

Figure 4—23 Transverse Coefficient of Thermal Expansion $[\theta_2/0/90]_{2T}$

Table 4—23 illustrates the results from Figure 4—23. The percent difference is none zero for all the laminates. The highest value for the percent difference is for the case of 75/75.

Table 4—23 Transverse Coefficient of Thermal Expansion $[\theta_2/0/90]_{2T}$

$\alpha_y(10^{-6}/F^0)$			
Θ/Θ	Modified method	Conventional method	% Difference
0/0	1.66E-06	2.54E-06	34.8
15/15	1.53E-06	2.43E-06	37.1
30/30	1.08E-06	2.17E-06	50.1
45/45	4.22E-07	1.79E-06	76.5
60/60	-3.79E-09	1.21E-06	100.3
75/75	-7.68E-08	4.09E-07	118.8
90/90	-6.35E-08	-6.07E-08	4.4

Figure 4—24 illustrates the transverse coefficient of thermal expansion for the symmetrical laminates with stacking sequence as $[\theta_2/0/90]_S$. The only cases that have the same results are 0/0 and 90/90. For the case of 15/15 the results are in a very close range from both methods.

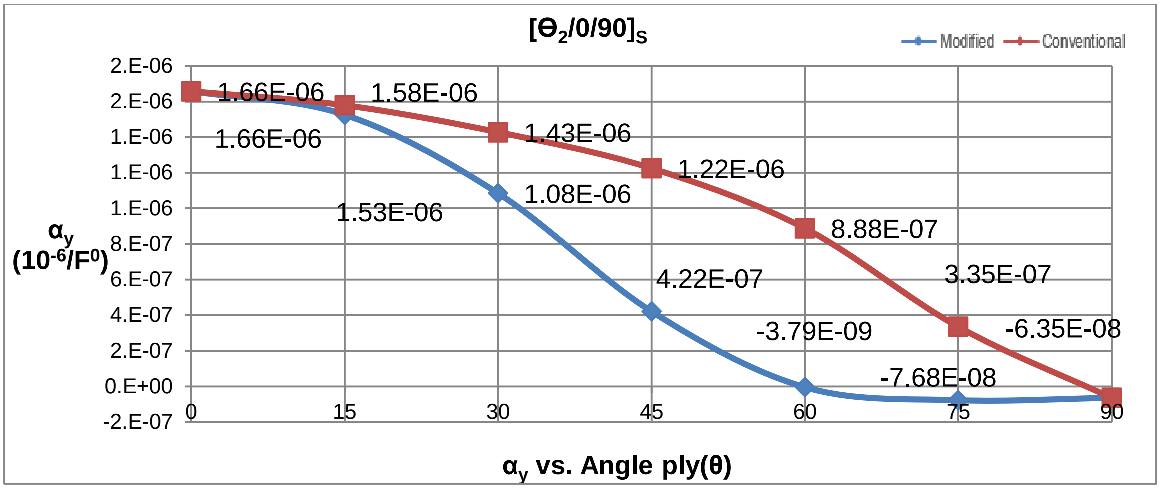

Figure 4—24 Transverse Coefficient of Thermal Expansion $[\theta_2/0/90]_S$

Table 4—24 illustrates the results from Figure 4—24. The percent difference for the case of 0/0 and 90/90 is zero. For the case of 15/15 the percent difference is as small as 3.4%.

Table 4—24 Transverse Coefficient of Thermal Expansion $[\theta_2/0/90]_S$

$\alpha_y(10^{-6}/F^0)$			
Θ/Θ	Modified method	Conventional method	% Difference
0/0	1.66E-06	1.66E-06	0.0
15/15	1.53E-06	1.58E-06	3.4
30/30	1.08E-06	1.43E-06	24.0
45/45	4.22E-07	1.22E-06	65.6
60/60	-3.79E-09	8.88E-07	100.4
75/75	-7.68E-08	3.35E-07	122.9
90/90	-6.35E-08	-6.35E-08	0.0

4.5 Stress analysis of laminate

In the previous sections equivalent properties of laminate were obtained by applying modified method and conventional method. These are the mechanical and thermal properties of a laminate but when it comes to analysis of laminates there is another key factor that plays a very important role in the analysis is the stress of each ply in the laminate. In this section the stress analysis of the laminate using the classical lamination theory is compared against the stress results obtained by employing the modified method and the conventional method.

For the case of an axial load, F_x=1(lb) is applied at the node on the mid-plane of each laminate. For the case of thermal load, ΔT =1(F^0) applied uniform temperature in the desired laminate. The stacking sequences that are considered for the stress analysis are $[45/-45/0/90]_{2T}$, $[45/-45/0/90]_{S}$, $[15/-15/0/90]_{2T,}$ $[15/-15/0/90]_{S}$, $[45_2/0/90]_{2T}$, $[45_2/0/90]_{S}$, and $[15_2/0/90]_{2T}$, $[30/-30/0/90]_{2T}$, and $[30/-30/0/90]_{S}$. For the case of thermal load the stacking sequences considered are $[45/-45/0/90]_{S}$, and $[45/-45/0/90]_{2T}$, and $[30/-30/0/90]_{S}$.

Equation (4.34) is derived in order to calculate the mid plane strain and curvature of the laminate.

$$\binom{\epsilon^0}{\kappa} = \begin{pmatrix} a & b \\ b^T & d \end{pmatrix} \binom{N}{M} \tag{4.36}$$

Recall equations (4.15) and (4.16), by using these two equations the P matrix and the stain mid-plane ca be obtained. Once the strain mid-plane is obtained then strain for each ply can be calculated. For the case of a symmetrical laminate since the [B] matrix is zero, the curvature will not exist. But for an un-symmetrical laminate with curvature, strain for each ply in the desired lumped laminate can be obtained by the following equation (4.35). “h” is the height measured from bottom of the lowest ply, and [k] is the curvature.

$$\epsilon = \epsilon^0 \; + \mathrm{h}\,[\mathrm{k}] \tag{4.37}$$

4.5.1 Ply-by-ply stress results

In ANSYS-APDL, an axial load of 1(lb) applied at a node in mid-plane (centroid) of the desired laminate with boundary conditions for the un-loaded side, all nodes in X-direction are set to zero displacement, nodes along the vertical line through the centroid in the Y-direction are set to zero displacement, and one node at the centroid in Z-direction is set to zero displacement.

For the case of the thermal load, assume temperature difference of $\Delta T=1(F^0)$ with the same boundary conditions as it was conducted for the axial load case.

Figure 4—25 illustrates ply-by-ply stress results for the laminate, subjected to an axial load of 1(lb) which is acting at the node in the mid-plane of the laminate, by employing both methods and also the ply stress for the actual laminate. This figure is for the case of un-symmetrical laminate with stacking sequence as $[45/-45/0/90]_{2T}$.

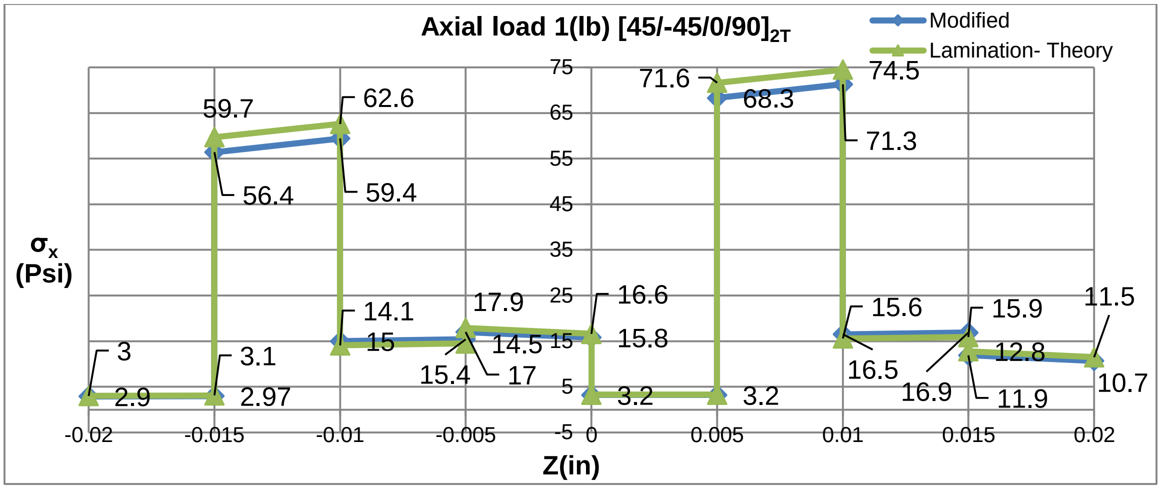

Figure 4—25 Ply-by-ply stress under axial load 1(lb) [45/-45/0/90]$_{2T}$

Table 4—25 displays the stress results obtained from the modified method and the lamination theory.

Table 4—25 Stress results under axial load 1(lb) [45/-45/0/90]$_{2T}$

σ_x(Psi)				
Z(in)	Ply(Θ)	Modified method	% Difference	Lamination theory
0.02	45	10.7	7.0	11.5
0.015	45	11.9	7.0	12.8
0.015	-45	16.9	5.9	15.9
0.01	-45	16.5	5.5	15.6
0.01	0	71.3	4.3	74.5
0.005	0	68.3	4.6	71.6
0.005	90	3.2	3.0	3.3
0	90	3.2	3.0	3.3
0	45	15.8	4.8	16.6
-0.005	45	17	5.0	17.9
-0.005	-45	15.4	5.8	14.5
-0.01	-45	15	6.0	14.1
-0.01	0	59.4	5.1	62.6
-0.015	0	56.4	5.5	59.7
-0.015	90	2.97	4.2	3.1
-0.02	90	2.9	3.3	3

Figure 4—26 illustrates ply-by-ply stress results under axial load of 1(lb), obtained for symmetrical, balanced laminate subjected to an axial load, by employing both methods and also the ply stress results by employing the laminate theory.

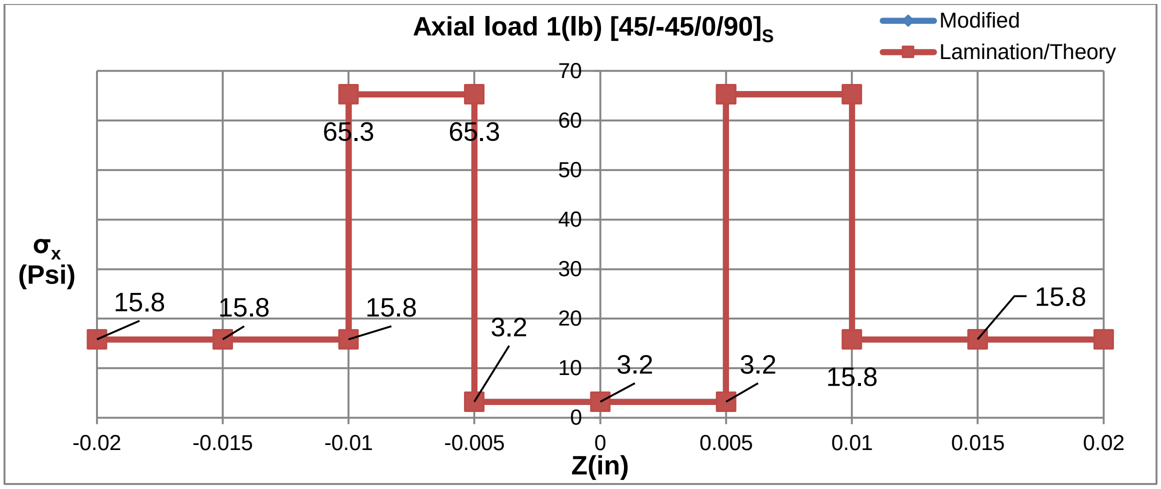

Figure 4—26 Ply-by-ply stress under axial load 1(lb) $[45/-45/0/90]_S$

Table 4—26 displays the results from Figure 4—26. The percent difference is zero for all the cases.

Table 4—26 Stress results under axial load 1(lb) $[45/-45/0/90]_S$

σ_x(psi)				
Z(in)	Ply(Θ)	%Difference	Modified method	Lamination theory
0.02	45	0	15.8	15.8
0.015	-45	0	15.8	15.8
0.01	0	0	65.3	65.3
0.005	90	0	3.2	3.2
-0.005	90	0	3.2	3.2
-0.01	0	0	65.3	65.3
-0.015	-45	0	15.8	15.8
-0.02	45	0	15.8	15.8

Figure 4—27 illustrates ply-by-ply stress under axial load of 1(lb) for the case of the symmetrical, balanced laminate with stacking sequence as: $[15/-15/0/90]_S$ by employing the modified method and the lamination theory. The results gained from both methods are identical.

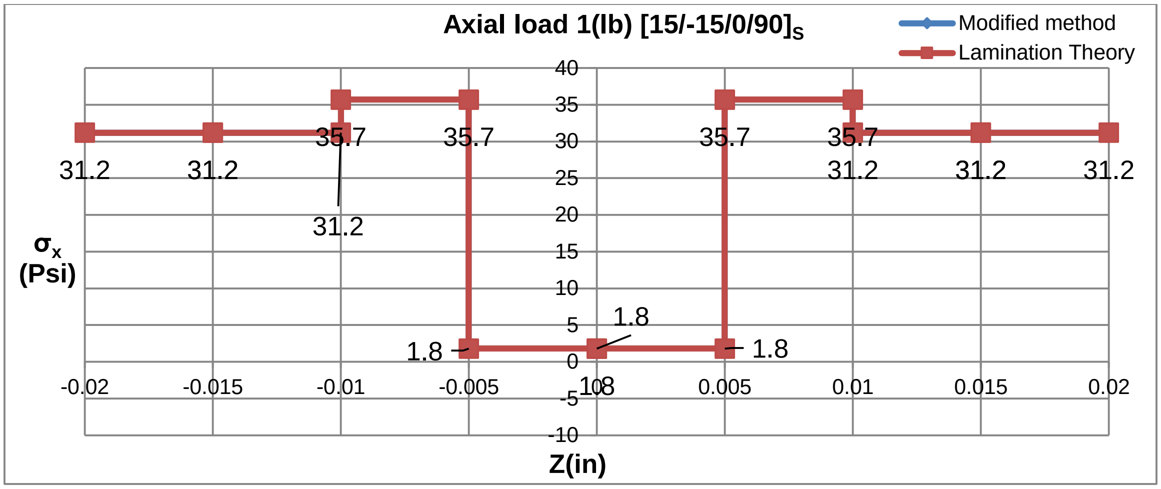

Figure 4—27 Ply-by-ply stress under axial load 1(lb) $[15/-15/0/90]_S$

Table 4—27 displays the stress results from Figure 4—27. The results gained from the modified method and the lamination theory are identical.

Table 4—27 Stress results under axial load 1(lb) $[15/-15/0/90]_S$

σ_x(psi)				
Z(in)	Ply(Θ)	Modified method	% Difference	Lamination theory
0.02	15	31.2	0	31.2
0.015	-15	31.2	0	31.2
0.01	0	35.7	0	35.7
0.005	90	1.8	0	1.8
-0.005	90	1.8	0	1.8
-0.01	0	35.7	0	35.7
-0.015	-15	31.2	0	31.2
-0.02	15	31.2	0	31.2

Figure 4—28 illustrates ply-by-ply stress results under axial load of 1(lb) for the case of the un-symmetrical, balanced laminate with stacking sequence as: $[15/-15/0/90]_{2T}$. Unlike the symmetrical model, the results are not identical. The largest difference is for the case of the 0 degree ply and 15 degree ply.

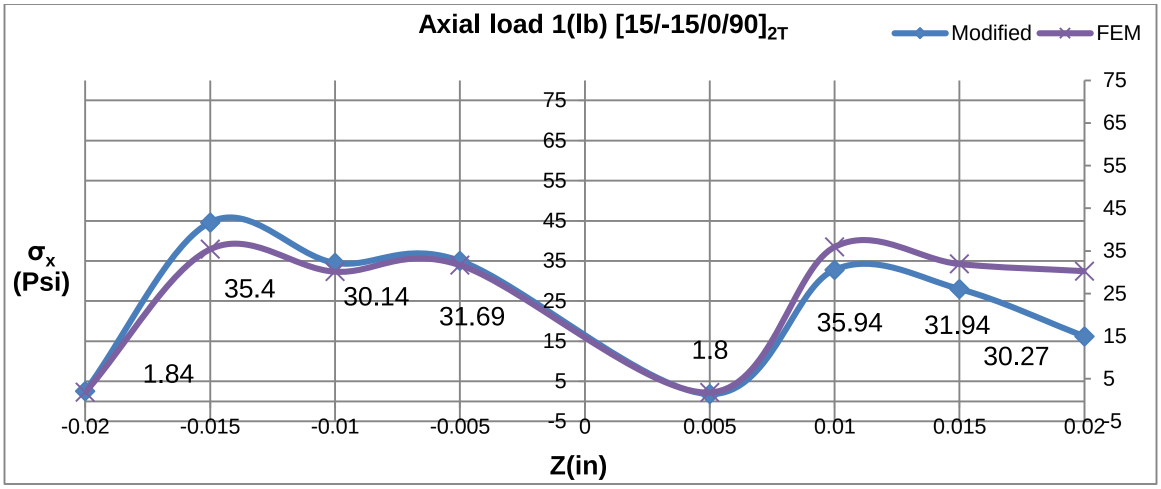

Figure 4—28 Ply-by-ply stress under axial load 1(lb) $[15/-15/0/90]_{2T}$

Table 4—28 displays the results from Figure 4—28. The largest difference between the results is for the 15 and 0 degree plies.

Table 4—28 Stress results under axial load 1(lb) $[15/-15/0/90]_{2T}$

σ_x(psi)				
Z(in)	Ply(Θ)	FEM	%Difference	Modified
0.02	15	30.27	46%	16.2
0.015	-15	31.94	12%	27.98
0.01	0	35.94	8.8%	32.78
0.005	90	1.8	0%	1.8
-0.005	15	31.69	9%	34.98
-0.01	-15	30.14	12.6%	34.48
-0.015	0	35.4	20.6%	44.59
-0.02	90	1.84	27.6%	2.54

Figure 4—29 illustrates ply-by-ply stress under axial load of 1(lb) for un-symmetrical, un-balanced laminate with stacking sequence as $[45_2/0/90]_{2T}$. The stress results gained by employing modified method for plies 45 and 90 degree are in a very close range with the results gained by FEM.

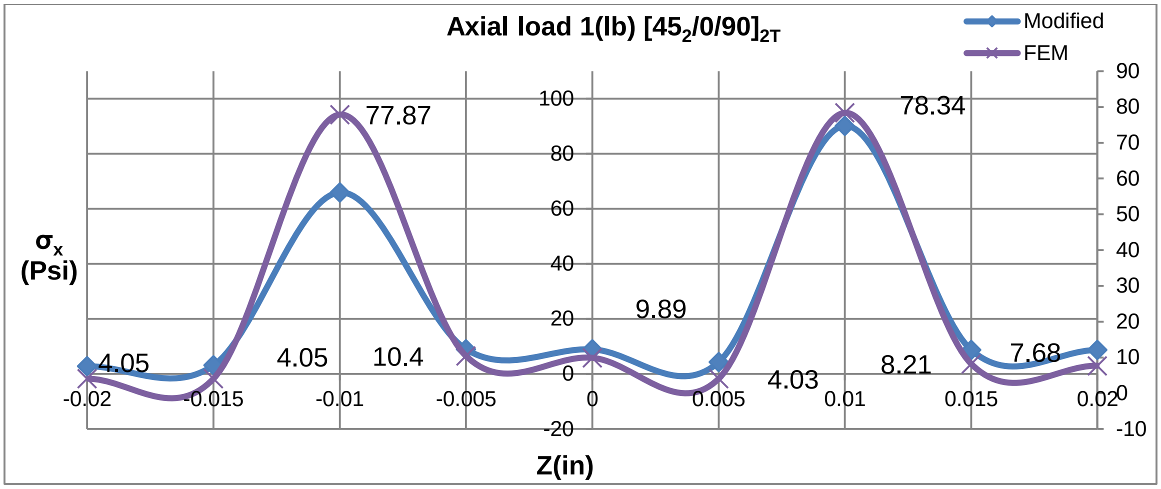

Figure 4—29 Ply-by-ply stress under axial load 1(lb) [45$_2$/0/90]$_{2T}$

Table 4—29 displays the results from Figure 4—29. The largest difference is for the 45 degree plies stress results gained by conventional method compared with the other two stress results.

Table 4—29 Stress results under axial load 1(lb) [45$_2$/0/90]$_{2T}$

σ_x(psi)				
Z(in)	Ply(Θ)	FEM	%Difference	Modified method
0.02	45	7.68	12%	8.73
0.015	45	8.21	6.6%	8.79
0.01	0	78.34	13%	90.13
0.005	90	4.03	7%	4.33
0	45	9.89	9.4%	8.96
-0.005	45	10.4	13.3%	9.02
-0.01	0	77.87	15.3%	65.95
-0.015	90	4.05	22.5%	3.14
-0.02	90	4.05	30%	2.84

Figure 4—30 illustrates ply-by-ply stress under axial load of 1(lb) for symmetrical, un-balanced laminate with stacking sequence as [45$_2$/0/90]$_S$. Stress results gained by employing modified method are identical compared with the results by FEM.

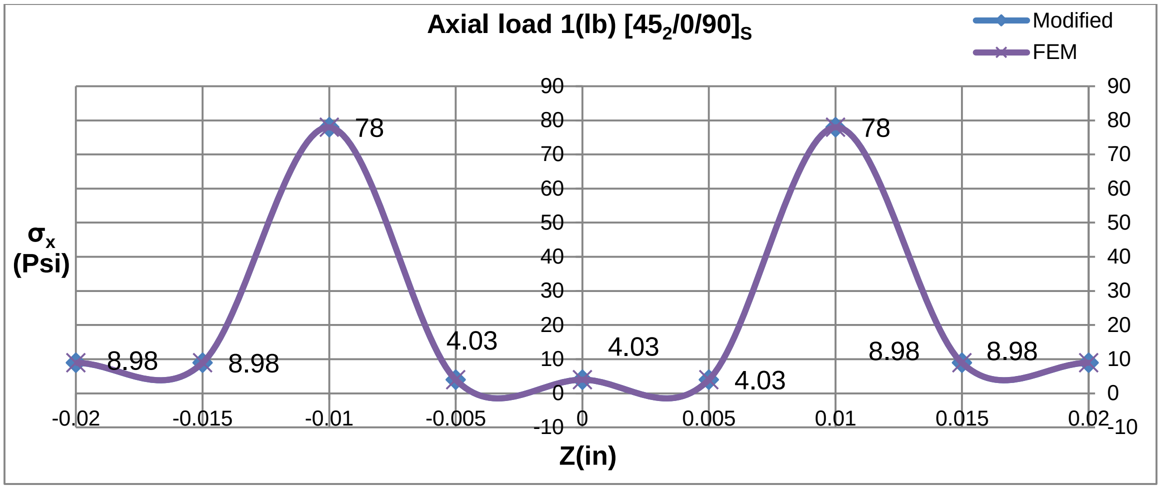

Figure 4—30 Ply-by-ply stress under axial load 1(lb) $[45_2/0/90]_S$

Table 4—30 displays the results from Figure 4—30. As it's displayed in the table, the stress results gained by conventional method have large differences compared with the results from modified method and FEM, for the cases of 45 degree plies.

Table 4—30 Stress results under axial load 1(lb) $[45_2/0/90]_S$

σ_x(psi)				
Z(in)	Ply(Θ)	FEM	%Difference	Modified method
0.02	45	8.98	0.2%	8.96
0.015	45	8.98	0.2%	8.96
0.01	0	78	0%	78
0.005	90	4.03	0%	4.03
-0.005	90	4.03	0%	4.03
-0.01	0	78	0%	78
-0.015	45	8.98	0.2%	8.96
-0.02	45	8.98	0.2%	8.96

Figure 4—31 illustrates ply-by-ply stress under axial load of 1(lb) for un-symmetrical, un-balanced laminate with stacking sequence as $[15_2/0/90]_{2T}$. It includes the stress results obtained from ANSYS. Conventional method stress result for the case of the 15 degree ply has a large difference compared with the actual data results and modified method results.

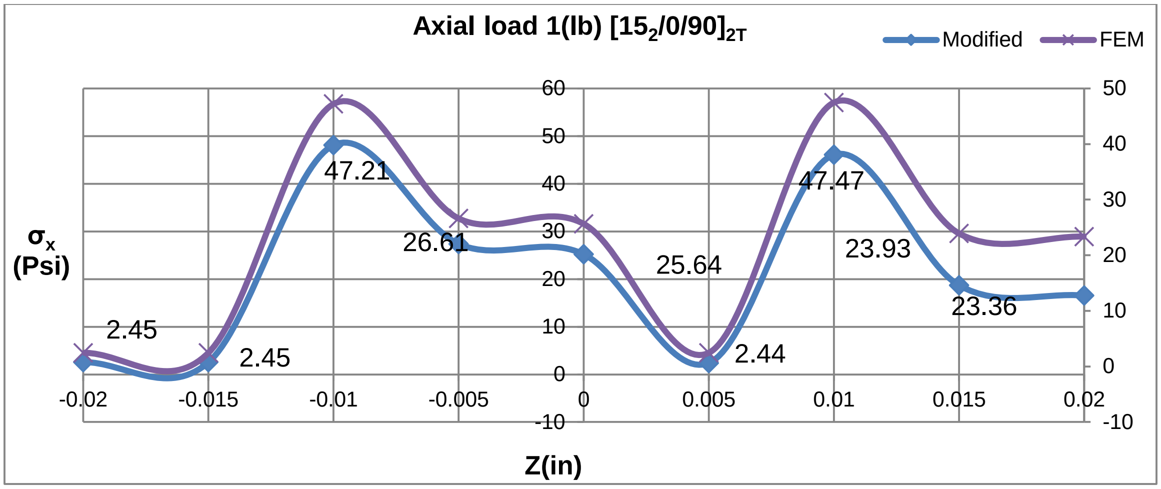

Figure 4—31 Ply-by-ply stress results under axial load 1(lb) [15$_2$/0/90]$_{2T}$

Table 4—31 displays the results from Figure 4—31. The stress results obtained from modified method are in closer range to the actual results (lamination theory) compared with conventional method. Conventional method has the largest difference for the stress results for the case of the 15 degree ply compared with the results from modified method and the actual results.

Table 4—31 Stress results under axial load 1(lb) [15$_2$/0/90]$_{2T}$

σ_x(psi)				
Z(in)	Ply(Θ)	FEM	%Difference	Modified method
0.02	15	23.36	29%	16.56
0.015	15	23.93	22%	18.73
0.01	0	47.47	3%	46.1
0.005	90	2.44	1.6%	2.4
0	15	25.64	1.6%	25.22
-0.005	15	26.61	2.8%	27.39
-0.01	0	47.21	2%	48.12
-0.015	90	2.45	5.8%	2.6
-0.02	90	2.45	5.8%	2.6

Figure 4—32 illustrates ply-by-ply stress under axial load of 1(lb) for un-symmetrical, balanced laminate with stacking sequence as [30/-30/0/90]$_{2T}$.

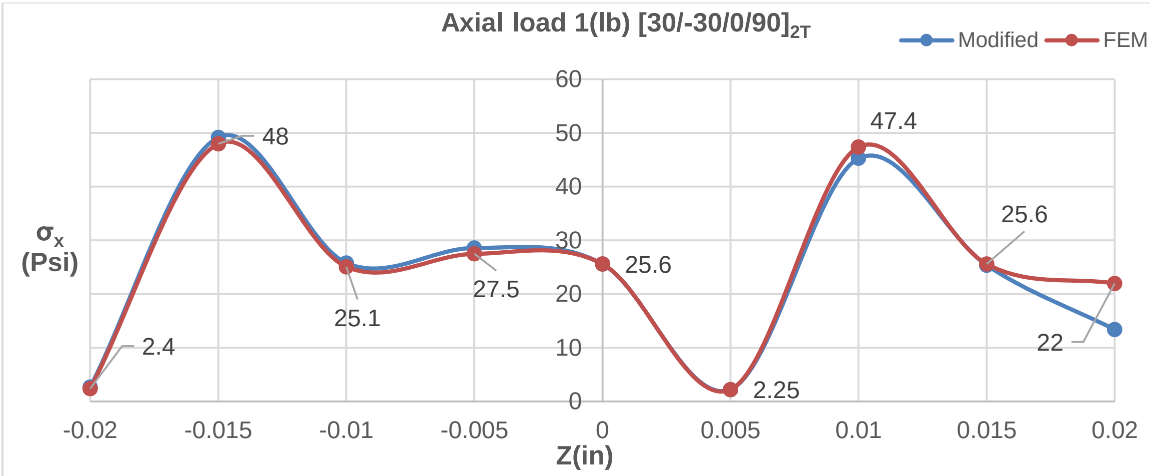

Figure 4—32 Ply-by-ply stress under axial load 1(lb) $[30/-30/0/90]_{2T}$

Table 4—32 displays the results from Figure 4—32.

Table 4—32 Stress results under axial load 1(lb) $[30/-30/0/90]_{2T}$

σ_x(psi)				
Z(in)	Ply(ϴ)	FEM	%Difference	Modified method
0.02	30	22	39%	13.4
0.015	-30	25.6	0.8%	25.4
0.01	0	47.4	4.4%	45.3
0.005	90	2.25	0%	2.25
-0.005	30	27.5	3.8%	28.6
-0.01	-30	25.1	2.7%	25.8
-0.015	0	48	2.4%	49.2
-0.02	90	2.4	11%	2.7

Figure 4—33 Illustrates ply-by-ply stress under axial load of 1(lb) for symmetrical, balanced laminate with stacking sequence as $[30/-30/0/90]_S$. Unlike conventional method, the stress results obtained from modified method are in a very close range with FEM results.

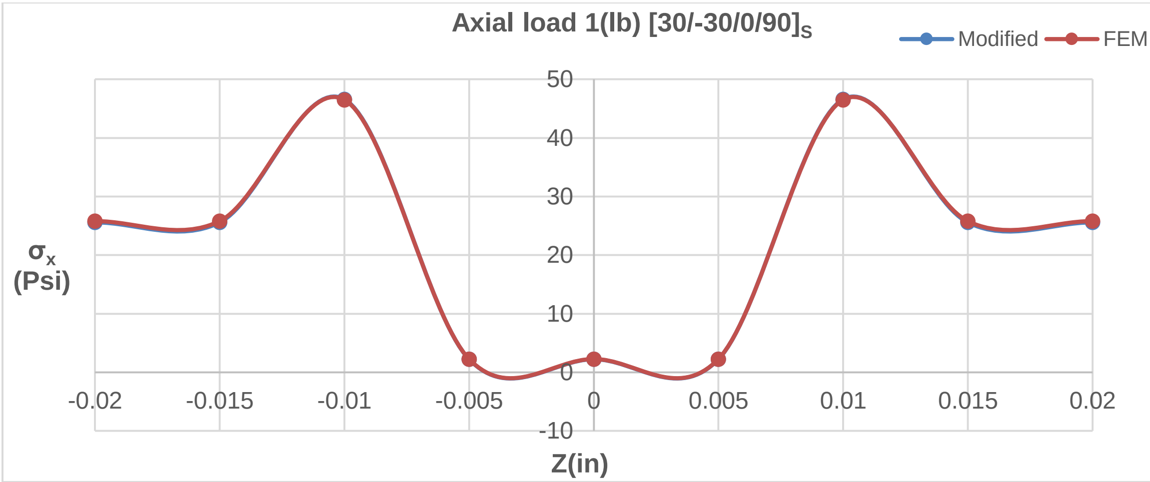

Figure 4—33 Ply-by-ply stress under axial load 1(lb) [30/-30/0/90]$_S$

Table 4—33 displays the results from Figure 4—33. The stress results obtained by modified method are almost identical to those obtained from FEM.

Table 4—33 Stress results under axial load 1(lb) [30/-30/0/90]$_S$

σ_x(psi)				
Z(in)	Ply(Θ)	FEM	%Difference	Modified method
0.02	30	25.8	0.8%	25.6
0.015	-30	25.8	0.8%	25.6
0.01	0	46.5	0.21%	46.6
0.005	90	2.26	0.44%	2.25
-0.005	90	2.26	0.44%	2.25
-0.01	0	46.5	0.21%	46.6
-0.015	-30	25.8	0.8%	25.6
-0.02	30	25.8	0.8%	25.6

Figure 4—34 illustrates ply-by-ply normal stress induced by the thermal load due to the temperature difference of $\Delta T=1(F^0)$ for the symmetrical, balanced laminate with stacking sequence as [45/-45/0/90]$_S$. The results obtained from modified method are identical with the stress results by FEM and the lamination theory. But the stress results gained from conventional method are not identical compare with the results gained from the lamination theory and FEM.

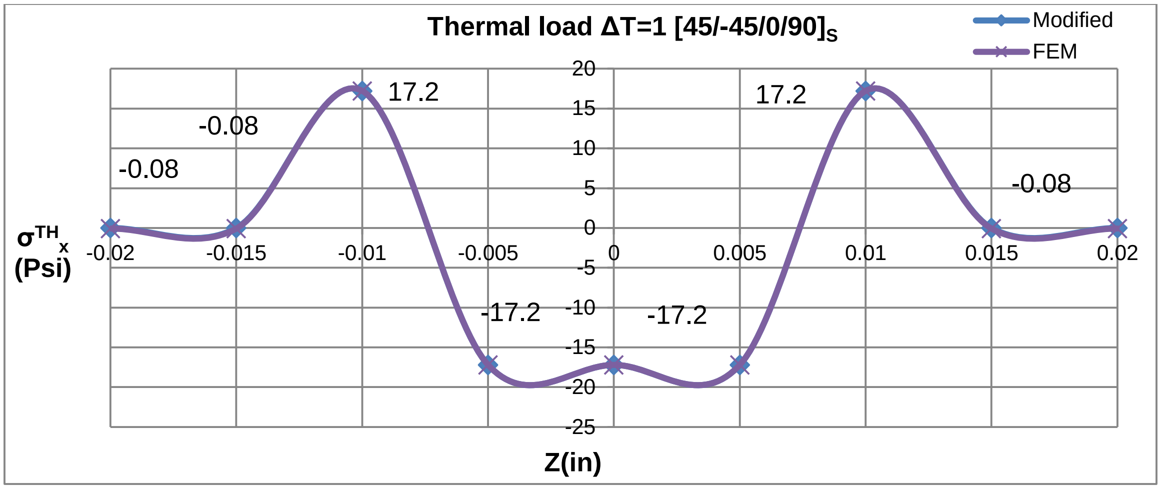

Figure 4—34 Ply-by-ply stress, σ_x^{TH} [45/-45/0/90]$_S$

Table 4—34 displays the stress results from Figure 4—34, plus it includes the thermal stress results obtained by employing FEM.

Table 4—34 Stress results, σ_x^{TH} [45/-45/0/90]$_S$

σ_x^{TH}(psi)				
Z(in)	Ply(Θ)	FEM	%Difference	Modified method
0.02	45	-0.08	0%	0
0.015	-45	-0.08	0%	0
0.01	0	17.2	0%	17.2
0.005	90	-17.2	0%	-17.2
-0.005	90	-17.2	0%	-17.2
-0.01	0	17.2	0%	17.2
-0.015	-45	-0.08	0%	0
-0.02	45	-0.08	0%	0

Figure 4—35 illustrates ply-by-ply shear stress induced by the thermal load due to the temperature difference as ΔT=1(F^0). The stress results gained from modified method are identical with FEM.

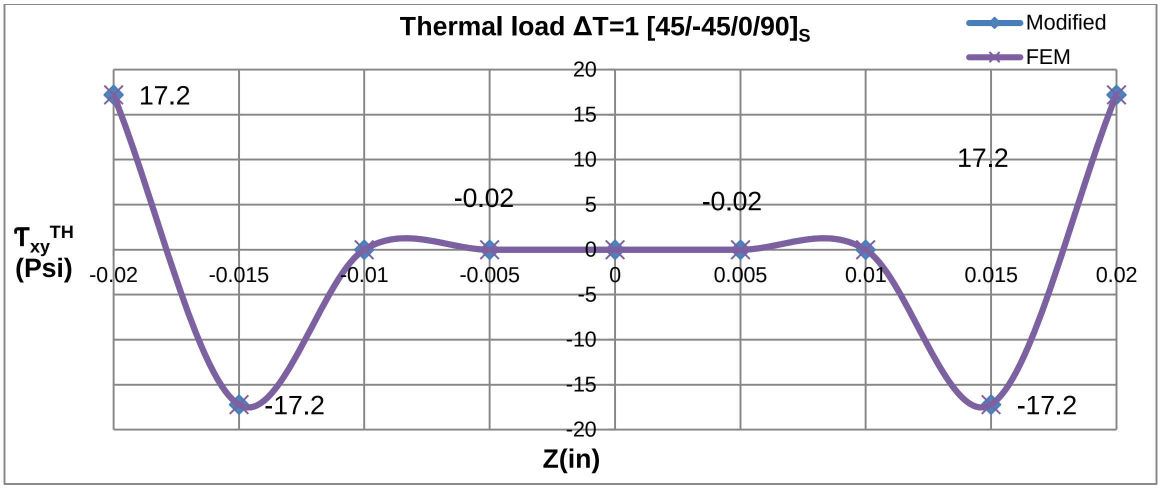

Figure 4—35 Ply-by ply Shear stress, τ_{xy}^{TH} [45/-45/0/90]s

Table 4—35 displays the results from Figure 4—35, including the stress results from FEM.

Table 4—35 Shear stress results, τ_{xy}^{TH} [45/-45/0/90]s

τ_{xy}^{TH}(psi)				
Z(in)	Ply(Θ)	FEM	%Difference	Modified method
0.02	45	17.2	0%	17.2
0.015	-45	-17.2	0%	-17.2
0.01	0	-0.02	0%	0
0.005	90	-0.02	0%	0
-0.005	90	-0.02	0%	0
-0.01	0	-0.02	0%	0
-0.015	-45	-17.2	0%	-17.2
-0.02	45	17.2	0%	17.2

Figure 4—36 illustrates ply-by-ply normal stress induced by thermal load due to the temperature difference of ΔT=1(F^0) for the symmetrical, balanced laminate with stacking sequence as [30/-30/0/90]s. The stress results for all the methods are identical to the FEM results.

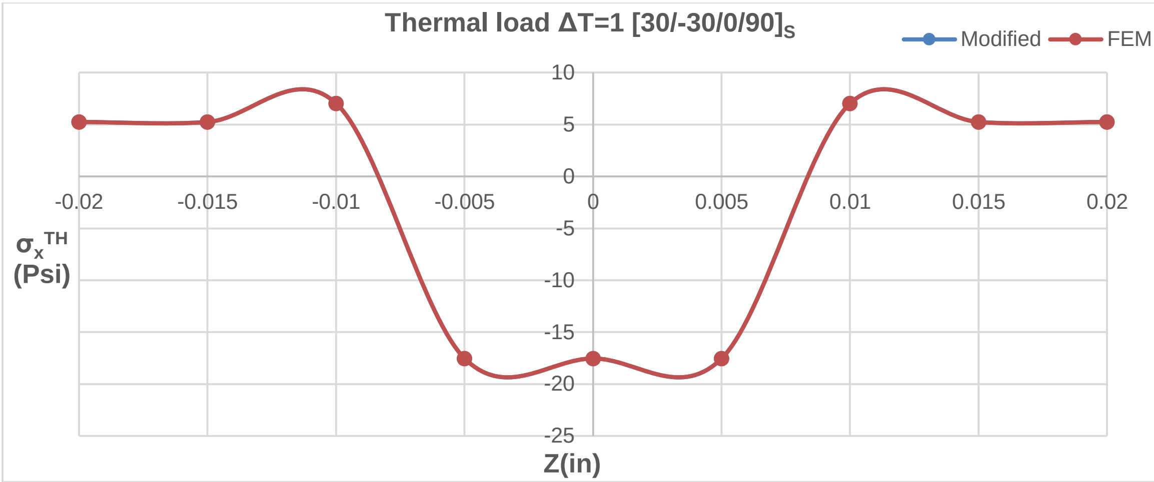

Figure 4—36 Ply-by ply Normal stress, σ_x^{TH} $[30/-30/0/90]_S$

Table 4—36 displays the results from Figure 4—36. The stress results obtained are identical to those results from FEM except for 30 and -30 plies which the percent difference is only 0.2%.

Table 4—36 Normal stress results, σ_x^{TH} $[30/-30/0/90]_S$

σ_x^{TH}(psi)				
Z(in)	Ply(Θ)	FEM	%Difference	Modified method
0.02	30	5.24	0.2%	5.25
0.015	-30	5.24	0.2%	5.25
0.01	0	7.03	0%	7.03
0.005	90	-17.53	0%	-17.53
-0.005	90	-17.53	0%	-17.53
-0.01	0	7.03	0%	7.03
-0.015	-30	5.24	0.2%	5.25
-0.02	30	5.24	0.2%	5.25

Figure 4—37 illustrates ply-by-play shear stress induced by thermal load due to the temperature difference of ΔT =1(F^0) for the symmetrical, balanced laminate with stacking sequence as $[30/-30/0/90]_S$. The stress results obtained by modified method are identical with the stress results from FEM.

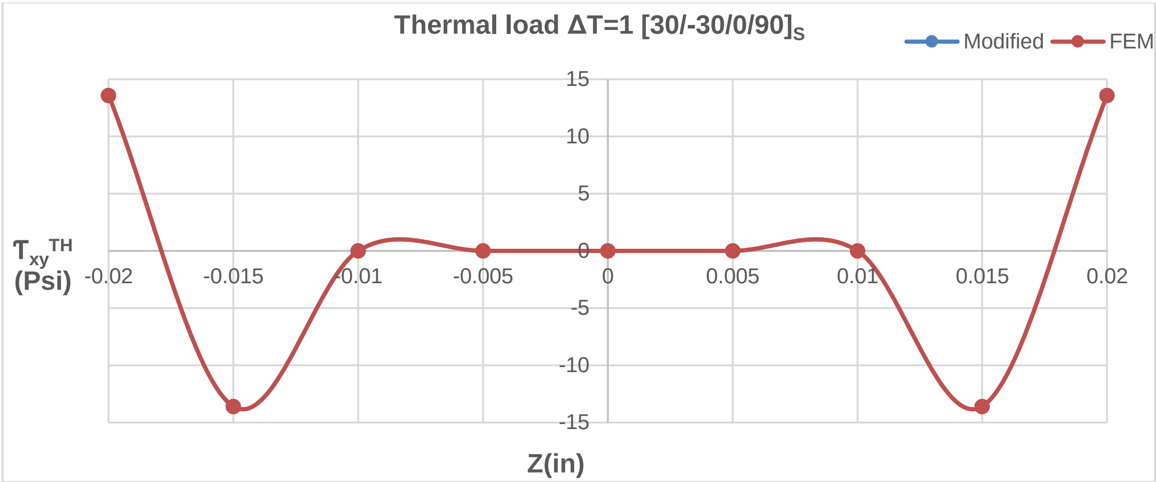

Figure 4—37 Ply-by ply Shear stress, τ_{xy}^{TH} $[30/-30/0/90]_S$

Table 4—37 displays the results from Figure 4—37. The stress results obtained are identical to the results obtained by FEM.

Table 4—37 Shear stress results, τ_{xy}^{TH} $[30/-30/0/90]_S$

τ_{xy}^{TH}(psi)				
Z(in)	Ply(Θ)	FEM	%Difference	Modified method
0.02	30	13.6	0%	13.6
0.015	-30	-13.6	0%	-13.6
0.01	0	0.0003	0%	0
0.005	90	0.0003	0%	0
-0.005	90	0.0003	0%	0
-0.01	0	-13.6	0%	-13.6
-0.015	-30	13.6	0%	13.6
-0.02	30	13.6	0%	13.6

Figure 4—38 illustrates ply-by-ply normal stress induced by thermal load due to the temperature difference of 1(F^0) in the un-symmetrical, balanced laminate with stacking sequence as $[45/-45/0/90]_{2T}$.

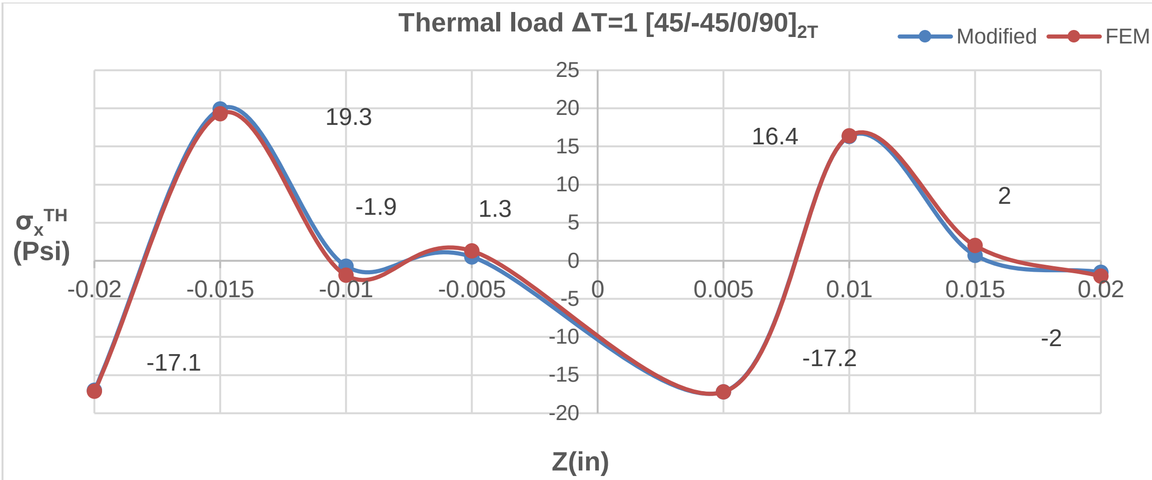

Figure 4—38 Ply-by-ply Normal stress, σ_x^{TH} [45/-45/0/90]$_{2T}$

Table 4—38 displays the results from Figure 4—38.

Table 4—38 Normal stress results, σ_x^{TH} [45/-45/0/90]$_{2T}$

σ_x^{TH}(psi)				
Z(in)	Ply(Ө)	FEM	%Difference	Modified method
0.02	45	-2	25%	-1.5
0.015	-45	2	64%	0.72
0.01	0	16.4	0.61%	16.3
0.005	90	-17.2	0%	-17.2
-0.005	45	1.3	61.5%	0.5
-0.01	-45	-1.9	62%	-0.72
-0.015	0	19.3	3%	19.9
-0.02	90	-17.1	0.58%	-17

Figure below illustrates ply-by-ply normal stress induced by thermal load due to the temperature difference of 1(F^0) in the un-symmetrical, un-balanced laminate with stacking sequence as [15$_2$/0/90]$_{2T}$.

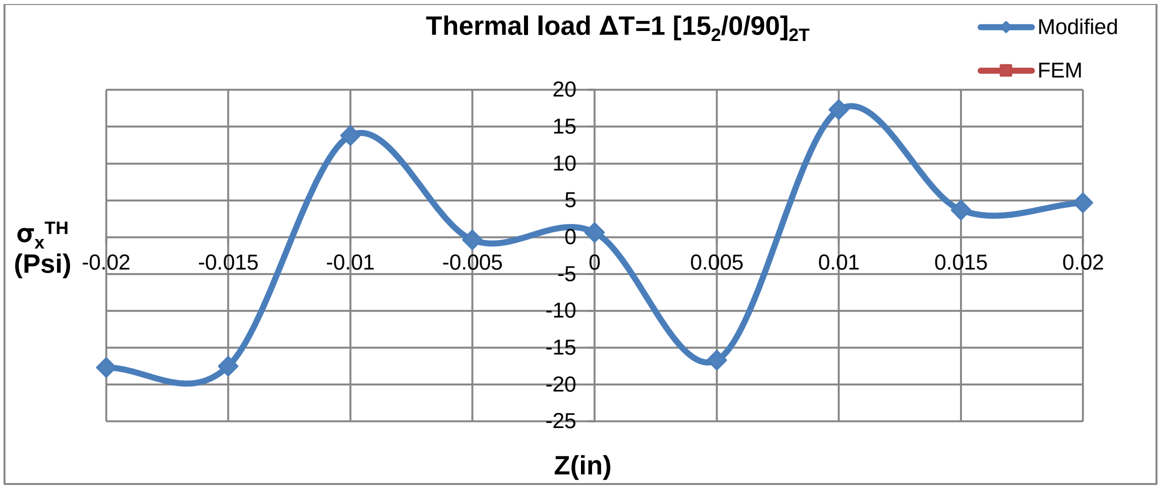

Figure 4—39 Ply-by-ply Normal stress, σxTH [152/0/90]2T

The table below displays the stress results obtained by modified method are in closer range to the results obtained by FEM in comparing them with conventional method's results.

Table 4—39 Normal stress results, σxTH [152/0/90]2T

σ_x^{TH}(psi)				
Z(in)	Ply(Θ)	FEM	%Difference	Modified method
0.02	15	4.6	2%	4.7
0.015	15	3.8	2.6%	3.7
0.01	0	17.3	0%	17.3
0.005	90	-16.7	0%	-16.7
-0.005	15	0.62	4.6%	0.65
-0.01	15	-0.28	20%	-0.35
-0.015	0	13.8	0%	13.8
-0.02	90	-17.5	0%	-17.5

The figure below illustrates ply-by-ply shear stress induced by thermal load due to the temperature difference of 1(F^0) in the un-symmetrical, un-balanced laminate with stacking sequence as [15$_2$/0/90]$_{2T}$.

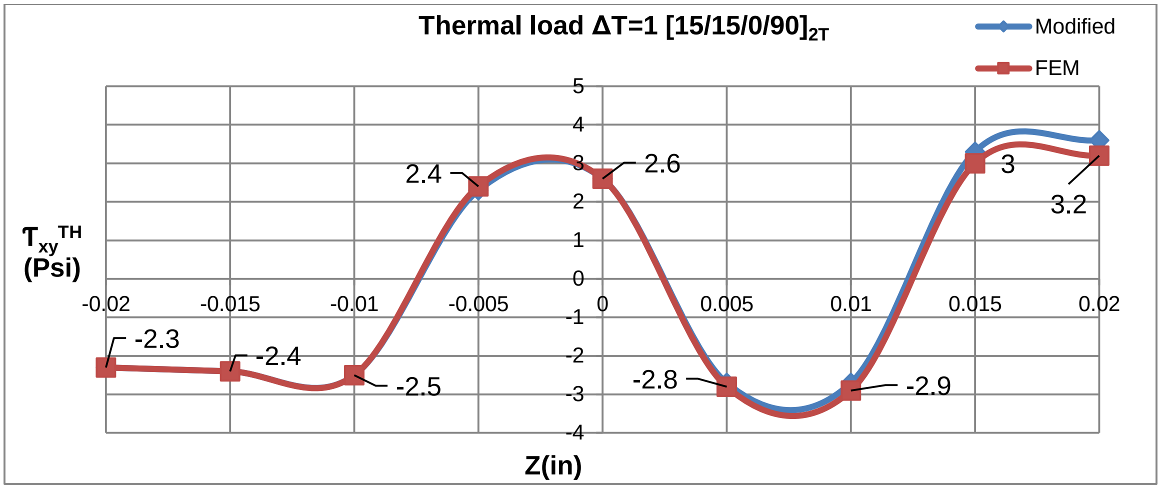

Figure 4—40 Ply-by-ply Shear stress, T_{xy}^{TH} $[15_2/0/90]_{2T}$

The table below displays the stress results are in a very close range in comparing them with the results from FEM.

Table 4—40 Shear stress results, T_{xy}^{TH} $[15_2/0/90]_{2T}$

T_{xy}^{TH}(psi)				
Z(in)	Ply(Θ)	FEM	%Difference	Modified method
0.02	15	3.2	11.1%	3.6
0.015	15	3	9%	3.3
0.01	0	-2.9	6.9%	-2.7
0.005	90	-2.8	3.6%	-2.7
-0.005	15	2.6	0%	2.6
-0.01	15	2.4	4.2%	2.3
-0.015	0	-2.5	0%	-2.5
-0.02	90	-2.4	0%	-2.4

4.6 Constructing laminate model by ANSYS

The finite element method is done by using ANSYS-APDL software. Laminate is subjected to F_x =1(lb) which is acting at a node on the centroid of the laminate. All the nodes on the loaded side of the laminate are coupled in X-direction, in order to achieve uniform load distribution through all the elements. On the un-loaded side of the laminate, all the nodes are constrained in the X-direction, the nodes displacements on the vertical line through the centroid in the Y-direction are set to be zero, and one node on the mid-plane (centroid) is only constrained in the Z-direction. The laminate length and width is 1 by 1 (X by Y), and Z axis is from 0 to top of the laminate thickness.

Figure 4—41 shows the induced thermal stress due to the temperature difference of $\Delta T = 1(F^0)$ for the laminate $[45/-45/0/90]_S$.

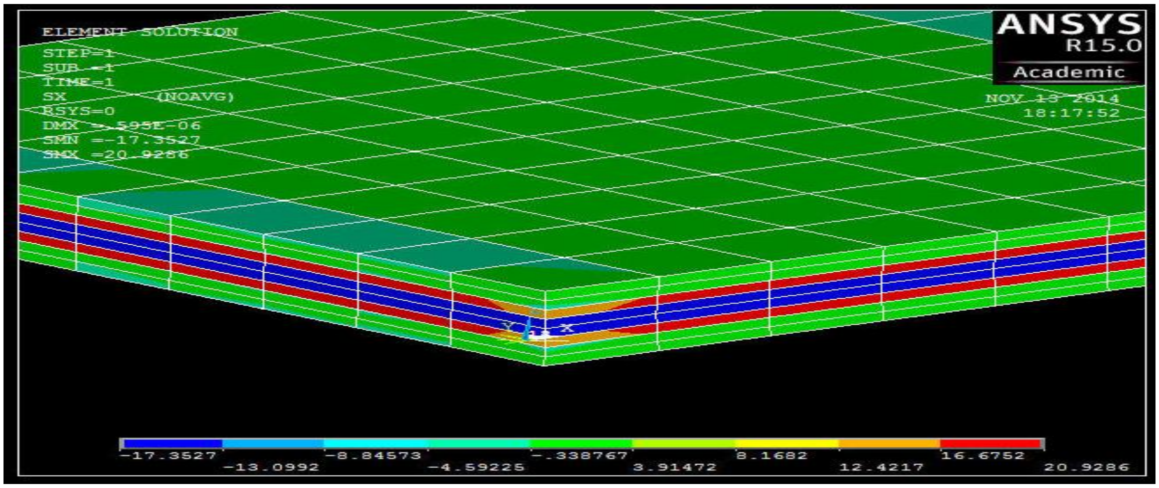

Figure 4—41 Induced σ_x^{TH} due to $\Delta T = 1(F^0)$, $[45/-45/0/90]_S$

Figure 4—42 shows the induced shear thermal stress due to the temperature difference for laminate $[45/-45/0/90]_S$.

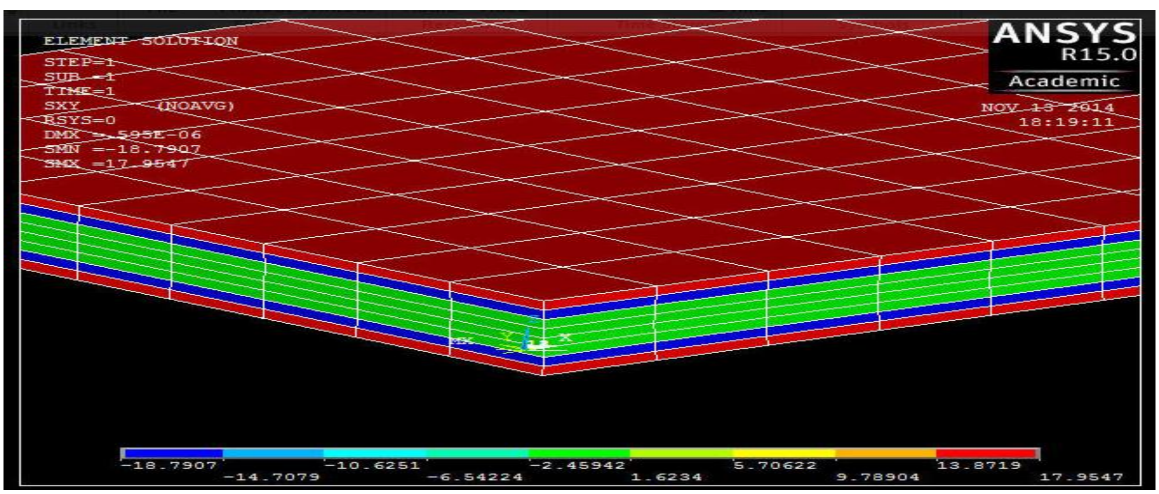

Figure 4—42 Induced T_{xy}^{TH} due to $\Delta T = 1(F^0)$, $[45/-45/0/90]_S$

Figure 4—43 shows the induced thermal stress caused by the temperature difference of $\Delta T = 1(F^0)$ for the laminate $[15/-15/0/90]_{2T}$.

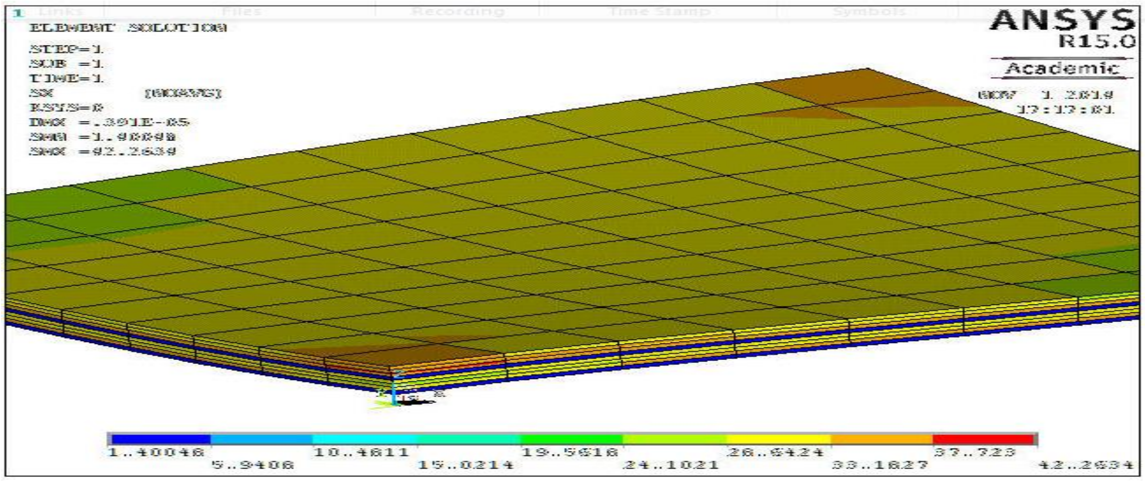

Figure 4—43 Induced σ_x^{TH} for $[15/-15/0/90]_{2T}$

Figure 4—44 shows the normal stress caused by an applied axial load of 1(lb) for the laminate with stacking sequence as $[45/-45/0/90]_{2T}$.

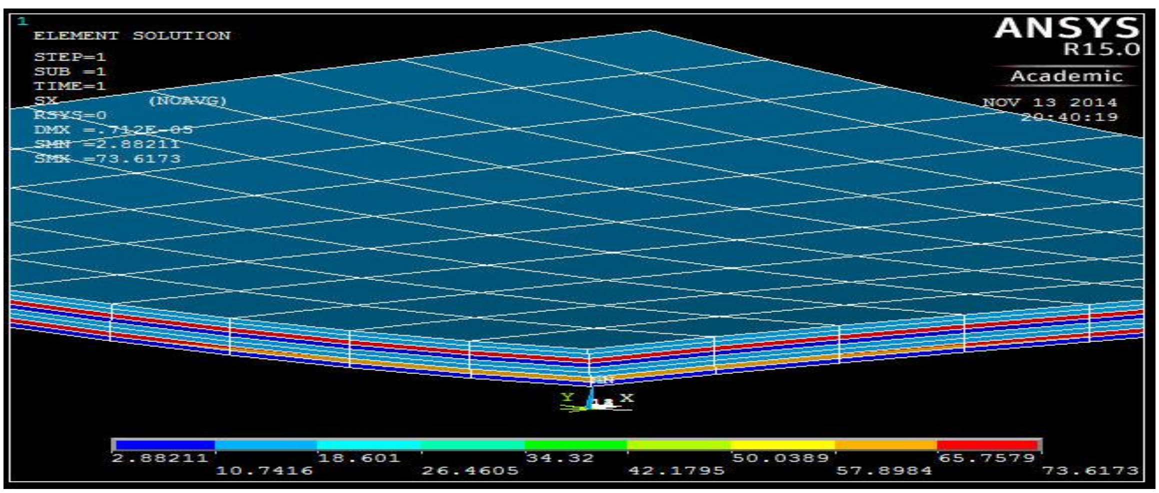

Figure 4—44 σ_x due to Axial load 1(lb), $[45/-45/0/90]_{2T}$

Figure 4—45 shows the induced normal stress results for the laminate $[45/-45/0/90]_{2T}$ due to the temperature difference of $1(F^0)$.

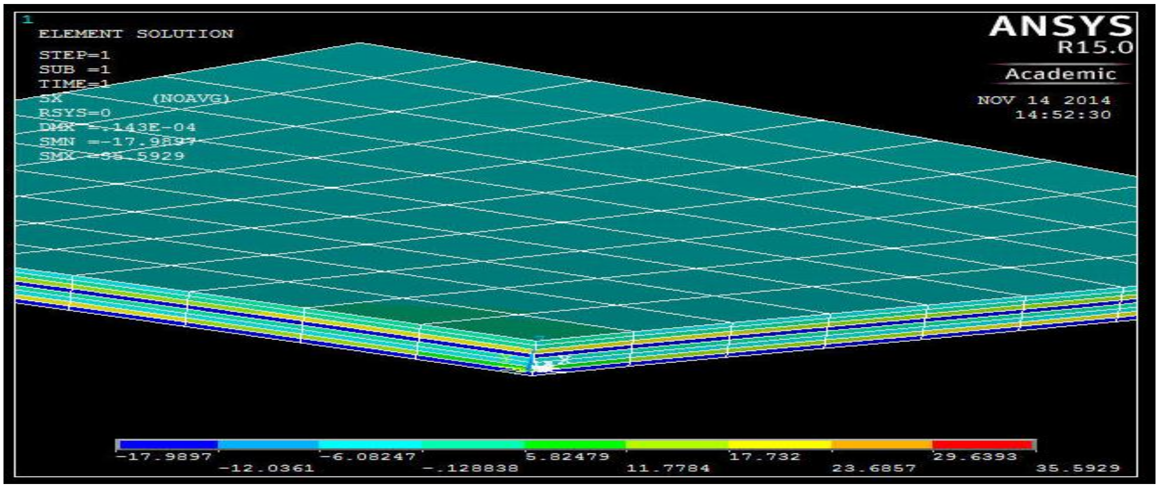

Figure 4—45 σ_x^{TH} due to Thermal load, 1(F^0) $[45/-45/0/90]_{2T}$

Figure 4—46 shows the induced shear stress results for the laminate $[45/-45/0/90]_{2T}$ due to the temperature difference of 1(F^0).

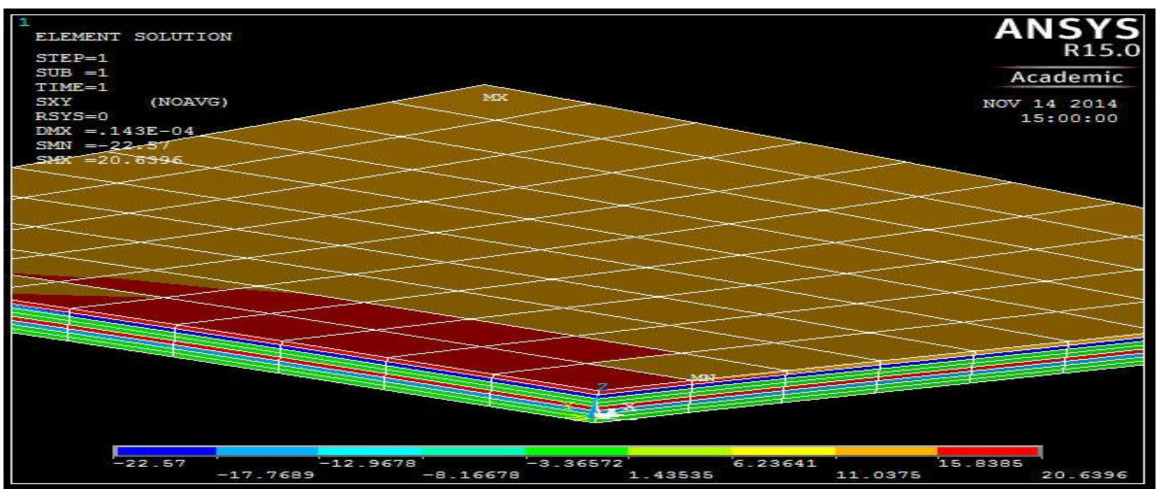

Figure 4—46 τ_{xy}^{TH} due to Thermal load, 1(F^0) [45/-45/0/90]2T

Figure 4—47 shows the induced normal stress results for the laminate $[30/-30/0/90]_S$, due to the temperature difference of 1(F^0).

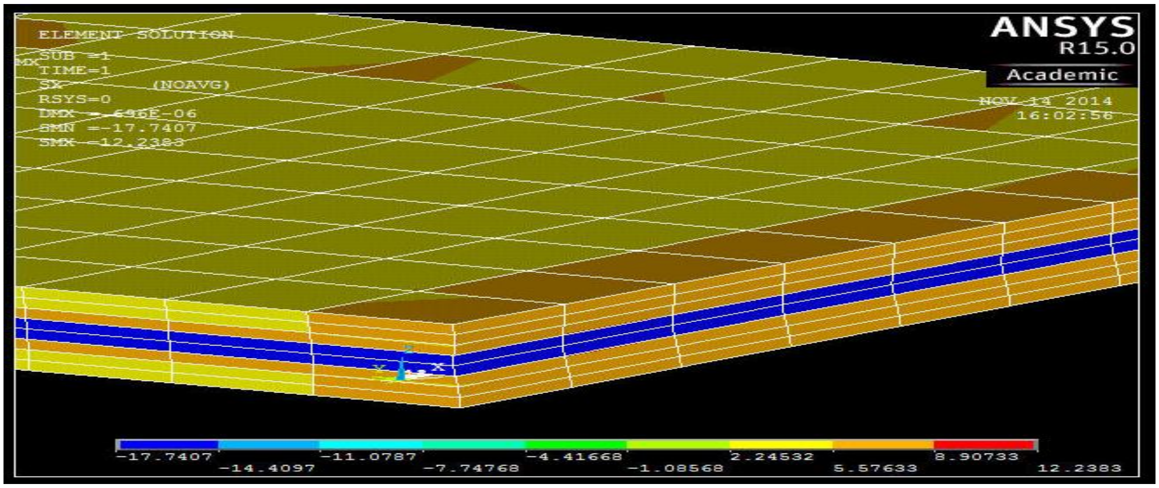

Figure 4—47 σ_x^{TH} due to Thermal load, 1(F^0) $[30/\text{-}30/0/90]_S$

Figure 4—48 shows the induced shear stress results for the laminate $[30/\text{-}30/0/90]_S$, due to the temperature difference of 1(F^0).

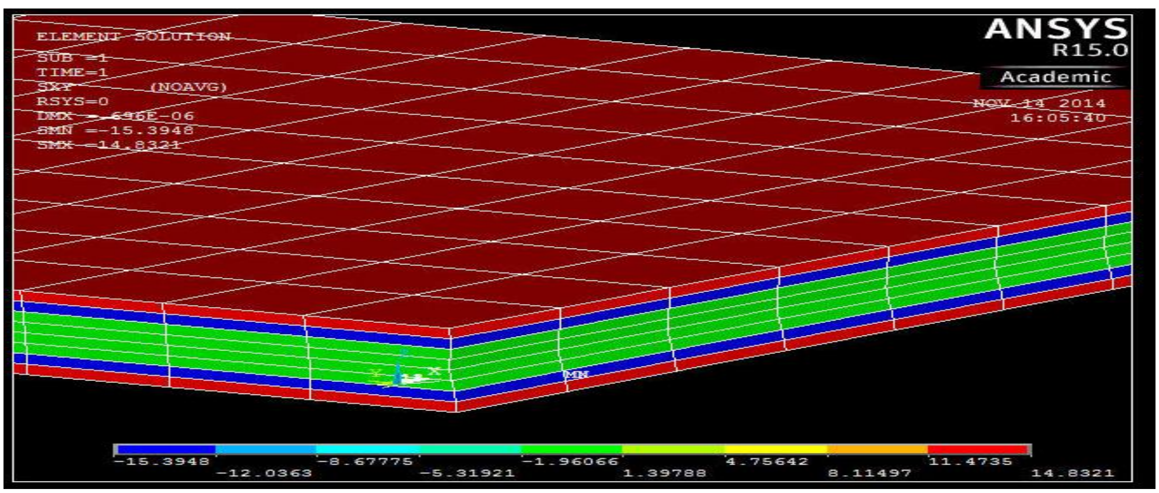

Figure 4—48 τ_{xy}^{TH} due to Thermal load, 1(F^0) $[30/\text{-}30/0/90]_S$

Figure 4—49 shows the boundary conditions, as an example for laminate with stacking sequence of $[45/\text{-}45/0/90]_S$. The nodal displacements for all the nodes in the X-direction is zero, nodes on the vertical line through the centroid in the Y-direction is zero, and only one node at the mid-plane (centroid) in the Z-direction is zero.

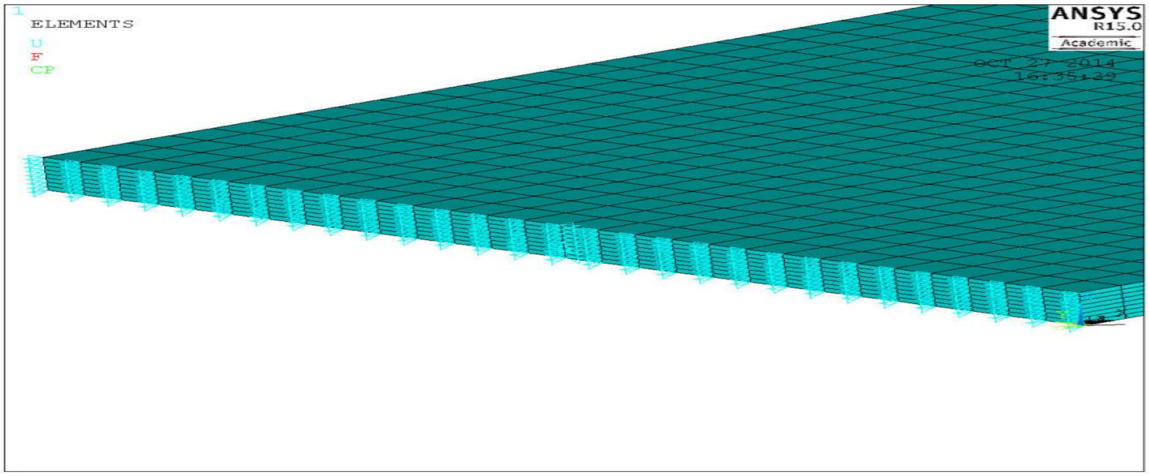

Figure 4—49 Laminate with Boundary Conditions by ANSYS-APDL

Figure 4—50 shows applied axial force of 1(lb), acting at the mid-plane of the laminate, and all the nodes are coupled in the X-direction.

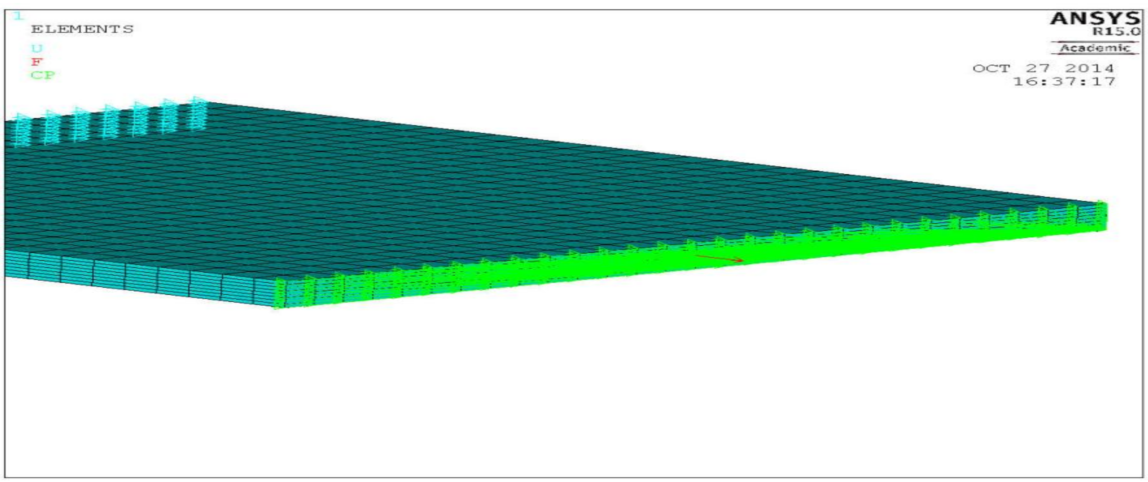

Figure 4—50 Laminate with applied axial load by ANSYS

In order to read the stress results in ANSYS, The data are chosen at least one element away from the edge of the laminate in order to avoid the edge effect.

Figure 4—51 illustrates how the results are obtained by FEM approach. For each laminate, the stack of 8 elements which represent the exact 8 layers in the desired laminate are chosen in order to obtain ply-by-ply stress. The stacks of elements are chosen one element away from the edge of the laminate, and each element is associated with each ply in the desired laminate in the same order as the stacking sequence.

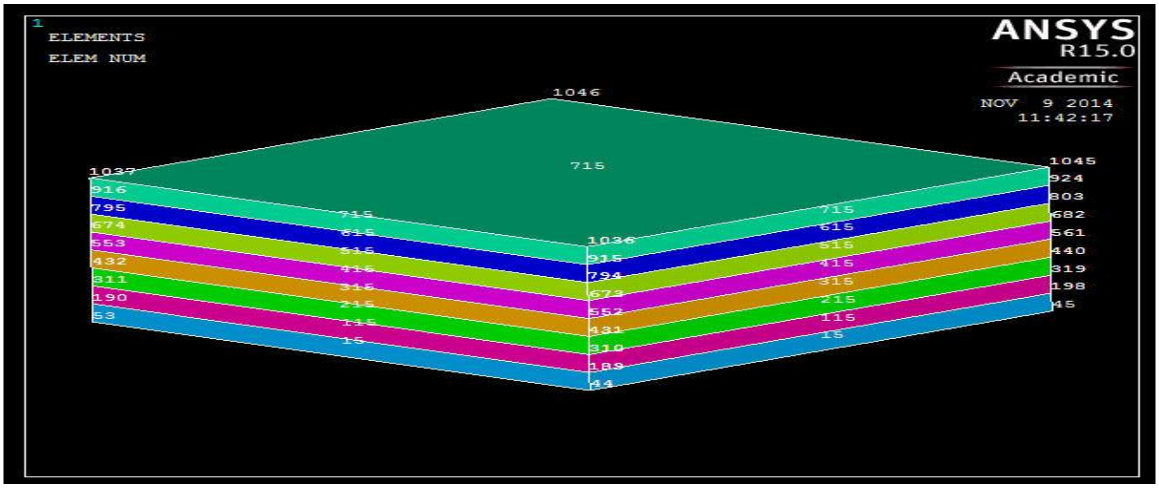

Figure 4—51 Stack of elements representing a laminate

Figure 4—52 illustrates as an example, the induced normal stress due to the temperature difference of 1(F^0) for the element number 715 (top ply) which is associated with the layer number 8 in the laminate $[30/-30/0/90]_S$.

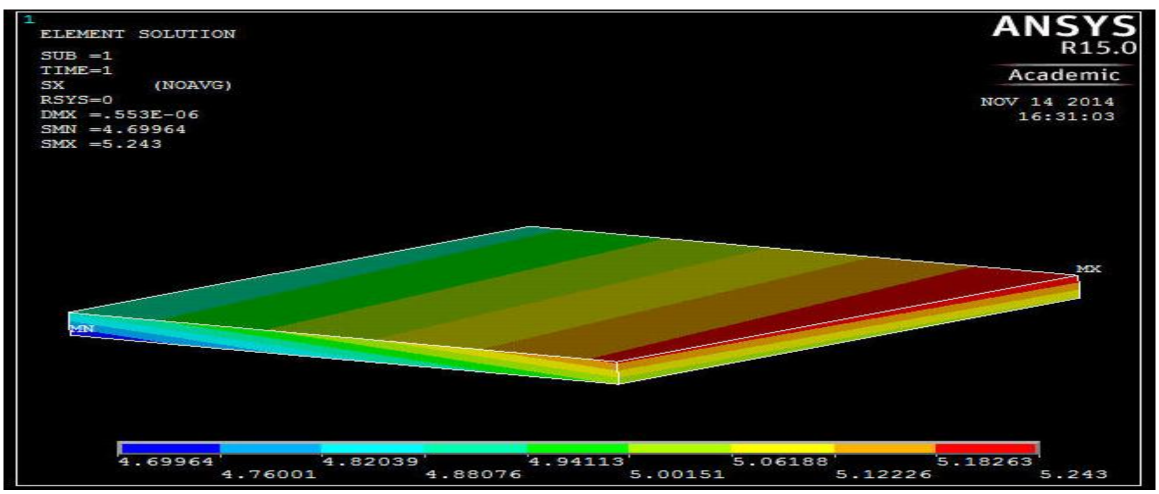

Figure 4—52 Element number 715 associated with layer # 8 of $[30/-30/0/90]_S$

Figure 4—53 shows the stress results obtained by ANSYS-APDL, using the “list results” command for the element number 515. It also displays the stress results for each node. For the

FEM approach, the stress for each layer in the laminate is obtained by employing the list results command for all of the laminate cases.

```
PRINT S     ELEMENT SOLUTION PER ELEMENT

***** POST1 ELEMENT NODAL STRESS LISTING *****

 LOAD STEP=     1  SUBSTEP=     1
  TIME=    1.0000      LOAD CASE=   0

 THE FOLLOWING X,Y,Z VALUES ARE IN GLOBAL COORDINATES

 ELEMENT=     515        SOLID185
   NODE     SX           SY           SZ           SXY          SYZ          SXZ
    673   17.049      -17.253     -0.30600E-02-0.19343E-01 0.26764      0.20465E-01
    682   17.050      -17.253     -0.30589E-02-0.17528E-01 0.26758      0.22158E-01
    683   17.117      -17.252     -0.62796E-02-0.17576E-01-0.58205E-01-0.77362E-02
    674   17.123      -17.251     -0.67988E-02-0.19391E-01-0.60093E-01-0.10326E-01
    794   17.192      -17.264      0.34567E-02-0.20885E-01 0.26739      0.20464E-01
    803   17.192      -17.264      0.34189E-02-0.19025E-01 0.26737      0.22156E-01
    804   17.260      -17.262      0.18667E-03-0.18976E-01-0.58414E-01-0.76982E-02
    795   17.267      -17.262     -0.29365E-03-0.20836E-01-0.60342E-01-0.10288E-01
```

Figure 4—53 Stress Listing for element 515, layer # 6 of [45/-45/0/90]S

Figure 4—54 shows the stack of elements that are chosen for the analysis for each and individual laminate. The stacks are carefully picked that they are one element away from the edge of the laminate. The element that is circled is the figure, is element number 715 which is the top layer of the laminate.

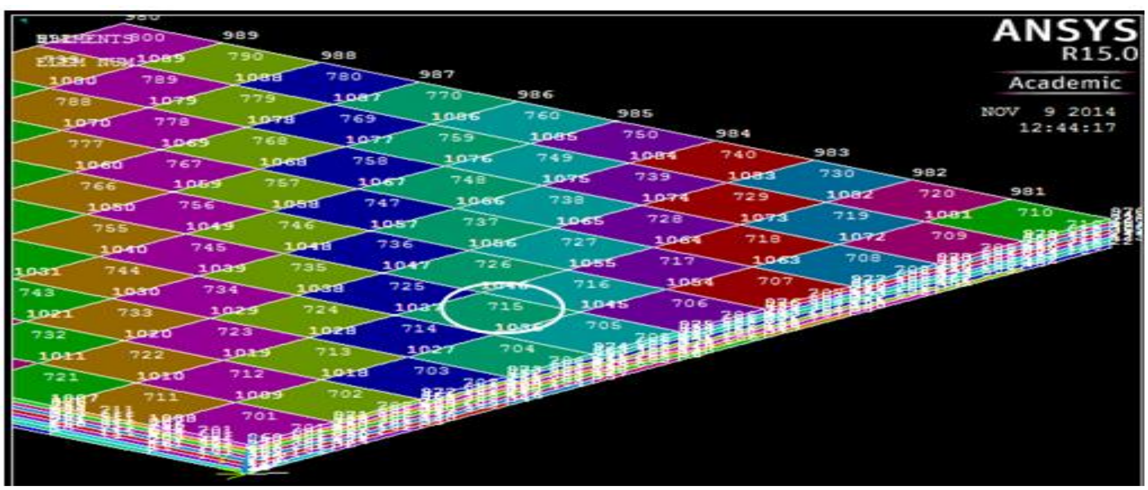

Figure 4—54 Stack of elements chosen for FEM analysis for each laminate

Chapter 5

Equivalent Properties of Structure

5.1 Overview

Composite materials are used in many different types of structures in industries. For example bridges, air craft wings, ballistic materials and much more. Composite structures are made of different geometries. The structure level of composite materials is laminated composites that are bonded together in order to form a new geometry such as I-Beams or aircraft wings. The focus of this chapter is on obtaining the equivalent properties and stress analysis of laminated or composite I-Beam.

In this chapter the stress analysis of composite I-Beam is conducted by finite element method using ANSYS-APDL software, and also by analytical method using Mathematica software. There are two methods that are considered in this chapter in order to obtain the equivalent properties of I-Beam cross section. One is conventional method using smeared properties, and the other is modified method. In the modified method, the constitutive equations of the top and bottom flanges and the web were first obtained based on a composite narrow beam behavior. The sectional properties, centroid, axial stiffness, and bending stiffness of composite I-Beam are derived. Once the strain and curvature are calculated then the resultant forces and moment can be obtained. With having the moment and the resultant forces calculated, then the stress for each ply in the sub-laminates can be calculated as well.

As far as analysis of I-Beam, most of them are considered to be one dimensional. The analysis of I-Beam is based on the moment and curvature relation along the longitudinal axis. In the laminate level, the classical laminated plate theory is employed in order to calculate the ply stresses.

In order to calculate the section property of structure by employing the analytical method (non-FEM) approach, first the equivalent stiffness of each sub-laminate by lamination theory needs to be calculated. Conventional method using in composite analysis is to calculate the equivalent stiffness of each sub-laminate by the lamination theory. But by employing this method, the coupling effect of the structural level would be ignored.

The focus of this chapter is to obtain and evaluate equivalent properties of I-Beam by employing conventional method using smeared properties, and modified method. The main factor that would make a big difference in comparing the two methods is the translation of axis. In structural modeling it may be necessary to translate the reference axis of a laminate. For instance, for the case of I-Beam, the flange laminate axis of I-Beam needs to be translated to the laminate axis of the entire cross section. The effect of this axis translation in obtaining the equivalent properties of laminated I-Beam using smeared properties and modified method will be discussed in details later on in this chapter.

In the analysis of a long I-Beam, moment M_y and twisting curvature k_{xy} in the Y-plane are neglected. For the case of a laminated I-Beam under an axial load acting at the centroid, the bending moment M_x and M_{xy} may be induced. In this thesis, transverse normal force F_y shear force F_{xy}, moment M_y, and twisting curvature k_{xy} are assumed to be zero. The laminated constitutive equation for a narrow beam in the form of a matrix can be constructed as:

$$\begin{pmatrix} N_x \\ M_x \end{pmatrix} = \begin{pmatrix} A_x^{narrow} & B_x^{narrow} \\ B_x^{narrow} & D_x^{narrow} \end{pmatrix} \begin{pmatrix} \epsilon_x^0 \\ \kappa_x \end{pmatrix} \tag{5.1}$$

A_x^{narrow} is the laminate axial stiffness, B_x^{narrow} is the coupling stiffness, and D_x^{narrow} is the bending stiffness. ϵ_x^0 and k_x are the mid plane strain and the curvature of the laminate, respectively.

5.2 Composite I-Beam geometry

I-Beam is constructed of two sub-laminates, top and bottom flanges, and the web sub-laminate. All the sub-laminates are to be perfectly bonded. The top flange is numbered 1, the web is numbered 2, and the bottom flange is numbered 3. The width of the top and bottom flanges are b_{f1} and b_{f3} respectively, and the height of the web is h_w. z_1 is measured from the bottom of the flange 3 to the mid thickness of the flange 1. z_2 or z_w is measured from the bottom of the flange 3 to the mid height of the web, and z_3 is measured from bottom of the flange 3 to its mid thickness.

Figure 5—1 it's an arbitrary geometry only to illustrates the dimensions and it's not to resemble the actual I-Beam that is used for the analysis. The width and the height of the I-Beam for this analysis are b_{f1} =1(in), b_{f3} =2(in), and h_w =1(in).

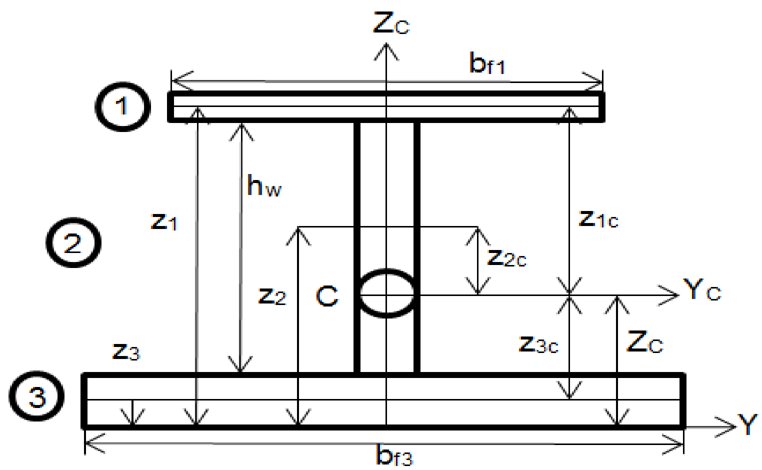

Figure 5—1 Composite I-Beam geometry and dimensions

5.3 Sectional properties of composite I-Beam

The significant difference between the smeared properties stiffness and the narrow beam bending stiffness (modified method) is that the bending stiffness in smeared properties does not consider the stacking sequence in the calculations. The smeared properties method only consider an equivalent young's modulus and multiply it by the inertia of the cross section of the beam. So that is why the effect of the stacking sequence on the bending stiffness is ignored. This is acceptable for the case of a very thin I-beam which the height from the bending axis is large. However in the case of a thick laminate which the height from the bending axis is small, then the stacking sequence will have a significant influence on calculating the bending stiffness. So for the case of a thick laminate it is more appropriate to employ the modified method rather than the smeared properties method.

5.3.1 Conventional method's approach

As it was mentioned before, this method does not consider the stacking sequence effect when obtaining the bending stiffness. It only take the young's modulus and multiply it by the inertia of the cross section of the beam.

Conventional method's approach uses smeared properties in order to obtain the axial and the bending stiffness.

$$A_x^{smeared} = \frac{w}{a_{11}} = E\,A \tag{5.2}$$

$$D_x^{smeared} = w\,D_x = E\,I \tag{5.3}$$

$$I = 2\left(\frac{1}{12}\,b_{fi}h_{fi}^3 + (b_{fi}\,h_{fi})\,Z_{iC}^2\right) + \frac{1}{12}\,t_w h_w^3 \tag{5.4}$$

Where Z_{iC} is the distance measured from the centroid of the I-beam to the mid axis of the laminate.

5.3.2 Modified method's approach

Since the ratio of the width to the depth of the beam is usually not greater than 6, a narrow beam assumption is employed in this study. The equation of constitutive of I-beam has been derived in [8]. The key equations used in this study are given below.

Total axial stiffness with "w" being the width of the beam is:

$$A_x^{narrow} = \frac{w\,d_{11}}{a_{11}\,d_{11} - b_{11}^2} \tag{5.5}$$

Total coupling stiffness can be calculated by:

$$B_x^{narrow} = \frac{w\,b_{11}}{b_{11}^2 - a_{11}\,d_{11}} \tag{5.6}$$

Total bending stiffness can be calculated as:

$$D_x^{narrow} = \frac{w\,a_{11}}{a_{11}\,d_{11} - b_{11}^2} \tag{5.7}$$

By having the sectional properties, then the equivalent axial stiffness of the entire cross-section can be defined by using equation (5.8).

$$EA^c = b_{f1}(A_{1,f1}) + b_{f2}(A_{1,f2}) + b_{f3}(A_{1,f3}) \tag{5.8}$$

The centroid of a structural cross-section is defined as the average location of forces acting on each part of the cross section. So the centroid can be located by using equation (5.9) and the bending stiffness of the entire I-Beam is defined as equation (5.10).

$$Z_c = \frac{b_{f1}(A_{1,f1})z_1 + b_{f2}(A_{1,f2})z_2 + b_{f3}(A_{1,f3})z_3}{b_{f1}(A_{1,f1}) + b_{f2}(A_{1,f2}) + b_{f3}(A_{1,f3})} \tag{5.9}$$

$$D_x^c = \sum_{i=1}^{2} b_{fi}\left(A_{1,fi}\, z_{ic}^2 + 2\, B_{1,fi} z_{ic} + D_{i,fi}\right) + A_{1,w}\left(\frac{1}{12} h_w^3 + h_w h_{wc}^2\right) \tag{5.10}$$

5.3.3 Results obtained by employing modified and Conventional methods

Mathematica software was used in order to calculate the sectional properties of the I-Beam cross section. The ply thickness is 0.005(in) and the stacking sequence of the top flange (1) of the I-Beam is $[45/\text{-}45/0/90]_S$, for the bottom flange (3) is $[45/\text{-}45/0_4/90]_S$, and for the web (2) is $[45/\text{-}45/0]_S$. The top flange width is 1(in), the bottom flange width is 2(in). For this case the height of the web h_w is 1(in).

Properties of the typical unidirectional composite in 2-D, used for this analysis are displayed in Table 5—1. Table 5—2 displays the results for the sectional properties of I-Beam, for the case of h_w=1(in) by employing both conventional and modified methods.

Table 5—1 Properties of Carbon/Epoxy (IM6G/3501-6)

Density ρ (lb/in^3)	Long. Modulus E_1(Msi)	Trans. Modulus E_2(Msi)	Shear Modulus G_{12}(Msi)	Poisson's Ratio υ_{12}	Long. TEC $\alpha_1(10^{-6}/F^0)$	Trans. TEC $\alpha_2(10^{-6}/F^0)$
0.059	24.5	1.3	0.94	0.31	-0.5	13.9

As it was expected for the axial stiffness, the results gained from both methods are identical, and the results for the bending stiffness have 58.3% difference.

Table 5—2 Sectional properties results for h_w =1(in)

Equivalent. Prop. of I-Beam	Modified method	Conventional method
Centroid (in)	0.229	0.229
Axial stiffness, EA^C(lb)	2.909 x 10^6	2.909 x 10^6
Percent Difference %	0%	
Bending stiffness, D_x^C(lb.in²)	382857	918475
Percent Difference %	58.3%	

5.4 Stress analysis of composite I-Beam

In composite materials, the centroid is defined to be at the location where an axial load N_x does not cause any change in the curvature $K^C{}_x$ and the bending moment M_x does not induce axial strain $\epsilon^C{}_x$. So it means if the load is applied at the centroid, it decouples the structural response between the axial extension and the bending.

Consider an I-Beam which is subjected to N_x and M_x acting at the centroid of the cross section. Since load is applied at the centroid, the axial and bending stiffness are decoupled. Equations (5.8) and (5.9) are the constitutive equations in the matrix form. It can be constructed based on the strain and curvature of the whole I-Beam section.

$$\begin{pmatrix} \epsilon_x^c \\ K_x^c \end{pmatrix} = \begin{pmatrix} a_{11} & b_{11} \\ b_{11} & d_{11} \end{pmatrix} \begin{pmatrix} N_x \\ M_x \end{pmatrix} \tag{5.11}$$

$$\begin{pmatrix} N_x \\ M_x \end{pmatrix} = \begin{pmatrix} EA^c & 0 \\ 0 & D_x^c \end{pmatrix} \begin{pmatrix} \epsilon_x^c \\ K_x^c \end{pmatrix} \tag{5.12}$$

N_x and M_x are the applied axial and moment loads, respectively. a_{11}, b_{11}, and d_{11} are the compliance, coupling, and flexibility components of each sub-laminate, EA^C and $D^C{}_x$ are the equivalent axial and bending stiffness of the I-Beam cross section, respectively.

5.4.1 Applied axial load

In the case of axial load acting at the centroid, the curvature $K_x{}^C = K_{x,fi} = 0$ and $\epsilon_{x,fi}{}^0 = \epsilon_x{}^C$ in order to obtain the strain at the centroid, $\epsilon_x{}^C$ equation (5.13) can be applied.

$$\epsilon_x^C = \frac{N_x}{EA} \tag{5.13}$$

The resultant force and moment per unit width of sub-laminates are:

$N_{x,fi} = A_{1,fi}\ \epsilon_x^C$ (5.14)

$M_{x,fi} = B_{1,fi}\ \epsilon_x^C$ (5.15)

Now the mid plane strain and curvature of each sub-laminate can be calculated by equation (5.16).

$$\begin{pmatrix} \epsilon_{x,fi}^0 \\ \epsilon_{y,fi}^0 \\ \epsilon_{xy,fi}^0 \\ K_{x,fi} \\ K_{y,fi} \\ K_{xy,fi} \end{pmatrix} = \begin{pmatrix} a_{11} & b_{11} & b_{16} \\ a_{12} & b_{21} & b_{26} \\ a_{16} & b_{61} & b_{66} \\ b_{11} & d_{11} & d_{16} \\ b_{12} & d_{12} & d_{26} \\ b_{16} & d_{61} & d_{66} \end{pmatrix} \begin{pmatrix} N_{x,fi} \\ M_{x,fi} \\ M_{xy,fi} \end{pmatrix} \tag{5.16}$$

Once the mid plane strains for sub-laminate is calculated, strain of each layer in the sub-laminate can be calculated by:

$\epsilon_{fi,k} = \epsilon_{fi}^0 + z_{fi,k}\ K_{fi}$ (5.17)

$\epsilon_{fi,k}$ is the strain for the desired layer in a sub-laminate, and $z_{fi,k}$ is the height from the center of the desired layer in a sub-laminate to the bottom of the I-Beam.

5.4.2 Applied bending moment

In the case of bending moment acting at the centroid, the curvature of the composite I-Beam can be calculated by using equation (5.18).

$$k_{x,fi} = K_x^C = \frac{M_x}{D_x^C} \tag{5.18}$$

The resultant force and moment can be obtained by using equations (5.16) and (5.17). Hint that for this case: $\epsilon^C{}_x = 0$ and $K^C{}_x = k_{x,fi}$.

$$N_{x,fi} = \left(A_{x,fi}^{narrow}\, z_{c,fi} + B_{x,fi}^{narrow} \right) = \frac{M_x}{D_x^C} \tag{5.19}$$

$$M_{x,fi} = \left(B_{x,fi}^{narrow}\, z_{c,fi} + D_{x,fi}^{narrow} \right) = \frac{M_x}{D_x^C} \tag{5.20}$$

Chapter 6

Conclusions

Materials have variety of properties which includes mechanical and thermal properties. It was found that the combination of materials can improve the properties of materials. So composite materials were introduced and they have been used in many industries for a long time. Also this would bring a great challenge when it comes to analysis of composite materials. It is a very time consuming process and it takes a large amount of computer memory. So obtaining equivalent properties would reduce the size of the problem.

A concept of equivalent properties for lamina, laminate, and structure levels is considered. Methods that are considered in this thesis are the modified or the present method, and the conventional method. Equivalent properties are calculated by the present method is taken consideration of the structure behavior of equivalent zero degree lamina. Hence, the induced curvature and the shear deformation are suppressed for un-symmetrical and un-balanced laminates under applied axial load, and the induced axial and shear deformation are suppressed under applied bending moment.

It was discussed at the lamina level how to obtain and derive the equivalent properties for variety of ply orientations and the results gained from both methods were compared against each other and the properties were plotted. At the laminate level, both methods were employed for different cases, for all of the properties E_x, E_y, G_{xy}, υ_{xy}, α_x, and α_x. Laminates with stacking sequences as $[\theta/\text{-}\theta/0/90]_{2T}$, $[\theta/\text{-}\theta/0/90]_S$, $[\theta_2/0/90]_S$, and $[\theta_2/0/90]_{2T}$ were considered. Longitudinal normal stress, due to an applied axial load for the cases of $[45/\text{-}45/0/90]_{2T}$, $[45/\text{-}45/0/90]_S$, $[15/\text{-}15/0/90]_{2T}$, $[15/\text{-}15/0/90]_S$, $[45_2/0/90]_S$, $[45_2/0/90]_{2T}$, $[15_2/0/90]_{2T}$, $[30/\text{-}30/0/90]_{2T}$, and $[30/\text{-}30/0/90]_S$ were analyzed and the results were plotted. Also induced normal and shear stresses caused by temperature load, due to the temperature difference for the case of $[45/\text{-}45/0/90]_S$, $[45/\text{-}45/0/90]_{2T}$, $[30/\text{-}30/0/90]_{2T}$, $[30/\text{-}30/0/90]_{2T}$, and $[15_2/0/90]_{2T}$ were calculated and analyzed by employing the two methods and compared the results against those that were obtained by the laminate theory. At the structure level, I-Beam cross section was considered for the analysis. The two methods, modified method and smeared properties approach were employed in order to obtain the sectional properties such as centroid, axial and bending stiffness. Stress analysis for flange 2 when I-Beam is subjected to an axial load and moment which were acting at the centroid of the I-Beam cross section were conducted and tabulated. The stress results with an applied axial load by employing both methods were compared against the results gained by employing FEM by using ANSYS. The method of constructing the model in ANSYS with the boundary conditions and the load cases were discussed and plotted.

Appendix A

Mathematica codes and calculations

Sample codes for laminate analysis and equivalent properties:

IM6G/3501-6:

E1 = 24.5e6, E2 = 1.3e6. G12 = 0.94e6, V12 = 0.31, α1 = -0.5e-6, α2 = 13.9e-6

Equivalent- properties for [+θ/-θ/0/90] 2T : lumped layer, θ = 0,15, 30, 45, 60, 75, 90

```
σnew=Table[0,{a,3}];

σ45=Table[0,{t,3}];

σmin45=Table[0,{s,3}];

σ0=Table[0,{aa,3}];

σnew0=Table[0,{b,3}];

σnewmin45=Table[0,{ee,3}];

σnew45=Table[0,{dd,3}];

σnew90=Table[0,{q,3}];

s=Table[0,{c,3},{d,3}];

snew=Table[0,{e,3},{f,3}];

q=Table[0,{o,3},{p,3}];

delta=Table[0,{g,3},{h,3}];

qnew=Table[0,{i,3},{j,3}];

A=Table[0,{k,3},{l,3}];

B=Table[0,{kk,3},{ll,3}];

b=Table[0,{mm,3},{nn,3}];

Dmat=Table[0,{oo,3},{pp,3}];

d=Table[0,{qq,3},{rr,3}];

a= Table[0,{m,3},{n,3}];

Q0=Table[0,{u,3},{v,3}];

P=Table[0,{r,3},{hh,3}];

Qmin45=Table[0,{gg,3},{ff,3}];
```

```
Q45=Table[0,{ii,3},{jj,3}];

NTtotal=Table[0,{w,3}];

Napply=Table[0,{z,3}];

Ntotal=Table[0,{bb,3}];

α=Table[0,{ss,3}];

αnew=Table[0,{tt,3}];

α45=Table[0,{tt,3}];

αmin45=Table[0,{av,3}];

αold=Table[0,{ww,3}];

L=Table[0,{xx,3},{yy,3}];

Q90=Table[0,{zz,3},{ab,3}];

α90=Table[0,{cd,3}];

ϵmid=Table[0,{ef,3}];

k=Table[0,{gh,3}];

ϵ45=Table[0,{ij,3}];

ϵmin45=Table[0,{kl,3}];

snew=Table[0,{mn,3},{op,3}];

deltanew=Table[0,{qr,3},{st,3}];

Qnew45=Table[0,{uv,3},{wx,3}];

σnewlump=Table[0,{yz,3}];

ϵmid=Table[0,{ba,3}];

Pnew=Table[0,{dc,3},{fe,3}];

NT=Table[0,{hg,3}];

αnew=Table[0,{ji,3}];

ϵnewlump=Table[0,{lk,3}];

ϵ0=Table[0,{nm,3}];
```

```
NTlump=Table[0,{po,3}];

MTlump=Table[0,{rq,3}];

ϵ90=Table[0,{ts,3}];

σ90=Table[0,{vu,3}];

Qnewlump=Table[0,{xw,3},{zy,3}];

MT=Table[0,{ac,3}];

bt=Table[0,{ad,3},{ae,3}];

ϵnewmidlump=Table[0,{af,3}];

s0=Table[0,{ag,3},{ah,3}];

s15=Table[0,{ak,3},{ai,3}];

s30=Table[0,{al,3},{aj,3}];

s45=Table[0,{an,3},{am,3}];

s60=Table[0,{ap,3},{ao,3}];

s75=Table[0,{ar,3},{aq,3}];

s90=Table[0,{at,3},{as,3}];

Q15=Table[0,{au,3},{av,3}];

Q30=Table[0,{aw,3},{ax,3}];

Q60=Table[0,{ay,3},{az,3}];

Q75=Table[0,{ba,3},{bb,3}];

α15=Table[0,{bc,3}];

α30=Table[0,{bd,3}];

α60=Table[0,{be,3}];

α75=Table[0,{bf,3}];

αnew0=Table[0,{bg,3}];

αmin15=Table[0,{bh,3}];

αmin30=Table[0,{bi,3}];
```

```
αnew45=Table[0,{bj,3}];
αmin60=Table[0,{bk,3}];
αmin75=Table[0,{bl,3}];
αnew90=Table[0,{bm,3}];
αold0=Table[0,{bn,3}];
αold15=Table[0,{bm,3}];
αold30=Table[0,{bn,3}];
αold45=Table[0,{bo,3}];
αold60=Table[0,{bp,3}];
αold75=Table[0,{bq,3}];
αold90=Table[0,{br,3}];
Qmin15=Table[0,{bu,3},{bv,3}];
Qmin30=Table[0,{bx,3},{bw,3}];
Qmin60=Table[0,{bz,3},{by,3}];
Qmin75=Table[0,{cb,3},{ca,3}];
Qmin90=Table[0,{cc,3},{cd,3}];
αmin90=Table[0,{ce,3}];
Qoldlump=Table[0,{cf,3},{cg,3}];
ϵnewmidlump=Table[0,{cj,3}];
Qnewlump=Table[0,{ck,3},{cl,3}];
Mapply=Table[0,{cn,3}];
knewlump=Table[0,{co,3}];
s[[1,1]]=1/E1;
s[[1,2]]=s[[2,1]]=-V12/E1;
s[[2,2]]=1/E2;
s[[3,3]]=1/( G12);
```

```
s;MatrixForm[%];
delta[[1,1]]=s[[1,1]]*s[[2,2]]-s[[1,2]]*s[[1,2]];
delta[[2,2]]=s[[1,1]]*s[[2,2]]-s[[1,2]]*s[[1,2]];
delta[[1,2]]=s[[1,1]]*s[[2,2]]-s[[1,2]]*s[[1,2]];
delta[[2,1]]=s[[1,1]]*s[[2,2]]-s[[1,2]]*s[[1,2]];
q[[1,1]]=s[[2,2]]/delta[[1,1]];
q[[2,2]]=s[[1,1]]/delta[[2,2]];
q[[1,2]]=(-1*s[[1,2]])/delta[[1,2]];
q[[3,3]]=1/s[[3,3]];
qnew[[1,1]]=Cos[θ]^4*q[[1,1]]+Sin[θ]^4*q[[2,2]]+2*Cos[θ]^2*Sin[θ]^2*q[[1,2]]+4*Cos[θ]^2
*Sin[θ]^2*q[[3,3]];
qnew[[2,2]]=Sin[θ]^4*q[[1,1]]+Cos[θ]^4*q[[2,2]]+2*Cos[θ]^2*Sin[θ]^2*q[[1,2]]+4*Cos[θ]^2
*Sin[θ]^2*q[[3,3]];
qnew[[1,2]]=qnew[[2,1]]=Cos[θ]^2*Sin[θ]^2*q[[1,1]]+Cos[θ]^2*Sin[θ]^2*q[[2,2]]+(Cos[θ]^
4+Sin[θ]^4)*q[[1,2]]-4*Cos[θ]^2*Sin[θ]^2*q[[3,3]];
qnew[[1,3]]=qnew[[3,1]]=Cos[θ]^3*Sin[θ]*q[[1,1]]-Cos[θ]*Sin[θ]^3*q[[2,2]]-
Cos[θ]*Sin[θ]*(Cos[θ]^2-Sin[θ]^2)*q[[1,2]]-2*Cos[θ]*Sin[θ]*(Cos[θ]^2-Sin[θ]^2)*q[[3,3]];
qnew[[2,3]]=qnew[[3,2]]=Cos[θ]*Sin[θ]^3*q[[1,1]]-
Cos[θ]^3*Sin[θ]*q[[2,2]]+Cos[θ]*Sin[θ]*(Cos[θ]^2-Sin[θ]^2)*q[[1,2]]+2*Cos[θ]*Sin[θ]*(Cos[θ]^2-
Sin[θ]^2)*q[[3,3]];
qnew[[3,3]]=Cos[θ]^2*Sin[θ]^2*q[[1,1]]+Cos[θ]^2*Sin[θ]^2*q[[2,2]]-
2*Cos[θ]^2*Sin[θ]^2*q[[1,2]]+(Cos[θ]^2-Sin[θ]^2)^2*q[[3,3]];
snew[[1,1]]=Cos[θ]^4*s[[1,1]]+Sin[θ]^4*s[[2,2]]+2*Cos[θ]^2*Sin[θ]^2*s[[1,2]]+Cos[θ]^2*Si
n[θ]^2*s[[3,3]];
snew[[2,2]]=Sin[θ]^4*s[[1,1]]+Cos[θ]^4*s[[2,2]]+2*Cos[θ]^2*Sin[θ]^2*s[[1,2]]+Cos[θ]^2*Si
n[θ]^2*s[[3,3]];
```

snew[[1,2]]=snew[[2,1]]=Cos[θ]^2*Sin[θ]^2*s[[1,1]]+Cos[θ]^2*Sin[θ]^2*s[[2,2]]+(Cos[θ]^4 +Sin[θ]^4)*s[[1,2]]-Cos[θ]^2*Sin[θ]^2*s[[3,3]];

snew[[1,3]]=snew[[3,1]]=2*Cos[θ]^3*Sin[θ]*s[[1,1]]-2*Cos[θ]*Sin[θ]^3*s[[2,2]]+2*(Cos[θ]*Sin[θ]^3-Cos[θ]^3*Sin[θ])*s[[1,2]]+(Cos[θ]*Sin[θ]^3-Cos[θ]^3*Sin[θ])*s[[3,3]];

snew[[2,3]]=snew[[3,2]]=2*Cos[θ]*Sin[θ]^3*s[[1,1]]-2*Cos[θ]^3*Sin[θ]*s[[2,2]]+2*(Cos[θ]^3*Sin[θ]-Cos[θ]*Sin[θ]^3)*s[[1,2]]+(Cos[θ]^3*Sin[θ]-Cos[θ]*Sin[θ]^3)*s[[3,3]];

snew[[3,3]]=4*Cos[θ]^2*Sin[θ]^2*s[[1,1]]+4*Cos[θ]^2*Sin[θ]^2*s[[2,2]]-8*Cos[θ]^2*Sin[θ]^2*s[[1,2]]+(Cos[θ]^2-Sin[θ]^2)^2*s[[3,3]];

α[[1]]=- 0.5*10^- 6;

α[[2]]=13.9*10^-6;

α[[3]]=0;

αnew[[1]]=Cos[θ]^2*α[[1]]+Sin[θ]^2*α[[2]]-Cos[θ]*Sin[θ]*α[[3]];

αnew[[2]]=Cos[θ]^2*α[[2]]+Sin[θ]^2*α[[1]]+Cos[θ]*Sin[θ]*α[[3]];

αnew[[3]]=2*Cos[θ]*Sin[θ]*α[[1]]-2*Cos[θ]*Sin[θ]*α[[2]]+(Cos[θ]^2-Sin[θ]^2)*α[[3]];

αmin15=αnew/.θ-> -(15*Pi)/180;

α90=αnew/.θ-> Pi/2;

α30=αnew/.θ-> (30*Pi)/180;

α60=αnew/.θ-> (60*Pi)/180;

α15=αnew/.θ-> (15*Pi)/180;

α75=αnew/.θ-> (75*Pi)/180;

α45=αnew/.θ-> Pi/4;

αmin45=αnew/.θ-> - Pi/4;

αmin30=αnew/.θ->- (30*Pi)/180;

αmin75=αnew/.θ-> -(75*Pi)/180;

```
αmin60=αnew/.θ-> -(60*Pi)/180;

αmin90=αnew/.θ-> - Pi/2;

t=0.005;

h0=- 4*t;

h1=- 3*t;

h2=- 2*t;

h3=- t;

h4=0;

h5=t;

h6=2*t;

h7=3* t;

h8=4*t;

Napply[[1]]=1;

Napply[[2]]=0;

Napply[[3]]=0;

Mapply[[1]]=0;

Mapply[[2]]=0;

Mapply[[3]]=0;

s0=snew/.E1-> 24.5*10^6/.E2-> 1.3*10^6/.V12-> 0.31 /.G12-> 0.94*10^6/.θ->0;

Q0=qnew/.E1->  24.5*10^6/.E2-> 1.3*10^6/.V12-> 0.31 /.G12-> 0.94*10^6/.θ->0;

Q45=qnew/.E1->  24.5*10^6/.E2-> 1.3*10^6/.V12-> 0.31 /.G12-> 0.94*10^6/.θ->Pi/4;

Q15=qnew/.E1->  24.5*10^6/.E2-> 1.3*10^6/.V12-> 0.31 /.G12-> 0.94*10^6/.θ-
>(15*Pi)/180;

Q30=qnew/.E1->  24.5*10^6/.E2-> 1.3*10^6/.V12-> 0.31 /.G12-> 0.94*10^6/.θ-
>(30*Pi)/180;
```

Qmin30=qnew/.E1-> 24.5*10^6/.E2-> 1.3*10^6/.V12-> 0.31 /.G12-> 0.94*10^6/.θ->-(30*Pi)/180;

MatrixForm[%];

Q60=qnew/.E1-> 24.5*10^6/.E2-> 1.3*10^6/.V12-> 0.31 /.G12-> 0.94*10^6/.θ->(60*Pi)/180;

Qmin60=qnew/.E1-> 24.5*10^6/.E2-> 1.3*10^6/.V12-> 0.31 /.G12-> 0.94*10^6/.θ->-(60*Pi)/180;

Q90=qnew/.E1-> 24.5*10^6/.E2-> 1.3*10^6/.V12-> 0.31 /.G12-> 0.94*10^6/.θ->Pi/2;

Qmin90=qnew/.E1-> 24.5*10^6/.E2-> 1.3*10^6/.V12-> 0.31 /.G12-> 0.94*10^6/.θ->-Pi/2;

Q75=qnew/.E1-> 24.5*10^6/.E2-> 1.3*10^6/.V12-> 0.31 /.G12-> 0.94*10^6/.θ->(75*Pi)/180;

Qmin45=qnew/.E1-> 24.5*10^6/.E2-> 1.3*10^6/.V12-> 0.31 /.G12-> 0.94*10^6/.θ->-Pi/4;

Qmin15=qnew/.E1-> 24.5*10^6/.E2-> 1.3*10^6/.V12-> 0.31 /.G12-> 0.94*10^6/.θ->-(15*Pi)/180;

Qmin75=qnew/.E1-> 24.5*10^6/.E2-> 1.3*10^6/.V12-> 0.31 /.G12-> 0.94*10^6/.θ->-(75*Pi)/180;

-----------------------θ 0/0

Extensional stiffness (lb / in)

A=2*(Q90*t)+6*(Q0*t);

({ {751834., 16202.6, 0.},

{16202.6, 285456., 0.},

{0., 0., 37600.}

})Extensional - Bending coupling stiffness (lb)

```
B=0.5*((Q90*(h1^2-h0^2))+(Q0*(h2^2- h1^2))+(Q0*(h3^2-h2^2))+(Q0*(h4^2-h3^2))+(Q90*(h5^2-h4^2))+(Q0*(h6^2-h5^2))+(Q0*(h7^2-h6^2))+(Q0*(h8^2-h7^2)));
})Bending stiffness ( lb-in)
Dmat=(1/3)*((Q90*(h1^3-h0^3))+(Q0*(h2^3- h1^3))+(Q0*(h3^3-h2^3))+(Q0*(h4^3-h3^3))+(Q90*(h5^3-h4^3))+(Q0*(h6^3-h5^3))+(Q0*(h7^3-h6^3))+(Q0*(h8^3-h7^3)));
({  {94.4148, 2.16035, 0.},
 {2.16035, 43.8905, 0.},
 {0., 0., 5.01333}
})ABD=({
   {A[[1,1]], A[[1,2]], A[[1,3]], B[[1,1]], B[[1,2]], B[[1,3]]},
   {A[[2,1]], A[[2,2]], A[[2,3]], B[[2,1]], B[[2,2]], B[[2,3]]},
   {A[[3,1]], A[[3,2]], A[[3,3]], B[[3,1]], B[[3,2]], B[[3,3]]},
   {B[[1,1]], B[[1,2]], B[[1,3]], Dmat[[1,1]], Dmat[[1,2]], Dmat[[1,3]]},
   {B[[2,1]], B[[2,2]], B[[2,3]], Dmat[[2,1]], Dmat[[2,2]], Dmat[[2,3]]},
   {B[[3,1]], B[[3,2]], B[[3,3]], Dmat[[3,1]], Dmat[[3,2]], Dmat[[3,3]]}
abd=Inverse[ABD];
a=({    {abd[[1,1]], abd[[1,2]], abd[[1,3]]},
   {abd[[2,1]], abd[[2,2]], abd[[2,3]]},
   {abd[[3,1]], abd[[3,2]], abd[[3,3]]}
  });b=({
   {abd[[1,4]], abd[[1,5]], abd[[1,6]]},
   {abd[[2,4]], abd[[2,5]], abd[[2,6]]},
   {abd[[3,4]], abd[[3,5]], abd[[3,6]]}
  });bt=({
   {abd[[4,1]], abd[[4,2]], abd[[4,3]]},
   {abd[[5,1]], abd[[5,2]], abd[[5,3]]},
```

```
    {abd[[6,1]], abd[[6,2]], abd[[6,3]]}
   });d=({    {abd[[4,4]], abd[[4,5]], abd[[4,6]]},
    {abd[[5,4]], abd[[5,5]], abd[[5,6]]},
    {abd[[6,4]], abd[[6,5]], abd[[6,6]]}
```

P is εmid

```
P=a-(b.Inverse[d].Transpose[b]);
 ({  {1.33171*10^-6, -7.55886*10^-8, 0.},
  {-7.55886*10^-8, 3.50746*10^-6, 0.},
  {0., 0., 0.0000265957}
 })Exnew=1/((P[[1,1]]-(P[[1,3]]^2/P[[3,3]]))*8*t)
1.87729*10^7
Eynew=1/((P[[2,2]]-(P[[2,3]]^2/P[[3,3]]))*8*t)
7.12766*10^6
υxynew=- ((P[[1,2]]-((P[[1,3]]*P[[2,3]])/P[[3,3]]))/(P[[1,1]]-(P[[1,3]]^2/P[[3,3]])))
0.0567606
delta=P[[1,1]]*P[[2,2]]-P[[1,2]]^2;
Gxynew=(1/(P[[3,3]]-((P[[1,3]]*(P[[2,2]]*P[[1,3]]-P[[1,2]]*P[[2,3]]))/delta)-((P[[2,3]]*(P[[1,1]]*P[[2,3]]-P[[1,2]]*P[[2,3]]))/delta)))*(1/(8*t))
940000.
```

Equiv-prop for α: thermal moment load, assume T = 1

(lb / in)

```
T=1;
NT=T*((6*(Q0.α)*t)+(2*(Q90.α90)*t));
 ({  {-0.0208704},
  {0.471979},
  {0.}
```

})(lb):

MT=(0.5*T)*

(((Q90.α90)*(h1^2-h0^2))+((Q0.α)*(h2^2- h1^2))+((Q0.α)*(h3^2-h2^2))+((Q0.α)*(h4^2-h3^2))+((Q90.α90)*(h5^2-h4^2))+((Q0.α)*(h6^2-h5^2))+((Q0.α)*(h7^2-h6^2))+((Q0.α)*(h8^2-h7^2)));

({ {-0.00184818},

{0.00184818},

{0.}

})αnew[[1]]=((P[[1,1]]-(P[[1,3]]^2/P[[3,3]]))*NT[[1]])+((P[[1,2]]-((P[[1,3]]*P[[2,3]])/P[[3,3]]))*NT[[2]])

$-6.34696*10^{-8}$

αnew[[2]]=((P[[1,2]]-((P[[1,3]]*P[[2,3]])/P[[3,3]]))*NT[[1]])+((P[[2,2]]-(P[[2,3]]^2/P[[3,3]]))*NT[[2]])

$1.65703*10^{-6}$

Smeared method

Exold=1/(a[[1,1]]*8*t)

$1.79603*10^{7}$

Eyold=1/(a[[2,2]]*8*t)

$5.38477*10^{6}$

υxyold=- (a[[1,2]]/a[[1,1]])

0.0677194

Gxyold=1/(8*t*a[[3,3]])

αold=a.NT+b.MT;

References

[1] Richardson, D., “The Fundamental Principles of Composite Material Stiffness Predictions”, University of the West England, Bristol

[2] Lydzba, D., “Effective Properties of Composites, Introduction to Micromechanics”, Wroclaw University of Technology, 2011

[3] Chan, W.S., and his associates, “Equivalent thermal expansion coefficients of lumped layer in laminated composites”, Composite science and Technology 66 (2006) 2402-2408, January of 2006.

[4] Chan, W.S., Chen, D.J., “Use of composite effective moduli for lumping layers in finite element analysis”, American Institute of Aeronatics and Astronautics, Inc. AIAA meeting papers on disc, pp. 2199-2209, 1996.

[5] Chan, W.S., and Wang, J.S., “Effects on Buckling Load of Rodpack Laminates due to Defects”, Center for Composite Materials, Department of Mechanical and Aerospace Engineering, University of Texas at Arlington, 2000.

[6] Chandra, R., and Chopra, I., “Experimental and Theoretical Analysis of Composite I-Beams with Elastic Couplings”, University of Maryland, AIAA Journal, VOL. 29, NO. 12, December of 1991.

[7] Kumton, T., “Analytical Method for analyzing C-Channel Stiffener made of Laminate Composite”, University of Texas at Arlington, December of 2012.

[8] Parambil, J.C., Chan, W.S., Lawrence, K.L., and Shanghavi, V.M., “Stress analysis for composite I-beam by a non-conventional method”, Proceedings of the 2011 ASC conference, Paper No. 1027, 2011.

Biographical Information

Kamran Tavakoldavani received his Bachelor of Science in Mechanical Engineering from the University of Texas at Arlington in December 2006.

Kamran joined The U T Arlington Mechanical Engineering graduate program in August 2012 and started his research under Dr. Chan in fall 2012. The focus of the research is on mechanical and thermal properties of composite materials. Computer software programing is used in order to conduct the analysis. Kamran received Master of Science in Mechanical Engineering from the University of Texas at Arlington in December 2014.